1-1-2012

Geodetic Method to Estimate Mass Balance of Himalayan Glaciers: a Case Study of the Sagarmatha National Park, Nepal

Kabindra Joshi

Geodetic method to estimate mass balance of Himalayan glaciers: a case study of the Sagarmatha National Park, Nepal

By

Kabindra Joshi

A Thesis
Submitted to the Faculty of
Mississippi State University
in Partial Fulfillment of the Requirements
for the Degree of Master of Science
in Geosciences
in the Department of Geosciences

Mississippi State, Mississippi

December 2012

Geodetic method to estimate mass balance of Himalayan glaciers: a case study of the Sagarmatha National Park, Nepal

By

Kabindra Joshi

Approved:

Shrinidhi S. Ambinakudige Associate Professor of Geosciences (Major Professor)	John C. Rodgers III Associate Professor of Geosciences (Committee Member)
Qingmin Meng Assistant Professor of Geosciences (Committee Member)	Michael E. Brown Associate Professor of Geosciences (Graduate Coordinator)
R. Gregory Dunaway Professor and Interim Dean College of Arts & Sciences	

Name: Kabindra Joshi

Date of Degree: December 15, 2012

Institution: Mississippi State University

Major Field: Geosciences

Major Professor: Shrinidhi S. Ambinakudige

Title of Study: Geodetic method to estimate mass balance of Himalayan glaciers: a case study of the Sagarmatha National Park, Nepal

Pages in Study: 166

Candidate for Degree of Master of Science

Mass balance records of glaciers help to understand long term climate change, yet there are very few *in-situ* measurements of mass balance in Himalayan glaciers. Mass balance of major glaciers in the Sagarmatha National Park was assessed using Digital Elevation Model prepared from ASTER images for period 2002 & 2005 and 2002 & 2008, employing geodetic model. Overall glacial mass balance during 2002-2005 was -2.978 plus/minus 0.89 and during 2002-2008 was -0.94 plus/minus 0.34 m.w.e per annum. Glacier melt could form glacial lakes in high Himalayas. One of the glacial lakes, Imja Lake in the study area increased its surface area by 268% from 1975 to 2010. Temperature analysis from MODIS data between 2000 and 2011 indicated increase in temperature in the study area. General loss of glacial mass in the Himalayan region indicated, and these loses if continue in the future will lead to catastrophic environmental and economic impacts.

Key Words: ASTER, DEM, Mass balance, Himalayan glacier, GLOFs

DEDICATION

This thesis is dedicated to my loving family members who have offered encouragement and support throughout the entire endeavor. Special thanks are given to my father, Govinda Joshi; mother, Sushila Devi Joshi, brother, Dr. Rabindra Joshi and sister-in-law, Dr. Samjhana Kashaju Joshi.

ACKNOWLEDGEMENTS

I greatly appreciate Dr. Shrinidhi Ambinakudige's guidance in developing me as a young professional while promptly assisting me with all of my research endeavors. Special thanks are also given to Dr. John Rodgers and Dr. Qingmin Meng who augmented this research through there countless critiques and assistance.

TABLE OF CONTENTS

LIST OF TABLES

LIST OF FIGURES

CHAPTER I

INTRODUCTION

Chapter one provides an introduction of various topics on glaciers and climate change within the Himalayas. Section 1.1 provides background information on climatic changes and evaluates the importance of studies related to glaciers using remote sensing techniques. Section 1.2 gives general information on glacier mass balance measurement techniques. Section 1.3 emphasizes the importance of glacier mass balance studies to the society as a whole. This study's objectives are listed in Section 1.4 and hypothesis in Section 1.5. Section 1.6 provides the research scope and the study's limitations. Section1.8 gives the thesis organization which is a synopsis of the individual chapters.

1.1 Background

The Himalayan mountain range is one of the largest ice-covered areas outside of Greenland and Antarctic. Himalaya glaciers account for approximately 15% of world glaciers (Ashish et al. 2006). The Himalayan glacial region has complex terrain which is often inaccessible and thus, making it difficult for regular field glacier monitoring and in-situ measurements (Ashish et al. 2006; Bolch et al. 2011a).

Changes in glaciers can be a direct indicator of climate change in areas where meteorological stations are rarely present or completely absent (Ageta and Kadota 1992; Raup et al. 2007). Himalayan glaciers have been retreating more rapidly than glaciers in

other regions (Ageta and Kadota 1992; Ambinakudige 2010; Ashish et al. 2006; Fujita et al. 2009; Nakawo et al.1997; Racoviteanu et al. 2008; Raup et al. 2007). Many small glaciers with less than 0.5 sq. km. around the world have melted and many more in the future will to melt due to increase in global temperature (Kadota et al. 1993; Fujita et al. 2009; Nakawo et al. 1997; Racoviteanu et al. 2008). Glaciers melting faster than normal rate in high altitude areas could create new moraine dammed lakes and increase the depths of existing moraine lakes (Bajracharya et al. 2007). Eventually, the melting glaciers will also contribute to global sea level rise (Church et al. 2008).

There are more than 15,000 glaciers and 9,000 glacial lakes in the Himalayan region of Nepal, Bhutan, Pakistan, selected basins of China and mountain range in India (Bajracharya et al. 2009). All of these aforementioned countries within the Himalayan region have experienced life-threatening Glacial Lake Outburst Floods (GLOF's) (Bajracharya et al. 2009; Bajracharya & Mool, 2009) which have a wide range of socio-economic impacts including loss of building infrastructure, property, livelihoods, as well as human causalities. GLOF's describes an instantaneous occurrence of discharge of large volumes of water from a moraine lake (Racoviteanu et al. 2008; Bolch et al. 2011; Waldmann et al. 2010). These moraine dam lakes are developed by loose stones, gravel and during its burst the flow of water carries small to huge pieces of solid ice blocks and rocks. Such incidents occur when external events such as intensive rainfall, high snowmelt, earthquake, avalanche triggers or when the moraine dam itself fails to hold the water pressure (Mergili et al. 2011).

1.2 Glacier Mass Balance Measurement

The glacier mass balance is the total loss or gain in a glacier's mass at the end of a hydrological year, which runs from 1st September to 31st August in a calendar year (Peterson 1998). Mass balance can be estimated using multi-temporal Digital Elevation Model (DEM) - a topographic representation of complex terrain (Paul and Haeberli 2007). The internal thermodynamics property change in a glacier bed due to changes in temperature is the main reason for glacier melt creating mass balance changes (Kaser *et al.* 2002). A typical glacier consists of accumulation and ablation zones. Accumulation describes the area for catchment of snow and ice that creates additional glacier volume. It is perceived as a positive mass balance if snow and ice remain after melting at the end of a hydrological year. Contrastingly, negative mass balance describes that, glacier mass losses more than what it accumulated at the end of hydrological year. The area from where ice and snow melted is known as ablation zone (Braithwaite, 2002).

Mass balance can be measured either by direct or indirect methods. The direct method requires *in-situ* collection of glacier information. This method has been in use since the 1940s to numerically evaluate glacier retreat from measurements taken at lower ablation regions (Rott *et al.* 2002; Nishida *et al.* 1995). In the last two decades, number of *in-situ* measurements have declined and the indirect method has become more common (Barry 2006; Dyurgerov and Meier 1997).

Indirect method of mass balance measurement involves use of satellite images, aerial photos, and photogrammetric methods (Racoviteanu *et al.* 2008; Ambinakudige 2010). This helps to calculate accurate volumetric mass balance measurement in regional to global scale excluding hectic field visit in rough terrain and inaccessible areas.

1.3 Problem Statement

Himalayan glaciers act as reserves of ice and water that when melting processes occurs, it provides water for millions of people downhill and this area is considered as the world's water tower (Dyugrov and Meier 1997a, Dyugrov and Meier 1997). Hence, mass balance measurement has a significant role in estimating the available water balance (Immerzeel et al. 2010). However, significant gaps in current and past data in glacier masses in the Himalayas and concurrent weather data in glacial areas have limited the scope of water balance estimations and global climate change studies in the Himalayas (Bolch, et al. 2011; Kulkarni, et al. 2004). This data gap calls for the development of a system to continuously and remotely monitor the changing volumetric and temporal characteristics of mountain glaciers in the Himalayas. Obtaining elevation data from multi-temporal satellite images and calculating elevation differences to augment in-situ field measurements to ascertain realistic mass balance changes (Bamber & Rivera, 2007).

There are only few studies on glacier mass balance changes in the Himalayas. Berthier et al. (2007) employed remote sensing techniques to study the western Himalayan glacier mass balance changes within the study period of 1999-2004. Similarly, Bolch et al. (2008) studied mass balance of major glaciers in Mt. Everest region in the Sagarmatha National Park area from 1960-1970. They found almost all debris covered glacier, D-type glaciers, lost glacial mass since 1962 and glacier melt rate increased. However, vast majority of Himalayan glaciers have no mass balance records.

Geospatial techniques such as Geographical Information System (GIS), Global Positioning System (GPS) and Remote Sensing (RS) are tools to extract, store, and

analyze large volumes of information from inaccessible glaciers (Gao & Liu, 2001). Using in-situ method of glacier measurement in the remote Himalayas is physically exhausting, time consuming, and logistically challenging (Racoviteanu et al. 2008). The recent development in the field of satellite remote sensing technology for acquiring very high resolution images over large areas, glacier monitoring and change in glacier volume has increased in remote inaccessible mountain areas, which would have been left behind (Bolch et al. 2008). Despite high resolution remote sensing data and advancement in technology, still there has not been in-depth studies which evaluate variations of glacier mass balance in the Himalayas using remote sensing method (Nuimura et al. 2012) . To bridge data gaps in mass balance of some of the Himalayan glaciers, the Sagarmatha National Park, one of the densely glaciated areas was chosen for this research.

As a result of glacier shrinkage, many small glacial lakes are forming and increasing the surface area of existing lakes which are potentially hazardous in the Sagarmatha National Park. The study area has already faced several GLOFs events such as Lake Dig Tsho outburst in 1985 due to an avalanche (Vuichard and Zimmermann 1987) and Lake Sabai Tsho which was partly drained in 1998 (Kattelmann 2003). For this study's purpose using remote sensing method, satellite data from ASTER (Advance Spaceborne Thermal and Emission and Reflection), LANDSAT and MODIS (Moderate Resolution Imaging Spectroradiometer) satellites images were used to fulfill objectives listed in Section 1.4; using geospatial technologies to evaluate glacier parameters such as glacier mass balance, glacier area, lake areas, and the temperature variation in the study area.

1.4 Study Objectives

The specific objectives of the proposed study were:

1. To estimate mass balance change of major glaciers in the Sagarmatha National Park (SNP) in the Himalayas, employing remote sensing techniques for the periods 2002 and 2005, and 2002 and 2008.
2. To measure planimetric changes in Imja glacial lake, one of the potential lakes for Glacial Lake Outburst Floods (GLOFs) within the study area.
3. To quantify temperature variations in the study area using Moderate Resolution Imaging Spectroradiometer (MODIS), Land Surface Temperature and Emissivity 8-Day L3 Global Satellite (MOD11A2) images with 1 km resolution.

1.5 Hypotheses

The hypotheses were tested in this study:

1. There was no change in glacier mass balance during the study periods in the study area.
2. Area of Imja glacial lake remained the same during the study period.
3. There was no significant increase in local temperature during the study period.

1.6 Study Area

The Sagarmatha National Park (SNP) is listed as a world heritage site by UNESCO. SNP is the home of the highest peak commonly known throughout the world as Mount Everest at an altitude of 8,850 meters. The SNP is situated in northeastern part

of Nepal, in the Solukhumbu District (Figure 1.1, Figure 1.2). Eight out of ten of the world's highest mountains are located in Nepal (UNEP 2008).

Figure 1.1 Location of the Study area, the Sagarmatha National Park

Source: Digitized from 1:100,000 scale Topographic Map published by Department of Survey, Nepal

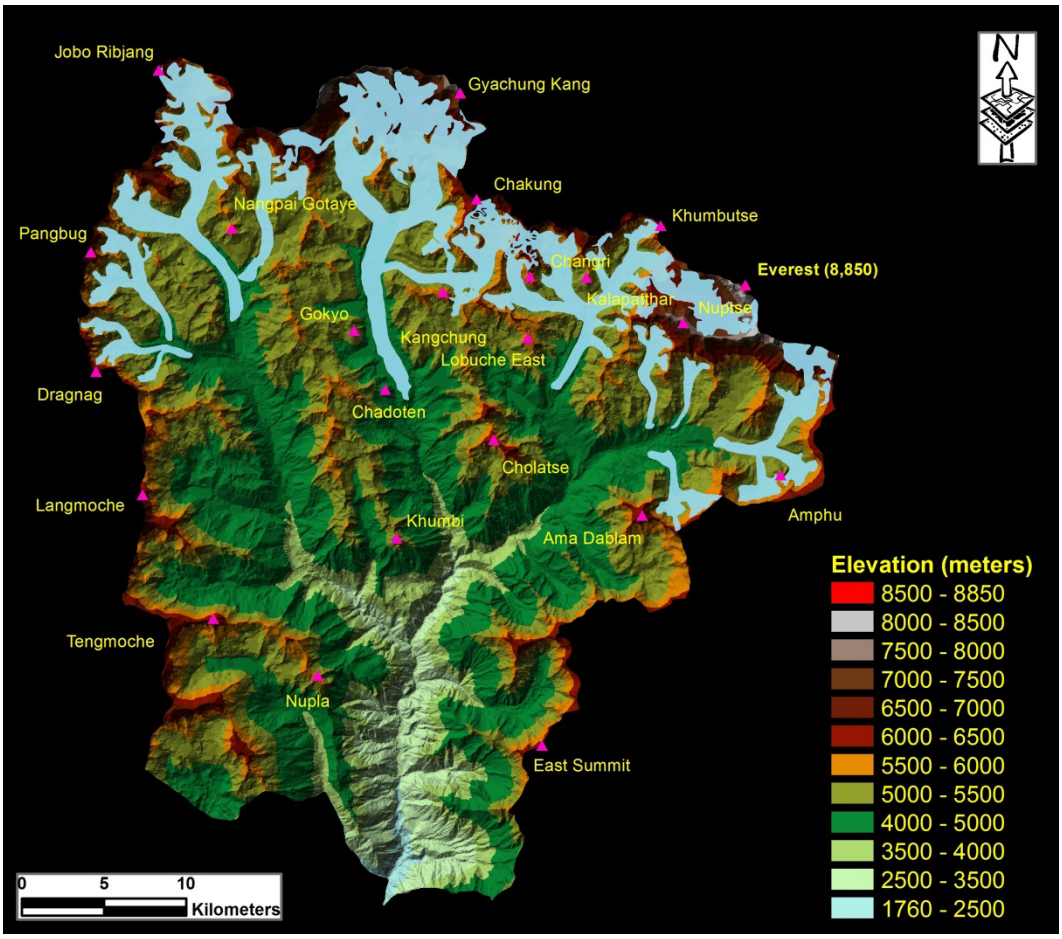

Figure 1.2 3D View of the Sagarmatha National Park, Nepal

Source: Digitized from 1:50,000 scale Topographic Map published by Department of Survey, Nepal and prepared 3D View using ArcGIS 10.0

There are around 3,552 glaciers and 2,315 moraine dam lakes above 3,500 mean sea level in Nepal Himalayas. SNP area alone consists of 296 glacial lakes and more than 12 major glaciers making it one of the densely glaciated regions in the world (Mool et al. 2002). The park includes the watershed catchment areas of the Dudh Koshi and Bhote Koshi Rivers. The Himalayan mountains have experienced several GLOFs in recent years, causing extensive damage to local infrastructure and loss of human life (Bajracharya 2009). The region still contains many potentially dangerous glacial lakes

(Mool et al. 2002). Since this area contains glacial lakes that could lead to GLOFs, scientists frequently measure, monitor, and map glaciers for building design planning and implementing of hazard mitigation measures.

The SNP consists of the Dudh Koshi River surrounded by high mountains around the Dudh Koshi River basin, which sustains 278 glaciers with a 482.20 sq. km. area and 473 glacier lakes of area 13.07 sq. km. (Mool et al. 2002) whose existence are threatened by the effects of global warming and could create additional bodies of water and eventually GLOFs. The area experiences a mix of South Asian monsoon, weather from mid-latitude and westerlies, and El Niño Southern Oscillation (ENSO) climate (Benn & Owen 2002).

1.7 Research Scope and Limitations

Baseline data is non-existent for research validation purposes except for studies performed by Bolch *et al.* in 2011. This thesis estimated mass balance of major glaciers in SNP area using geodetic methods. The study's overall objective is to facilitate understanding amongst fellow scientists that the behavior of the studied glaciers exhibits the same pattern of retreat as similar glaciers in the Himalayan range.

Limitations of this study include no *in*-situ data from the study area, possible errors from the low resolution ASTER satellite data of 15m in VNIR band and lack of ground control points (GCPs) from field to georeference satellite images effecting the creation of high accuracy DEMs. Another limitation of this research is the absence of socioeconomic data to understand the ongoing glacial changes, and information from local people within this area would have assisted in the interpretation of the glacier retreat affecting the low lying areas.

1.8 Thesis Organization

Chapter 1 “Introduction” provides a general synopsis of the thesis title, research hypothesis, and brief introduction of study area, study limitations, and the significance of this study to the scientific community. Chapter 2; “Literature Review” provides the knowledge of previous research, and with the data gaps of mass balance studies within the Himalayan Mountains. Chapter 3 “Research Methods” presents the overall flow diagram of mass balance estimations using geodetic method which employs the use of photogrammetry and remote sensing technology to generate the input data DEM. Also, Chapter 3 describes the methods to fulfill the second and third objectives and third objectives of this research. Chapter 4 “Results and Discussion” provides the glacier mass balance estimation in accumulation and ablation areas changes, micro analysis of glacier bed changes over the time period, and comparison of this study’s results with those of peer reviewed journals. Chapter 5 “Conclusions and Recommendations” summarizes the entire study, challenges faced during the study, and offers suggestions for further research options.

CHAPTER II

LITERATURE REVIEW

This chapter provides the knowledge of previous research, and with the data gaps of mass balance studies within the Himalayas.

Himalayan glaciers are considered as highly inaccessible glaciers. Its harsh and irregular terrain makes it difficult for in-situ measurements for regular monitoring. Because of (add all those related to logistic and border problems) only very few mass balance of Himalayan glaciers have been studied in field (Kulkarni et al. 1962). Mass balance of glaciers can be estimated from various methods; however, the geodetic or the remote sensing method coupled with photogrammetric technique will be discussed in detail as they directly related to this thesis's methodology. The Geodetic method has been used to estimate mass balance to augment insufficient glacier mass balance studies within the Himalayas (Kulkarni et al.2004; Berthier et al. 2007). This method requires accurate GCPs to georeference satellite images and during DEM production phase for triangulation and epipolar image creation.

This chapter discusses previous mass balance studies, its methods, data used, problems associated and data gaps. A separate topic on Himalayan glaciers of Nepal is also discussed to give a glance of the Himalayas of Nepal and glaciers.

2.1 Mass Balance Measurement of glaciers

There are different techniques to monitor and measure mass balance of glaciers that have been adopted throughout the years. Each methodology has its own advantages and inherent disadvantages. The most common research methods for measuring glacier mass balance changes have been reviewed in this section.

2.1.1 Glaciological Method

The traditional method of *in-situ* measurement of glacier characteristics and glacier mass includes direct interaction with glacier known as Glaciological method (Frenierre, 2009). This method was first used for quantitative analysis of glacier in Europe's Rhone glacier around end of 19th century (Dyurgerov and Meier 2000). *In-situ* method is labor intensive, uses stakes for measuring the change in snow depth over two different times. Pits are excavated for analyzing the density of ice at various depths in different location. The change in snow depth is measured from a reference surface through geodetic surveying technique (Mayo 1972). The volume change is computed by multiplying the glacier area and depth change between two different times (Kaser *et al.* 2003). Numerous ablation stakes are drilled several meters below glacier surfaces at reference points (Frenierre 2009). The distance from the glacier surface to the other end of stake is recorded at the time of placement and a repeated measurement is taken to determine the snow mass added or melted between measurements (Racoviteanu 2008b). The number of ablation stakes to be placed is not accurate, but generally 10 stakes should provide good representation for glaciers less than 20 sq. km. in area, whereas 10-20 stakes for to quantify glacier area up to 500 sq. km. (Hagen and Reeh 2003). The ablation of the glacier thickness is calculated by measuring the total length of stake above the

glacier surface and subtracting the original length. The accumulation of snow is determined by excavating snow pits, and the thickness of the snow layer is detected by the presence of layer of dust between two different time periods or the change in grain sizes between the layers. The specific winter balance at that particular point on the glacier surface is obtained by dividing the accumulation by average density of ice or snow. For consistent measurements, such field measurements are carried out between hydrologic seasons, either at the end of accumulation or ablation seasons (Racoviteanu 2008), or from one hydrologic year to another (Kaser *et al.* 2003; Hagen and Reeh 2003; Hubbard and Glaser 2005).

Direct method provides the most accurate quantitative data and so that the true mass balance changes can be estimated (Kaser *et al.* 2003); however, this method cannot be easily applied in remote mountainous terrain because of heavy manual labor, logistical issues to transport equipment's to and from the field; time consideration to reach, conduct, return from the site and data analysis as well the financial burden for every visit (Frenierre 2009). In addition to all of the aforementioned difficulties, the process involves sampling from different point locations and crevasses, steep headwalls, icefalls; and avalanches which could endanger the researchers (Hagen and Reeh 2003).

2.1.2 Geodetic Survey

A traditional geodetic survey using quantitative measurements at two different time periods can be used to calculate the topographic elevation changes over the glacier surface. At the beginning of hydrologic year, a survey can be made from recognized points on the glacier surface from a stationary station; the respective changes in x, y, and z axis of the points can be calculated measuring the angle and distance from the same

fixed position (Kaser *et al.* 2003). The volumetric changes can be calculated subtracting the earlier volume by the recent volume multiplied by the average density gives the change in mass balance (Hubbard and Glasser 2005). This method also has logistical and hazard issues as in glaciological method; however, Global Positioning System (GPS) has increased the accuracy of geodetic surveying (Hagen and Reeh 2003) but the hazardous conditions for the researcher's remains a prominent issue.

2.1.3 The Hydrological Method

The hydrological method is another direct method of mass balance calculation. This method treats a glacier as a reservoir with a gain in mass during winter as a seasonal gain and a loss in mass known as summer losses. The amount of precipitation that the glacier catchment area collects equals the volume of water lost through runoff and evaporation, and then there is a hydrological balance in glacier (Frenierre 2009). Positive difference refers to an increasing in glacier mass and negative value as a loss of glacial mass. This method is very challenging in applying it to high altitude glaciers as it requires precise measurement of each variable. A good gauging station is required for measuring the volume of water discharged; as well this method involves extrapolation of precipitation from the single station over the rough terrain which might produce inaccurate results (Kaser *et al.* 2003), as well in mountainous area, snow is accumulated not only with precipitation but with wind, avalanche, and other natural factors (Hubbard and Glasser 2005).

$$B = P\text{-}Q\text{-}E \pm dS \qquad (2.1)$$

Where:

P = precipitation

Q = runoff

E = evaporation

dS = variation of storage elements of the catchment area other than glaciers such as groundwater or interception.

2.1.4 Estimation from Climatic Record

The mass balance of glaciers can be calculated from climatic records excluding the non-climatic factors such as surge, avalanches that affect the accumulation process (Kaser *et al.* 2003). Majority of the mass balance calculation model algorithms are based on the correlation of mass balance elements with meteorological parameters (Sobota 2007) and depends on simple extrapolation from temperature and precipitation data (Kaser *et al.* 2003). Most of the climatic models require calibration to ascertain reliable results from these models (Kaser *et al.* 2003).

2.1.5 Precipitation Temperature Area Altitude Model (PTAA)

The Precipitation Temperature Area Altitude Model (PTAA) model utilizes the daily meteorological data to calculate the glacier mass balances. This model can be used in places where climatic stations are not close to the glaciers and in low lying elevations; however, climatic stations should be within 50 km distance from the glacier and be located 1200m lower than the glacier termini. The PTAA model holds the concept that, there is a correlation between low-altitude climate and glacier mass balance as well the correlation between mass balances variables from which coefficients can be generated to

run the algorithm. The model is iterative and the climatic data obtained from low-elevation temperature and precipitation is converted to variables such as snowline altitude, accumulation area ratio, zero balance altitude, to calculate glacier mass balance changes. The daily precipitation and temperature value is regressed against each mass balance variable for every available date from the researchers' studies in the ablation season from May to August.

The conceptual model has shown very good results when various mass balance components are simulated by the PTAA model and compared with corresponding *in-situ* data 1959 – 1996 periods (Tangborn 1999).

2.1.6 Remote Sensing Technique

In the absence of in-situ data, mass balance can be estimated using an indirect method ("geodetic method"), and this method consists of evaluating elevation changes from different times within various digital elevation models (DEMs) created over the glacial surface (Racoviteanu et al. 2008). Subtracting elevations of an older DEM from more current DEMs calculated by remote-sensing images such as ASTER, SRTM, ALOS or SPOT5, can create an elevation differential map for a glacier. Glacier thickness changes are evaluated pixel by pixel and the difference is multiplied to the glacier area to obtain the glacier volume change. The volume is multiplied with the density of glacier generally considered as 900 kg·m-3 to obtain mass balance (Paterson 1994).

The volume change can be interpreted into mass balance change by multiplying the volume with the density of glacier or firn. In the ablation zone, 900 kg·m-3 of ice is generally considered for the conversion of volume changes to mass balance. Paterson

(1994) used the following information in regards to accumulation area density of ice can range from (900 kg·m-3) for ice to firn (550-600 kg·m-3) for his research.

The geodetic approach has been used in several studies on the basis of historical topographic maps and DEMs derived from SPOT imagery (Berthier et al. 2007), SRTM (Racoviteanu et al. 2008), ASTER (Casey et al. 2012). Studies have also used high resolution DEMs derived from ALOS PRISM and Corona (Narama et al. 2010) to estimate mass balances with the geodetic method.

2.2 Digital Elevation Model Creation and Accuracy

Digital Surface Models (DSM), Digital Terrain Models (DTM), Triangulated Irregular Networks (TIN) are different form of Digital Elevation Models. DSM provides information about the highest elevation (elevation of natural terrain, bare earth plus vegetation and manmade features such as buildings, road) of the object at a given location. DTM provides elevation information about bare earth, elevation of vegetation and manmade features such as buildings, road, and trees are digitally removed. TIN provides information about the earth surface using point elevation data creating continuous polygon over the surface (Prima *et al. 2002*).

Digital Elevation Models (DEM) is digital illustration of the Earth's irregular complex terrain (Prima *et al.* 2002). Each point on the DEM represents the elevation of the undulating earth's surface in a two dimension.

A DEM has high capability to solve many problems related to surface topography in various fields that requires spatial location studies, such as engineering, scientific and many other disciplines like resource management, hydrology, transportation, geology, utility applications (Bolstad 2002). DEM's can produce contour maps, help in making

Orthophoto, and create three dimensional model of the terrain. DEM can be used to study morphometric characteristics such as slope, glacier profile curvature, and aspect. DEM is one of the most important components used in glacial studies for calculating volume change; in inaccessible areas (Bolch *et al.* 2011a).

Creating DEM from satellite images such as ALOS, AVNIR-PRISM, ASTER, SPOT (expand) images are becoming more common(Ambinakudige 2010, Racoviteanu *et al.* 2008). Advance improvement in satellite sensors have been achieved in the past decades, but still acquiring accurate vertical data for glacier volume change study is limited (Stevens *et al.* 2004). DEM from more than one satellite sensors need to be generated and their vertical error and accuracy need to be analyzed for better result (Ye 2010). From the satellite image we can easily calculate the planimetric data in x and y, but calculating volume with z value requires creation of DEMs. Very high resolution satellite sensor, SPOT from 1986 provided cross-track stereo images. DEMs from SPOT images generated using automated stereocorrelation is said to be accurate within RMSE ±5m and ±20m, depending on B/H ratio (Hirano *et al.* 2003). SPOT image being very expensive due to its high spatial resolution, and swath width being very less, obtaining cloud free images for large area has limited its use in creating DEMs (Hirano *et al.* 2003).

The manual method of DEMs creation require huge amount of time in collection of GCPs and tie points. In order for fast processing and greater accuracy automated stereocorrelation method is widely used (Hirano *et al.* 2003). DEM products can be relative or absolute, based on the Ground Control Point (GCP), map datum information available about the study area and the nature of the stereo image. A relative DEM does not consider GCP and not tied to map datum resulting possible shift in position, scale,

and rotation with respect to horizontal reference system on ground and vertical reference system with respect to the mean sea level defined as geodetic coordinate system. On other side, absolute DEM uses GCPs considering geodetic coordinate system referencing from above mean sea level resulting more accurate representation of the earth's terrain (Hirano *et al.* 2003). One of the advantages of ASTER (along-track) compared to cross-track image is that along-track images are acquired in uniform environment and lightening condition providing consistent information (Fujisada 1994, Fujisada 1998). Hirano *et al.* (2003) tested the ASTER image in producing DEMs in four different locations Mt. Fuji, Japan; Andes Mountains, Chile-Bolivia; San Bernardino, CA and Huntsville, AL.

The DEM produced for Mt. Fiji, from ASTER L1A had a vertical elevation difference of approximately 2100m. Using topographic maps of 10m contour interval, scale 1:25,000, were used to collect 50 GCPs and 331 check points. The result yielded an accuracy of ±5m in both planimetric and vertical measurement.

The elevation range difference in the study site, Mt. Andes was from low flat lava flowing areas to high cone-shaped volcanoes with elevation reaching 5,700m with a total relief difference of 2,200m. ASTER L1A image was used to create DEM. 18 GCPs and 46 check points were used using 1:50,000 scale topographic map of contour interval 20m and found the accuracy of approximately ±10m in planimetric and elevation.

Similarly, the accuracy of ±6m was obtained in planimetric and elevation, when ASTER L1A image was used to create DEM in San Bernardino area, CA. Total of 17 GCPs collected using Trimble Pathfinder R Pro XRS DGPS unit was used and more than

100 check points were digitized. The range difference in elevation from 200m to 1,700m was 1,500m.

The study in Huntsville by Hirano *et al.* (2003) was relatively low altitudinal area, with an elevation difference of 300m. Using ASTER L1A image, the planimetric and vertical height difference came to be ±1.5m.

Thus, the above different study correlates with, the accuracy of the DEM increases by increasing the number of GCP in ASTER L1A (San and Suzen, 2006).

2.3 DEM from Ground Elevation Data

DEMs can be generated from points collected on ground using the traditional method of surveying using theodolite or total station or from topographic maps; however, the modern digital equipment's Global Position System (GPS) has great influence on geospatial technology for collecting fast and precise data (Scherzinger *et al.* 2007). GPS technology consists of multiple satellites revolving around the earth 24/7 providing very accurate location of the earth's surface, stored using ground receiver. The resulting data is downloaded from ground receiver in the form of point data. The point data provides x, y, and z or elevation value. When a large number of points are collected a DEM can be created using the interpolation algorithm. The algorithm helps to calculate the elevation value statistically between the points using TIN data model. The accuracy of such DEM is dependent on the precision and accuracy of the point data collected using GPS Technology. DEM can also be generated interpolating the contour line. The contour line is the line joining points of equal elevation. The contour lines can be digitized from the topographic map or created from point data. The disadvantage of creating DEM from

contour line is there are no point information between two lines and may not result true topography.

2.4 DEM from ASTER Stereo Image

DEM generation with ASTER image requires two images, Nadir view and Backward view (Ye 2010). Qinghua Ye (2010), created DEMs of Northern slope of Qomolangma, Mt. Everest region using ASTER and ALOS/PRISM image using PCI Orthoengine module. Separate DEM from 1:50,000 topographic image and DEM from ALOS image were generated. The author found a mean difference of 1.7m, when 215 random points were selected in non-glaciered area. Comparing the ASTER DEM with ALOS, the author found mean difference of 45m and found that ALOS/PRISM DEM to be better than ASTER DEM.

2.5 Remote Sensing and Glacier Studies

Remote sensing technology has been one of the effective methods in the study of glaciers and related hazards (Barry 2006). The availability of various satellite images from low to high resolution has made the research scalable. Generally, medium resolution image (5-30m), provided by the satellite sensors Landsat TM, ETM+, ASTER can be used for areal coverage studies. The development of advance sensor system has led the technology to produce imagery with very high resolution (< 5m), provided by IKONOS, Quickbird. The capability of sensors to produce stereo pair images has helped to prepare 3D visualization and modeling of glaciers comparing different times and allowing for the calculation of movement rates. Regular monitoring by satellite has produced a large volume of images, which can be utilized to map and study glaciers continuously over a

long time (Kaab *et al.* 2002). GIS, GPS and remote sensing can be used as a tool to extract, store and analyze large volume of information about remote, inaccessible glaciers (Gao and Liu 2001). Studies have shown that remote sensing methods are more appropriate, cost effective and faster in decision-making than traditional in-situ method. Previous studies have shown the use of various satellite images in glaciological studies (Barry 2006). Medium resolution satellite images such as, Landsat, ASTER, IRS, ALOS and very high resolution satellite image Quickbird, IKONOS, SPOT have been used to measure glacial parameters (Racoviteanu *et al.* 2008).

2.6 Spectral Resolution of Satellite Image

Understanding the spectral resolution of a satellite image is required to apply the particular image in an appropriate research application (Quincey *et al.* 2005). In glacial studies, there are various jobs to performed, including: a) separating snow from ice or snow from fresh and turbid water, and b) delineation of the glacier boundaries. Thus, spectral characteristics play a vital role in selecting the images. Bronge and Bronge (1999) suggest visible (0.4-0.7 μm) and NIR band can be used to extract the important information about ice and snow. For automatic delineation of glacier boundary, Short Wave Infra-Red (SWIR) band (1.3-3.0 μm) is helpful (Paul and Kaab 2005). The separation of cloud from snow can be done by using SWIR (Bronge and Bronge 1999). Thermal Infra-Red (TIR) though the spatial resolution is low (3.0-14.0 μm), can be used to detect the water temperature present and very useful in forecasting the potential of glacial lake formation by melting ice and snow (Wessels *et al.* 2002).

2.7 Glacier and Glacial Lake Inventory

An inventory of glaciers and glacial lakes in the study area should be created as a baseline, to measure the change in area and volume over time (Kargel *et al.* 2005). Digital classification of multispectral images is not recommended for glacial lake boundary detection, however, manual interpretation with the use of stereo photography, is recommended. The GLIMS consortium handles the glacier database from all around the globe at the National Snow and Ice Data Center (NSIDC) in Boulder, Colorado (Raup *et al.* 2007). The Himalayan glaciers fall under regional center 12 of GLIMS to which the researcher herein is associated. The GLIMS database has an inventory of more than 180,000 ASTER images over glaciers by February 2008. However, ASTER data availability in the future is uncertain, because of the problem in SWIR ASTER sensor.

2.8 Glacial Lake Outburst Floods

Glacier Lake Outburst Flood (GLOF) is a catastrophic discharge of large volume of water, by breaking the moraine dammed lakes (Yamada and Sharma 1992). Glacier lake formation is due to melting of glacier ice and snow, which is a regular event in high mountains and Himalayan regions at an altitude of 4,500 – 5,500m (Kattelmann 2003). Outbursts of such glacier lakes in different parts of the world have repeatedly caused loss of human lives as well as severely damaging cropland and property (Clague and Evans 2000, Richardson and Reynolds 2000). Consequently, due to the high rate of glacier melting, the threat of glacial lake outburst in high mountain range is severe (Huggel *et al.* 2002). Rapidly advancing glaciers around the melt water path can block the water, thereby temporarily forming a new glacier lake, where as various natural phenomenon

like avalanche; can be one of the causes of outburst (Clague and Evans 2000), earthquake or even the weight of water itself breaking the moraine dams.

There is record on GLOFs event that have occurred since the 1960 in the Arun and Sunkoshi river basins in the Nepal Himalayas (LIGG/WECS/NEA 1988) and is known for thirteen times. Similarly, minimum of 5 GLOFs event have occurred in the Bhutan Himalayas (Iwata *et. al.* 2002), suggesting that the repetition of similar types of disasters in the Himalayan area is likely to continue. The world is experiencing global warming, and the Himalayan region is experiencing the most, which can be seen by a rapid melting of Himalayan glaciers (Fujita *et al.* 2001). At the end of studies conducted by ICIMOD on glacial lakes, they found about 3,252 glaciers and 2,323 glacial lakes in Nepal, (Mool *et al.* 2001) and 20 of them were listed as dangerous, and could cause GLOF hazards in future and continuous monitoring of those lakes was suggested (Mool *et al,* 2001).

One of the potentially dangerous glacial lakes, Imja Glacial Lake, situated at the base of Imja glacier collects huge amount of melting water from two other connected glacier Ambulapcha and Lhotse Shar glacier, in addition to Imja glacier. The volume of water measured in 1992 and 2002 is presented in (0).

Table 2.1 Volume of Water in Imja Lake

Measurement	**April-1992**	**April-2002**
Average depth (m)	47	41.6
Maximum depth (m)	99	90.5
Area (×106 m^2)	0.6	0.86
Stored water (×109 m^3)	28	35.8

Source: Yamanda 1998 & Fujita 2009

Researchers have used many different approaches to study the formation of such lakes and the consequences behind their formation. Some of the sophisticated methods used in studying the characteristics of such catastrophic lakes include the use of photographs from field, field work, satellite images, topographic maps and *in situ* methods (Yamada 1989; Bolch et al. 2011a). Since, the human reach in such mountainous terrain where such lakes form is very rare, its change detection study in regular interval is possible only with satellite images.

2.9 Glacier Change and Vulnerability

Changes in glacier dynamics can bring vulnerability in high mountain areas. The development of glacial lakes can cause the threat of potential GLOF events in downstream settlements and can change the availability and distribution of water resources in the watershed area as well as impacting the drainage system. In an effort to recognize the probability of future GLOF's in the Nepalese Himalayas, ICIMOD and other researchers have studied the impact of the GLOF (Bajracharya *et al.* 2007).

2.10 Temperature Studies with Satellite Images

IPCC (2001) claims glacier retreat around the world occurred during the 20th century, as the global mean annual temperature increased dramatically and these effects were still experienced till the end of the century. Since, there has been a decrease in precipitation from the 1940s the cause for melting of Himalayan glaciers has been documented to be associated with global warming (Ageta and Higuchi 1984). *In-situ* measurement on glacier melt requires a huge amount of time, resources, and manual labor. Theories have been developed to facilitate understanding the causes of glacier

melting from the temperature rise. Temperature increase in upper elevation and low precipitation rate definitely reduces accumulation, as Himalayan glaciers are summer accumulation type. Climatic stations around remote glaciated terrain rarely exist and in most parts there are absences of them. Climatic data around the glacier helps to understand relation between temperature increase and glacier melt. Where climatic stations are absent, temperature records from satellite image such as MODIS LST, AVHRR (Advanced Very High Resolution Radiometer) over large area provides reliable data continuously. Studies have been performed using MODIS LST data for the generation of temperature records.

Qin *et al.* (2009) used Moderate Resolution Imaging Spectroradiometer (MODIS) monthly averaged land surface temperature (LST) product for studying the warming trend over the change in elevations throughout the Tibetan Plateau (TP). Qin *et al.*(2009) used MODIS product as the meteorological stations were unavailable above 4,800m, and very few meteorological stations in western Tibetan Plateau. Qin *et al.* (2009) research validated the MODIS LST trend with the trend of near-surface air temperatures measured at meteorological stations from China Meteorological Administration (CMA). This validation helped the researchers to conclude that the higher elevations were experiencing increased temperatures. The results of Qin's study indicated the warming rate increased from 3,000 to 4,800m ASL and then remained fairly constant with fewer drops in temperature towards the highest elevation (Qin *et al.* 2009).

2.11 Glacier Studies in Nepal

Glacier studies in Nepal started in the beginning of 1970, to assess the rate of glacier melt (Higuchi 1976). In 1970, Nepal and Japan launched a joint research project

for studying the glaciers in Nepal Himalayan region, which is considered as the first known First Glaciological Expedition of Nepal (Higuchi 1976, 1977, 1979, 1980; Yamada *et al.* 1993). This joint research performed Topographic surveys, estimation of mass balance of various glaciers, photogrammetric studies of various glacier regions Dhaulagiri, Langtang, Khumbu, Kanchanjunga and Shorang Himal Region (Higuchi 1980; Yamada *et al.*1993).

2.11.1 Dhaulagiri Region

One of the most studied glaciers in Dhaulagiri region is Rika Samba. It was first studied in 1974 and according to that study, the location for this glacier is 28°50'N, 83°30'E (Nakawo *et al.*1976). In the year 1994 - 1998, several studies have been repeated for Rika Samba evaluating with other six glaciers in this region (Fujita *et al.* 2001). The glacier retreated 200m within 1974-1998 periods, a study conducted by Fujita *et al.* 1997. It was concluded that the melting of glacier occurred in similar ratio within the Dhaulagiri regions.

2.11.2 Langtang Region

Glaciers in this region were not studied until late 1982. Yala and Lirung are the two glaciers mostly studied in this region. Later both traditional and photogrammetric methods of estimating mass balance were studied (Thomas and Rai 2005). Later, within Langtang region, more glaciers were studied in 1987, 1989, 1994, and 1996 (Fujita *et al.*1998). The glacier retreat in this region was documented through photographs; however the study did not find a great change in surface lowering.

2.11.3 Khumbu Region

Glaciers in Khumbu region are mostly studied because of its nature of complex topographic terrain and densely glaciated in whole country, Nepal. Most of the early studies were based on the study of position of glacier tongue. There was significant melting of glacier recorded within 1960 - 1975 Higuchi *et al.* (1978). Fushimi and Orate (1980) found most of the glaciers were retreating based on glacier snout. Out of 15 glaciers studied in this region, they found eight of them retreating, three of them were advancing, three were found to be stationary with negligible change and one showed very irregular pattern of advance and retreat (Yamada *et al.* 1993). Because the Khumbu region is very densely glaciated region, a study from Yamada *et al*. (1993) estimated evaluated seven glaciers in the Khumbu region from 1970 – 1989, and the majority of these glaciers retreated in snout position from 30-60m within this study period.

2.11.4 Kanchanjunga Region

Morphological changes were found in Kanchanjunga region from the aerial photo interpretation and field study Asahi and Watanabe (2001). This clearly showed a variation in glacier growth. They found 57 glaciers in 1958; when compared to 1992 aerial photo, almost 50% of glacier were found to be retreated completely with no existence, 38% remained unchanged and only 12% advancement. This made a conclusion glaciers in this region started to retreat in 20th century.

2.11.5 Shorong Himal

Shorang Himal was divided into three individual glaciers in the Dudh Koshi basin as AX000, AX010, and AX030 (Yamada *et al*. 1993). Out of these three, AX010 has

been highly studied. AX000 has two glacier snouts in 1978 whereas in 1989 there was only one clear snout, and concluded that the terminus retreated approximately by 160m (Yamada *et al*.1993). Mass balance in glacier AX010 were studied from 1996-1999 and in all years it was found to have negative mass balance indicating glacial mass loss due to melting of glacier.

This chapter provided the knowledge on mass balance data gaps in Himalayas. Mass balance of glaciers is extremely important to forecast future water supply, future vulnerability in mountains. The regular monitoring can be done with geodetic method producing accurate results. Chapter 3 discusses about the data requirement, technique and research methods applied in this study.

CHAPTER III

RESEARCH METHODOLOGY

This chapter will discuss about the geodetic method of mass balance estimation of major glaciers that were studied within the SNP area. The data, methods, statistical tests conducted, and detail processes involved during Digital Elevation Models (DEMs) creation using PCI Geomatica 2012 software will be discussed.

3.1 To Estimate Mass Balance of Major glaciers in the Himalayas Using Remote Sensing Techniques

The geodetic method of mass balance calculation (Figure 3.1) uses elevation change at pixel level from at least two DEMs of different times (dh/dt) to determine surface depth changes (Bamber and Rivera 2007; Racoviteanu *et al.* 2008b). The aforementioned dh and dt represent change in elevation and change in time respectively providing change in glacier thickness over time. An elevation difference (dh/dt) per pixel is multiplied by the pixel area to ascertain the volume changes of that pixel, resulting (dv/dt). Where, dv represents change in volume with respect to change in time (dt). The volumetric changes are multiplied by density of snow (generally considered as 900 kg. m-3) which provides the mass balance change. The change is divided by the density of water 1,000 kg/m3 to compare with the water volume, usually expressed as meter water equivalent ($m.w.e.a^{-1}$). Rabatel et al. (2005), found a very good relationship between in-situ data and result from geodetic method.

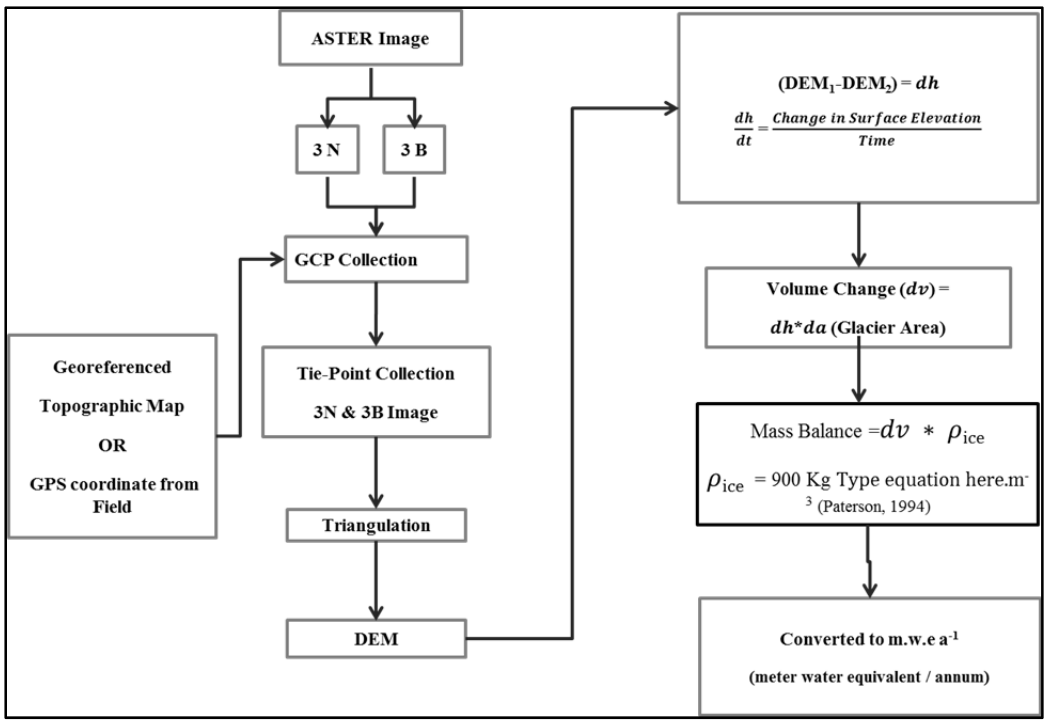

Figure 3.1 Flow Chart for Calculating Mass Balance of Glaciers using Geodetic Method

To calculate glacier mass balance using remote sensing method, multi-temporal DEMs are required (Bolch et al. 2011a; Berthier et al. 2007; Kobelt et al. 2010; Racoviteanu et al. 2008). Satellites which have sensors for acquiring stereo pair image such as ASTER, SPOT5, IRS-1C, and CORONA KH-4, KH 4A, and KH 4B satellites are predominantly employed for generating DEMs. The detail and accuracy of the final DEM differs based on the satellite's spatial resolution, Ground Control Points (GCPs), and other external parameters.

Himalayan glaciers are summer accumulation types which have higher precipitation in summer than in winter. Hence, accumulation as well as ablation takes place from May until mid-September (Ageta and Higuchi 1984; Benn and Owen 2002).

Thus, images captured toward the end of September months are optimal for mass balance analysis purposes. Because the end of September is recognized as the end of the hydrological year, a time period where significant glacier melt has occurred and also transitional period awaiting new snowfall (http://academic.emporia.edu/aberjame/gage/glacier7.htm).

ASTER images were purchased from Earth Remote Sensing Data Analysis Center (ERSDAC), Japan (https://ims.aster.ersdac.jspacesystems.or.jp). However, due to the unavailability of images during the month of late September in ASTER's archive, near ablation period images were used (Table 3.1).

Table 3.1 ASTER Images used for this Study and DEM Characteristics

Observation Date	Sensor	Image Identification	Spatial Resolution (m)	DEM Resolution (m)
21-Nov-02	ASTER	ASTL1A_021121050034021207070 7B	15	15
23-Oct-03	ASTER	ASTL1A_031023045929031105056 3B	15	15
10-Nov-04	ASTER	ASTL1A_041110045819041121013 1B	15	15
13-Nov-05	ASTER	ASTL1A_051113045841051119011 1B	15	15
7-Feb-08	ASTER	ASTL1A_080207045935090301060 8B	15	15
2-Nov-10	ASTER	ASTL1A_101102050508101104051 7B	15	15

ASTER is an advanced multispectral imager capable of collecting stereo images launched on National Aeronautics and Space Administration's (NASA's) Terra satellite sensor by NASA and Japan's Ministry of Economy in December of 1999. It is capable of acquiring land surface temperature, reflection, emissivity and stereo images for elevation measurement. A single image nearly covers ground area of 60km by 60km (Hirano et al. 2003). The purchased images came in a bundle and each layer was extracted to an individual image layer using ERDAS 10.0 software. Each extracted layer was

georeferenced to WGS84 datum UTM projection and UTM Zone 45. ASTER has 14 bands in its three subsystems Very-Near Infrared (VNIR), Short Wave Infrared (SWIR) and Thermal Infrared (TIR) (Table 3.2). Bands 3N and 3B in the NIR wavelength range from 0.78 to 0.86 µm records stereo information using Nadir and after-looking telescopes (Hirano et al. 2003). Along-track stereo-pair with base to height ratio (B/H) of nearly 0.6 is capable of producing DEMs (Toutin 2008; Bolch et al. 2011a; Racoviteanu et al. 2008a). The ASTER sensor stopped operating 6 SWIR bands during April of 2008. The original data values of the ground feature is stored in Level-1A (L1A) ASTER image. Once the L1A image is processed for radiometric and geometric correction depending on the cloud coverage, it is called L1B level data

Table 3.2 Characteristics of ASTER Sensor Systems

Subsystem	Band No.	Spectral Range (µm)	Spatial Resolution, m	Quantization Levels
VNIR	1	0.52-0.60	15	8 bits
	2	0.63-0.69		
	3N	0.78-0.86		
	3B	0.78-0.86		
SWIR	4	1.60-1.70	30	8 bits
	5	2.145-2.185		
	6	2.185-2.225		
	7	2.235-2.285		
	8	2.295-2.365		
	9	2.360-2.430		
TIR	10	8.125-8.475	90	12 bits
	11	8.475-8.825		
	12	8.925-9.275		
	13	10.25-10.95		
	14	10.95-11.65		

. Source: ASTER User Handbook Version 2

3.1.1 DEM Creation

Creating a DEM from stereo pair images employing geodetic software is a straightforward process. However, it can be time consuming in collecting accurate tie

points in stereo-pair images. A tie point is a mark representing same ground features in more than two overlapping images (Figure 3.4). The selection of representative tie points over image area describing different terrain to georeference as well normalize the error during intermediate products such as epipolar images and DEMs itself.

ASTER Level 1A data consisting of bands 3N and 3B was used to generate multi-temporal DEMs (Table 3.1) using OrthoEngine extension of PCI Geomatica 2012. The band 3N refers to Nadir image and 3B refers to the backward image. First, the same pixel on both images was identified, and a mark with a tie point in the 3N image. Another tie point representing the same feature on the 3B image was identified (Figure 3.4) and a tie point is placed. Theses tie points assisted in orienting stereo-pair images and defining epipolar geometry for individual images during the DEM extraction process (Figure 3.2).

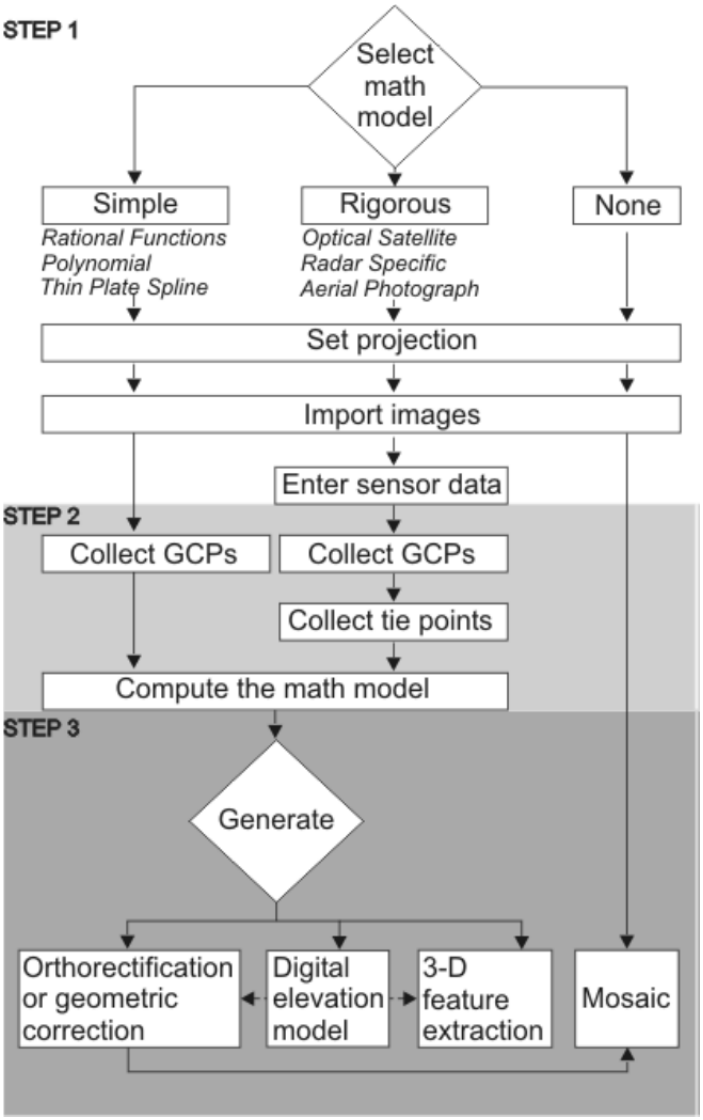

Figure 3.2 Flow Chart in PCI Geomatica Software

Source: PCI Geomatica OrthoEngine Manual

The four DEMs prepared for analysis 2002, 2005, 2008, and 2010 were georeferenced automatically to 30 meter AGDEM v2 during DEM extraction process in PCI Geomatica software. ASTER 2002 image was the earliest image located in ASTER archive, and was treated as the reference DEM. The path and row of the ASTER image for every year being different, individual ASTER images covered different areas (Figure

3.3). DEMs were clipped to outline covering glaciers within SNP area fast processing and reduction of unwanted image data.

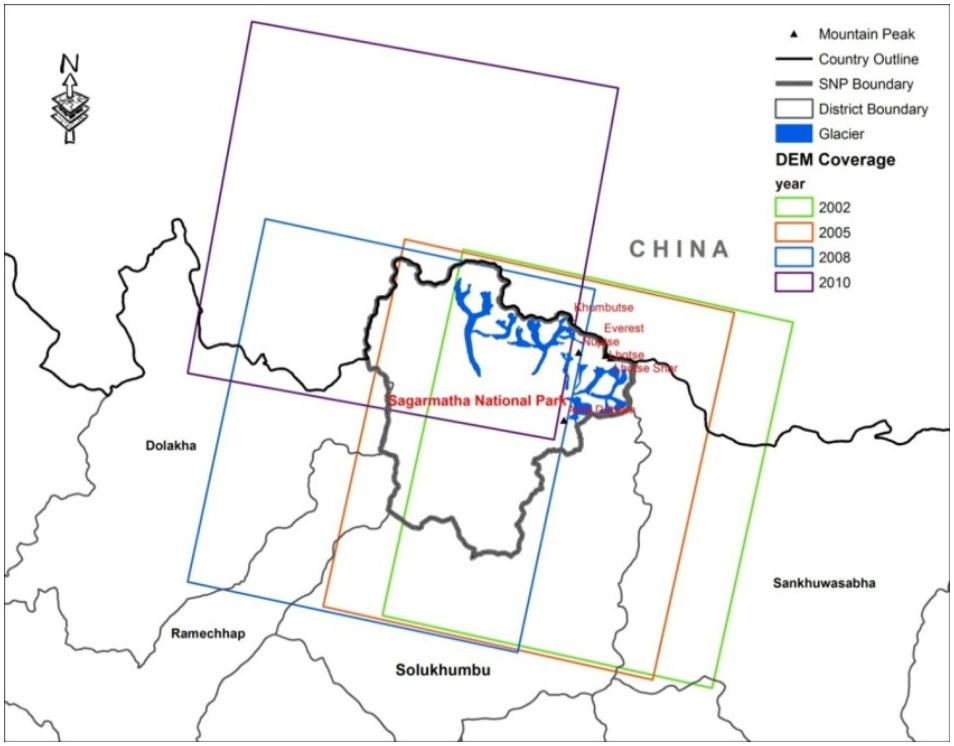

Figure 3.3 Portion Covered by Individual Year ASTER DEM of The Study Area Presenting Major Glaciers, SNP

In the absence of GCP a relative DEMs with the help of only tie points can be generated. Hence, relative DEMs above mean sea level (a.m.s.l.) were generated using 90 well distributed tie-points throughout the image in each individual year.

Images as well as elevations of their tie points ascertained from the ASTER satellite were georeferenced to NASA's AGDEM v2, 30m pixel size during the process of tie point collection.

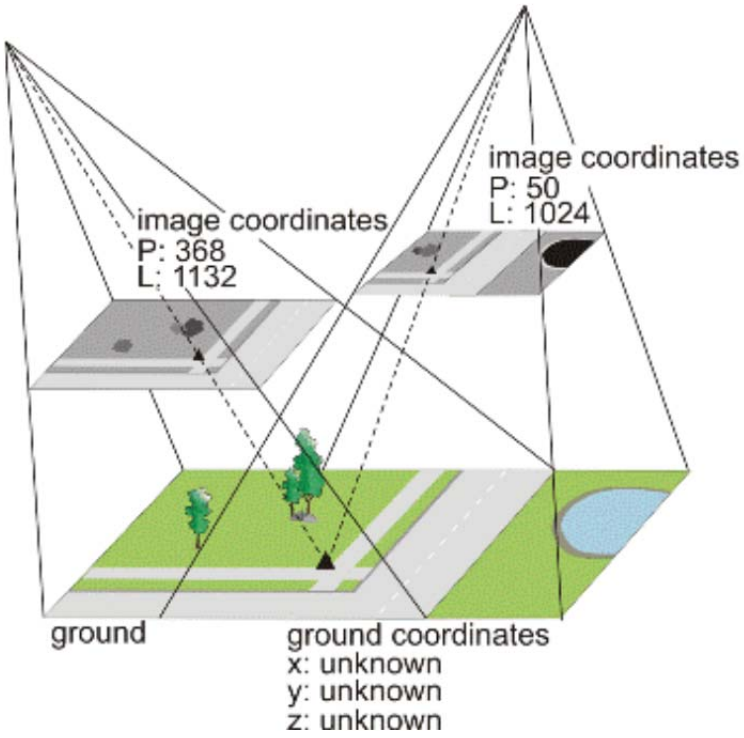

Figure 3.4 How Tie Point is represented in Stereo Pair Images

Source: PCI Geomatica manual 2012

While collecting tie-points, features such as road intersections, bridge and mountain peaks were given priorities as they are not rapidly changed in the ground unless some natural disaster washes them away. Elevation information from shadow cast area could introduce inaccuracy measurements. To limit the aforementioned inaccuracies, glaciated areas, and clouded areas, shaded and snow covered areas were completely excluded in tie point collection process, as these areas have high degrees of variation in elevation and could introduce outliers in the generated DEMs.

Once tie-points were collected, epipolar images were generated. During epipolar image creation (Figure 3.5) the software orients images in such a way that the left and right images have same coordinate system (PCI Geomatica manual, 2012).

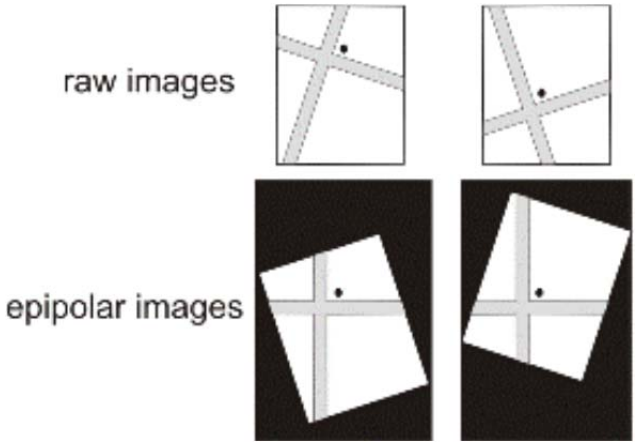

Figure 3.5 Epipolar Generation

Source: PCI Geomatica manual 2012

DEM was generated once epipolar images were processed and final DEMs were georeferenced to UTM Projection (Universal Transverse Mercator) and UTM Zone 45, and mean sea level altitude as reference datum. The DEMs were filled to remove any sinks; depression pixels. However, due to the very steep slopes and numerous mountain peaks within a small area, DEM still showed some data gaps in shaded, steep slopes, and snow-covered areas. Those areas had values tremendously different than neighboring pixels and such areas were identified and excluded in mass balance analyses.

3.1.2 Estimating Surface Elevation Change

DEM differencing from later images to earlier ones provide surface elevation changes; however, this accounts for entire pixels in the image. Though pixels under shadow, clouds and glaciated areas were excluded in tie point collection, still some pixels in high rough terrain resulted in high elevation difference. Considering such inaccuracies that could occur from pixels differencing, concept of random points generation within non-glaciated and glaciated area was applied. The corresponding pixel value was

extracted using "Extract Multi Values to Points" from overlapping DEMs using ArcGIS 10.0. Surface elevation profile at various sections in accumulation and ablation area for each glacier at various transects was studied to estimate the thinning of glacier surfaces.

3.1.3 Digitizing glacier Boundary

Glacier area of different times informs the viewer of change in accumulation and ablation as well as the change in position of glacier tongue. To acquire physical information about the study area and the glacier characteristics, the available large scale Topographic Maps published by Department of Survey (DoS), Nepal of scale 1:50,000 were purchased (Table 3.3). These maps were digitally scanned and georeferenced to the datum and projection information provided in topographic map using ERDAS Imagine 2010 software.

Table 3.3 List of 1:50,000 Scale Topographic Maps Covering SNP area

Sheet Numbers of Purchased Topographic Maps of SNP Area, Nepal			
2786 03	2786 04	2787 01	2787 06
2786 07	2786 08	2787 02	2787 09
2786 15	2786 16	2787 05	2787 10

Table 3.4 Projection Information Used to Georeference Aforementioned Topographic Maps

Spheroid	Everest 1830
Projection	Modified Universal Transverse Mercator
Origin	Longitude 870° East, Latitude 00° North
False coordinate of origin	500000m Easting; 0m Northing
Scale factor at Central	0.9999

The glacier boundary digitized from topographic maps were revised with individual year ASTER images in False Color Composite 5, 4, 2, and modified where required. Individual years had separate glacier boundaries as changes in snow area and volume occurred in later years.

3.1.4 Elevation Difference by Using Random Points

In the digitized non-glaciated and glaciated area random points were generated at distances of 21.22m; the hypotenuse of 15m X 15m square pixels. The distance was chosen such that no two random points lie within a same pixel. The random points were used to extract elevation values from individual DEM pixels. ASTER 2002 image was the earliest image ascertained for ASTER archive, therefore, the 2002 DEM was considered as reference or master DEM. The results of the study compared the elevation differences of random points in non-glaciated ice free terrain, which is supposed to be constant unless changes occurred due to natural disaster. However, complex topographic and terrain nature of the SNP area high elevation differences were examined.

3.1.5 DEM Accuracy Test

The vertical elevation of master DEM was also compared with the elevation of 1:50,000 topographic maps published by Survey Department of Nepal in 1997, based on 65 well distributed control points in a non-glaciated area. The topographic map was prepared from 1:50,000 aerial photographs taken in 1992 that were field verified in 1996. Relative uncertainties were calculated in non-glaciated terrain using equations 1 and 2. The uncertainty (e) for such rugged, high terrain study area is statistically significant.

$$SE = \frac{\text{STDV non-glacier}}{\sqrt{n}} \quad (3.1)$$

$$e=\sqrt{(SE)^2+(MED)^2} \quad (3.2)$$

Where,

SE = Standard Error

STDV= Standard Deviation

MED = Mean Elevation Difference

n = Number of included pixels in

e = uncertainty

Standard Error of mean, Uncertainty tests and T-test were conducted between the DEM and topographic map to determine the significance of data. The generated DEMs were compared with 30m resolution ASTER Global Digital Elevation Model (GDEM) ver. 2 (NASA, USA and METI, Japan) in non-glaciated area to see the correlation of elevation points. The created DEMs were resampled to 30m resolution using Nearest Neighborhood technique to match AGDEM pixel size. The profile of the surface elevation from generated DEM compared with AGDEM showed limited changes in non-glaciated areas.

To normalize the differences elevation, individual DEM values of non-glaciated areas were compared with ice free terrain values of a master DEM using regression analysis employing SPSS 21.0 software and regression coefficients were obtained (Table 3.5). 2005 and 2008 random points elevation values from non-glaciated were regressed with 2002 non-glaciated values with 95% confidence intervals. The regression coefficient was obtained that would assist in the normalization of the non-glaciated terrain of 2005 and 2008 with 2002 data.

Table 3.5 Regression Coefficient

Years	α	β
2005-2002	-8.72	0.999
2010-2008	2.695	0.999

The regression coefficient was applied to the old glacier surface to ascertain the new regressed elevation values for individual year glacier surfaces. The elevation values of master DEM subtracted from new glacier surface provided the change in surface elevation at that particular random point. Elevation values within 5th and 95th percentiles were considered in the analysis. Separate statistical calculations for uncertainty of the elevation difference in glacier and non-glacier areas were computed using the standard error of the mean (SE) as calculated by Bolch et al. (2011a).

$$SE_{glacier} = \frac{STDV_{non-glacier}}{\sqrt{n}} \quad (3.3)$$

Where,

$STDV_{non-glacier}$ = Standard Deviation of non-glaciated pixel

n = number of pixels considered for calculation.

Another way of estimating the uncertainty according to law of error propagation, e, as computed by Bolch et al. (2012a) was analyzed:

$$e = \sqrt{(\mathrm{SE})^2 + (\mathrm{MED})^2} \quad (3.4)$$

Where,

SE = Standard Error

MED = Mean Elevation Difference

3.1.6 Volume Change and Mass Balance Calculation

Volume change was computed for each glacier as the product of individual area of the glaciers and the mean elevation difference. The volume change multiplied by the density of ice, generally considered 900 kg•m-3 provided the mass balance of glacier measured in kg•m-2 yr-1. Mass balance of individual glaciers may vary depending on area, altitude, amount of snow in accumulation and ablation area, though they are close to one another within the study area. The specific mass balance is converted to meter water equivalent unit by it dividing the density of water (1,000 kg•m-3). Hence, mass balance of individual glaciers in SNP area was estimated with standard error.

3.2 To Measure Planimetric Changes in Glacial Lake within Study Area

Imja glacier Lake (Figure 3.6) has around 28 million cubic meters of water (Yamada 1993) and in 2009, field verification by ICIMOD study team estimated 35.5 million cubic meters of water stored. If the lake's weak moraines burst, water would inundate the valley and trigger a devastating natural disaster in the downstream area by washing away communities along and below the flood path (Figure 3.7).

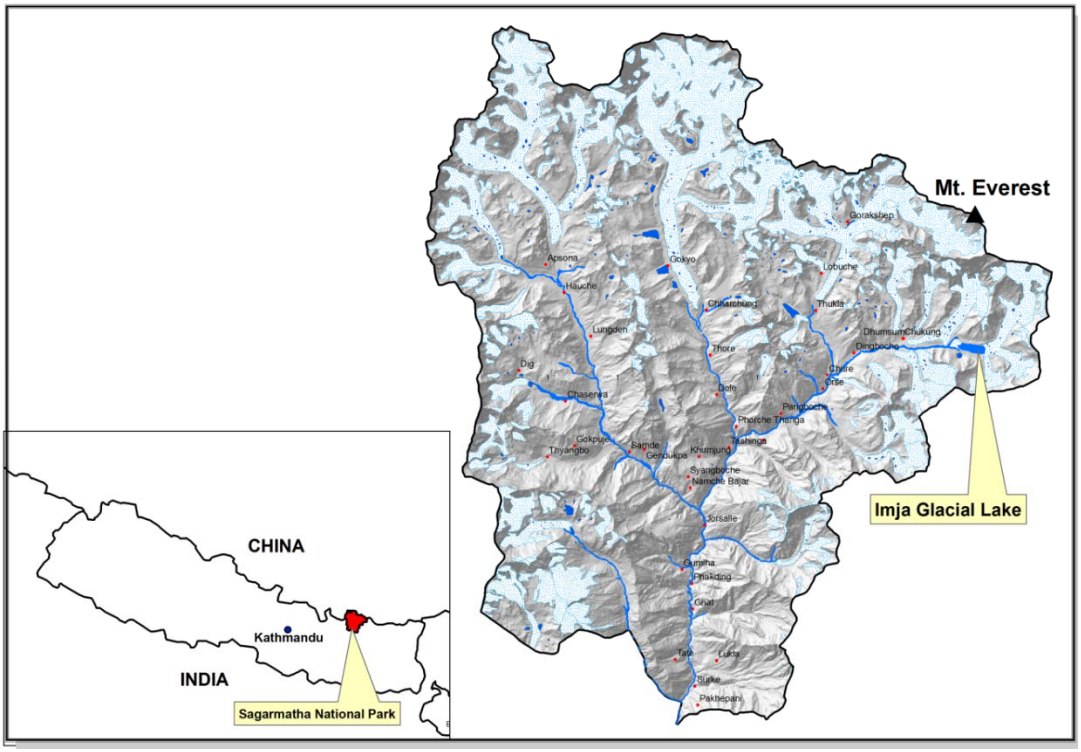

Figure 3.6 Location Map of Imja Glacial Lake, SNP

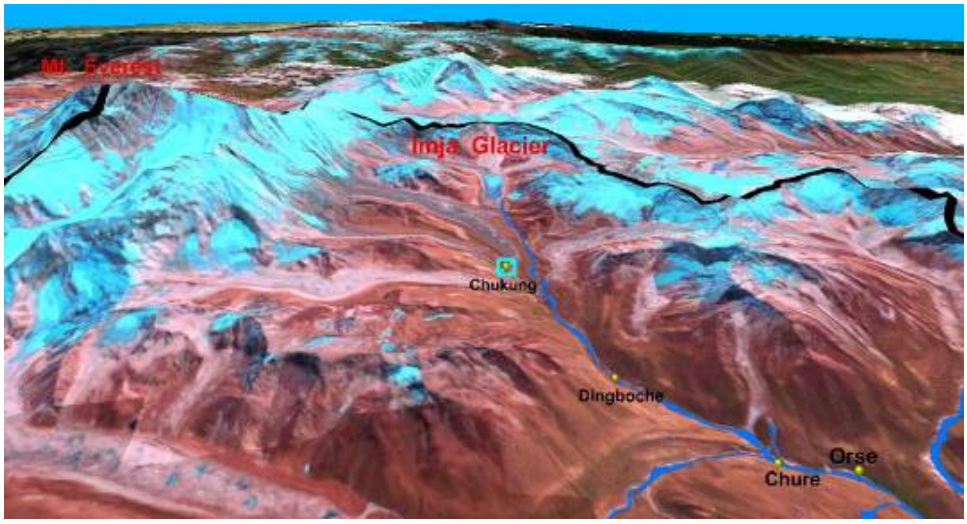

Figure 3.7 Vulnerable Settlements along Imja Khola

Source: Settlements Digitized From 1:50,000 Topographic Maps Overlaid on Top of ASTER 3D Model Prepared in ArcScene 10.0

Thus, regular monitoring can provide information preventing natural disasters and this can be done with temporal satellite images in inaccessible areas (Mool *et al.* 2002). Here, the study evaluated planimetric changes in Imja proglacial Lake using Landsat images from 1975 to 2010. Images were downloaded from USGS EROS website (http://earthexplorer.usgs.gov) and re-projected to WGS 84 UTM Zone 45N. Manual inspection of the image was performed to check any presence of clouds, shadow cast by high mountains surrounding the lake, or any other visual obstructions. Normalized Differenced Water Index (NDWI), which uses the (Near Infrared) NIR and Blue band to differentiate water bodies from other features (Huggel *et al.* 2002) in conjunction with manual delineation of the glacial was performed.

$$NDWI = \frac{B_{NIR} - B_{blue}}{B_{NIR} + B_{blue}} \quad 3.5$$

Imja glacial lake area was digitized using ArcGIS 10.0 software for different years and change in lake surface area was measured. This study method can be utilized in other inaccessible regions to monitor the formation as well analyze change in glacial lake area.

3.3 Temperature Variation using MODIS Imagery

Hence, this section of the study will emphasize the effects of temperature on glacier melting using MODIS, MOD11A2 product. MOD11A is an 8 day composite data generated from 1km MOD11A1 product stored on Sinusoidal Grid. MOD11A1 is obtained daily and mean temperature of eight day based on clear-sky image is produced. It covers an area ~1100km X 1100km and is, stored in Sinusoidal projection with a spatial resolution of 1km. There are 12 layers stored in HDF-EOS (Hierarchical Data

Format for Earth Observing System developed by NASA) data format. Each layer stores temperature of land surface at different times with its respective units along with a conversion factor to generate real data for research purposes. LST_Day_1km: 8-Day daytime 1km gird land surface temperature in Kelvin units were ascertained from this satellite and employed for this study's purpose. The pixel value in Kelvin was multiplied by a factor of 0.02 (provided by MODIS documentation) to obtain the real temperature value in Kelvin which was sequentially converted to degrees Centigrade.

A particular month contains three scenes. All images present from January to December was downloaded for 11 years spanning from 2001-2011. A subset of each image covering study area was generated and zonal statistics were extracted from all images writing a python script in ArcGIS10. Each image layer was analyzed visually to detect presence of any visual obstacles within the study area and if these anomalies were observed the scene was discarded from analysis. The temperature value was extracted using zonal statistics in ArcGIS for all eleven years and exported to Microsoft Access for further analysis. Any large negative temperature values outside the normal range was re-evaluated and considered as outliers. Time series temperature analysis graphs were prepared using maximum monthly temperature during summer months. The mean elevation time-series temperature graph is provided in Chapter 4.

CHAPTER IV

RESULTS AND DISCUSSION

Sections 4.1-4.3 of this chapter will explain the research results while fulfilling the defined objectives 1, 2, and 3 respectively, from Chapter I. As described in Chapter I, the three objectives of this study were:

1. To estimate mass balance change of major glaciers in the Sagarmatha National Park (SNP) in the Himalayas, employing remote sensing techniques for the periods 2002 and 2005, and 2002 and 2008.
2. To measure planimetric changes in Imja glacial lake, this is one of the potential lakes for Glacial Lake Outburst Floods (GLOFs) within the study area.
3. To quantify temperature variations in the study area using Moderate Resolution Imaging Spectroradiometer (MODIS), Land Surface Temperature and Emissivity 8-Day L3 Global Satellite (MOD11A2) images with 1 km resolution.

4.1 Estimation of Mass Balance of Major Glaciers

Profile A-B in non-glaciated region was compared with AGDEM v2 (Figure 4.1). However, more precise DEMs could have been prepared with field GCPs, which remains a future study validation task.

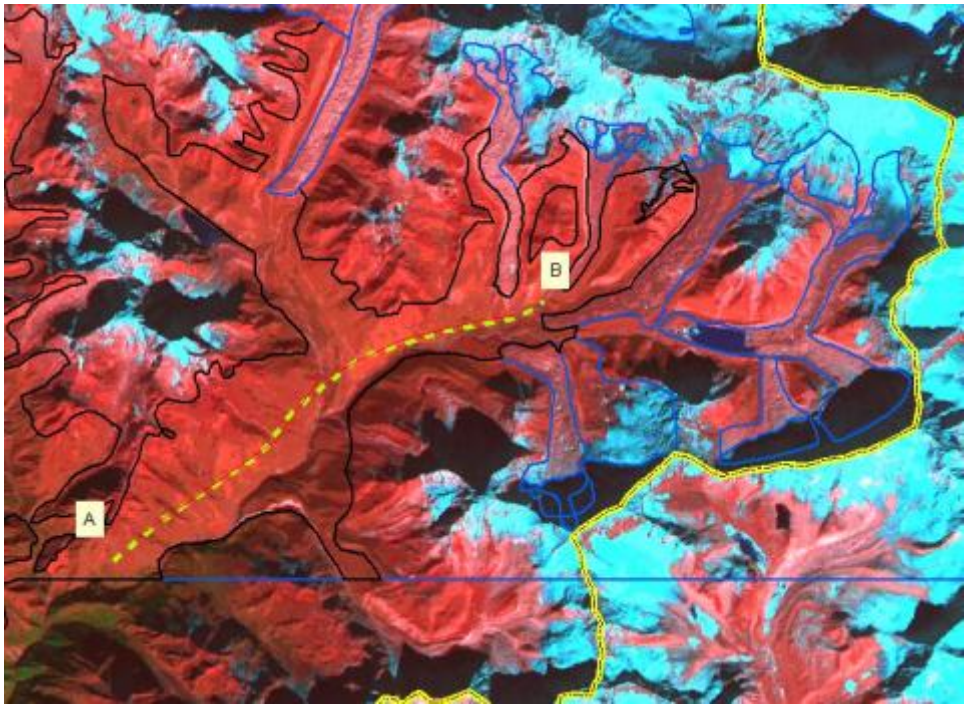

Figure 4.1 Profile A-B in non-glaciated region compared with individual DEM and AGDEM v2

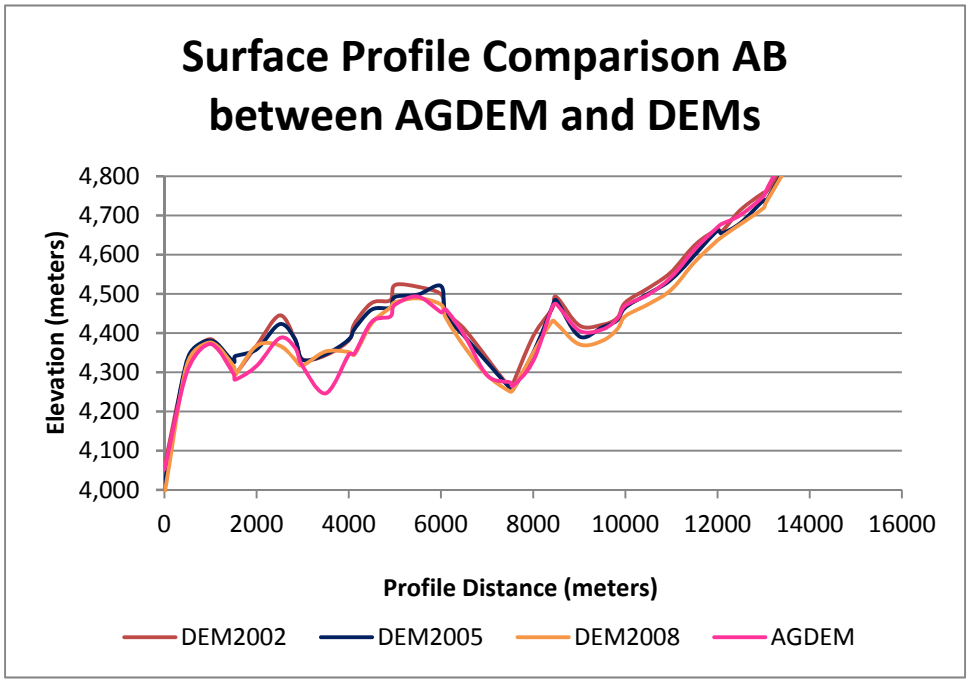

Figure 4.2 Surface Profile Comparison Between ASTER DEMs And AGDEM

The maximum elevation differences between all of the DEMs in comparison to the AGDEM produced by NASA were within acceptable ranges of other studies (Hirano et al., 2003).

The result of uncertainty tests is shown in Table 4.1.

Table 4.1 Uncertainty Calculation of Master DEM With Respect to Topographic Map

Error Analysis of 2002 DEM with respect to Topographic Map	
Number of elevation points (n)	49
Mean Elev. Difference (m)	9.79
Avg. STDV	17.15
Standard Error (SE)	2.42
Uncertainty (e)	10.08

The average standard deviation (Avg. STDV) of the non-glaciated area was ±17.15m. The STDV ±17.15m implies an overestimation of elevation for the calculated area because this technique does not utilize small glacier areas and excludes data from large surface areas (Bolch et al.2011b). Therefore, the propagation of error was employed to determine a more realistic value of uncertainty. The uncertainty, (e), had a confidence level of ±10m in glacier elevation differences.

Two independent paired t-tests were performed. Both t-tests employed the master 2002 DEM for comparisons with the mean elevations for 2005 and 2008 DEMs. The mean elevations of individual glaciated areas and non-glaciated areas for 2002 and 2005 were the first statistical paired t-test. While the second paired statistical t-test evaluated 2002 and 2008 DEMs of glaciated and non-glaciated regions. The statistical t-test results are shown in Appendix A and showed most of the glaciers in the study area and in the study period showed statistical, t-tests were significant.

Regression analysis was performed for 2005 and 2008 random points value with 2002 master DEM values in the non-glaciated area. The coefficient for linear regression "α" and "β" had very good correlation as β was ~1 for both analyses (Table 4.6).

Table 4.2 Correlation Coefficients Obtained From Regressing 2005 Point Values With Master DEM

Year	α	β
2005-2002	-13.584	1
2008-2002	12.63	0.999

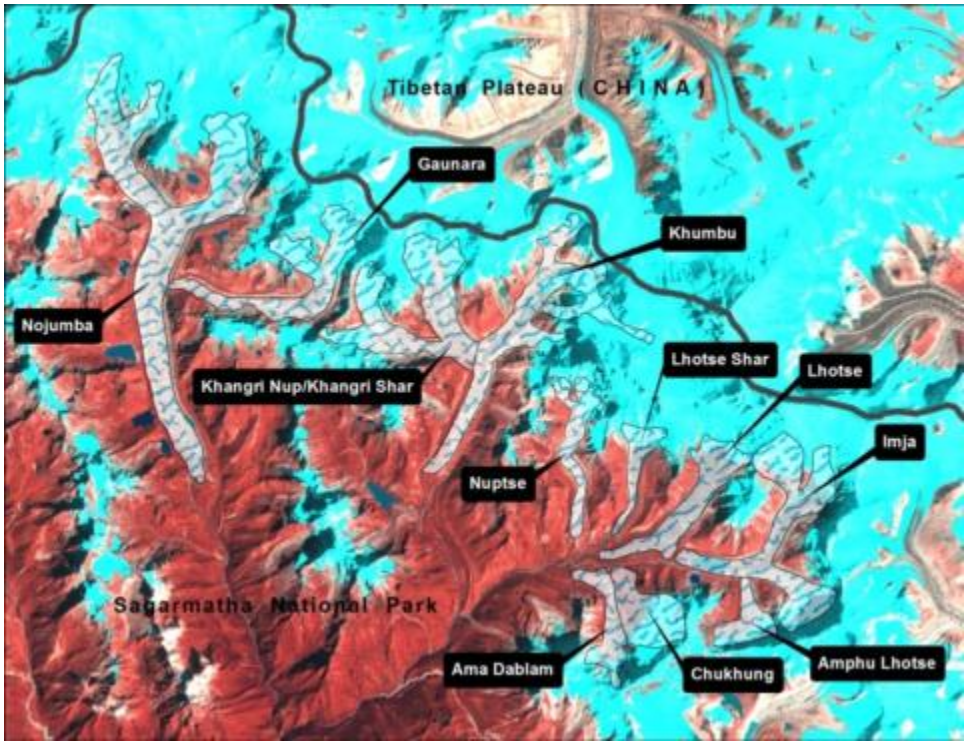

Figure 4.3 Major Glaciers Analyzed in SNP Region, Nepal

Almost all of the glaciers in their accumulation, clean ice (C-type) and ablation, debris mixed ice (D-type) region clearly indicated reduction of glacier mass during both

study periods (Table 4.3-4.8). Surface profiles along centerline and at various transects for individual glaciers were studied to evaluate internal glacier bed elevation changes over the study periods. Each glacier is described in detail, their characteristics and results.

Table 4.3 Mass Balance of Common Glaciers In 2002 and 2005 DEMs

Name	Area (sq. km)	No. of Random Points	Mean (m)	STDV	MB (m w.e.a^{-1})	SE	Uncertainty	Specific mass balance (m w.e.a^{-1})
Ama Dablam_D	3.96	271	0.35	5.49	0.11	0.6	0.75	0.10 ± 0 .61
Amphu Lhotse_D	3.24	321	-8.67	4.37	-2.61	0.6	8.71	-2.6 ± 0.56
Changri Nup Shar_D	5.99	1875	3.54	5.54	1.15	0.2	3.83	1.14 ± 0.23
Chukhung_D	6.94	748	-4.6	7.66	-1.36	0.4	4.54	-1.3 ± 0.37
Duwo_D	1.84	76	1.25	4.2	0.44	1.2	1.89	0.44 ± 1.16
Imja_D	9.52	1336	-10.59	7.39	-3.17	0.3	10.57	-3.1 ± 0.27
Imja_C	4.7	1044	-10.71	14.75	-3.47	0.3	11.57	-3.4 ± 0.31
Khumbu_D	9.42	1550	-4.98	6.26	-1.63	0.3	5.43	-1.6 ± 0.25
Khumbu_C	9.43	1388	-1.42	7.51	-0.33	0.3	1.14	-0.3 ± 0.27
Lhotse Nup_D	1.88	272	-4.35	8.77	-1.23	0.6	4.16	-1.2 ± 0.61
Lhotse Nup_C	0.86	128	-14.83	28.1	-2.85	0.9	9.54	-2.8 ± 0.89
Lhotse_D	5.69	1195	-3.34	6.85	-1.11	0.3	3.71	-1.1 ± 0.29
Lhotse_C	1.49	309	-10.24	9.73	-2.84	0.6	9.49	-2.8 ± 0.57
Nuptse_D	3.25	580	-1.72	5.2	-0.56	0.4	1.9	-0.5 ± 0.42
Nuptse_C	1.75	270	-1.55	12.91	-0.22	0.6	0.96	-0.2 ± 0.61
Gaunara_C	3.83	1290	-8.9	7.76	-1.33	0.5	8.91	-1.33 ± 0.48
Gaunara_D	5.54	1867	-5.71	9.18	-0.86	0.4	5.73	-0.85 ± 0.40
Nojumba_C	8.2	2778	0.34	31.05	0.05	0.3	0.47	0.050 ± 0.32
Nojumba_D	20.02	6724	3.08	18.73	0.46	0.2	3.09	0.462 ± 0.21
Sum/Average	69.96		-4.79		-1.31	0.5		-2.978 ± 0.89

C = Clean type; D = Debris mixed ice type; STDV = standard deviation; SE = standard Error

Table 4.4 Mass Balance of Common Glaciers in 2002 and 2008 DEMs

Mass Balance 2002-2008								
Name	Area (sq.km.)	No. of Random Points	Mean (m)	STDV	MB (m w.e.a^{-1})	SE	uncertainty	Specific mass balance (m w.e.a^{-1})
Gaunara_C	3.83	1290	-8.9	7.76	-1.33	0.5	8.91	-1.33 ± 0.48
Gaunara_D	5.54	1867	-5.71	9.18	-0.86	0.4	5.73	-0.85 ± 0.40
Khumbu_C	11.44	1867	-5.71	9.18	-0.86	0.4	5.73	-0.85 ± 0.40
Khumbu_D	18.5	6235	-20.75	7.73	-3.11	0.2	20.75	-3.11 ± 0.22
Nojumba_C	8.2	2778	0.34	31.05	0.05	0.3	0.47	0.050 ± 0.32
Nojumba_D	20.02	6724	3.08	18.73	0.46	0.2	3.09	0.462 ± 0.21
Nuptse_C	0.9	302	-124.99	185.5	-18.75	1	124.99	-18.7 ± 1.00
Nuptse_D	3.95	1332	-28.17	8.81	-4.23	0.5	28.17	-4.22 ± 0.47
Sum/Average	67.53		-6.28	13.94	-0.94	0.34		-0.94 ± 0.34

C = Clean type; D = Debris mixed ice type; STDV = standard deviation; SE = standard Error

4.1.1 Khangri Nup/Shar Glacier

Khangri Nup and Khangri Shar glaciers(Figure 4.4) are the two tributaries of Khumbu glaciers in Khumbu valley, SNP region. Average elevation of the glacier area for the individual year 2002, 2005, 2008 and 2010 from 30m ASTER DEM was determined (Figure 4.4, Table 4.5).

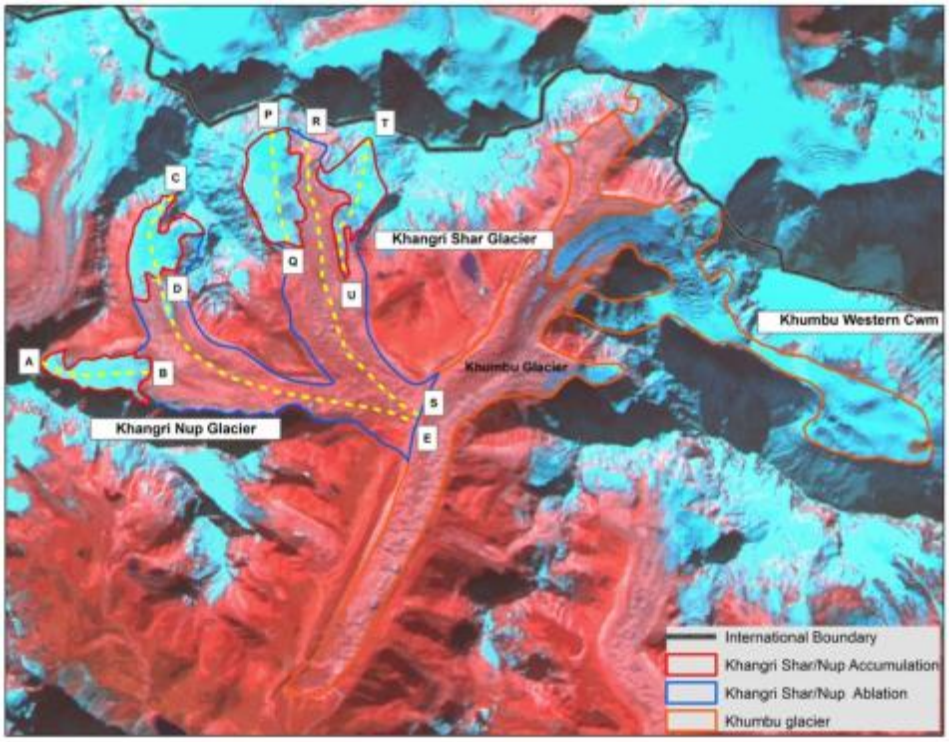

Figure 4.4 Khangri Nup/Shar Glacier Adjacent to Khumbu Glacier

Table 4.5 Mean Elevation of Khangri Nup/Shar Glacier (2002-2010)

Mean Elevation (meters)				
Year	2002	2005	2008	2010
Mean Elevation	5431.75	5427.23	5402.2	5383.83

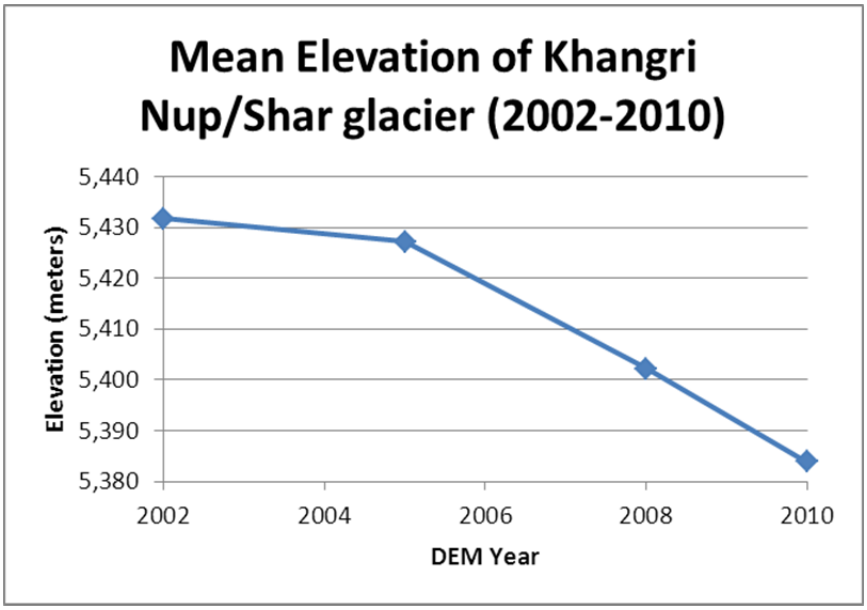

Figure 4.5 Mean Elevation of Khangri Nup/Shar Glacier

The ice and debris from these two glaciers mixes with Khumbu glacier (Figure 4.4). Khangri Nup/Shar glacier covers an area 6.939 sq. km, according to the glacier boundary digitized based on ASTER 15m resolution image. According to 1:50,000 topographic maps, the elevation of Khangri Nup/Shar glacier tongue stands at ~5160 m joining Khumbu glacier. The glacial head for Khangri Nup and Khangri Shar glaciers stands are at an elevation of ~5600m and ~5400m, respectively.

Khangri Nup/Shar glacier is greatly covered with debris in most of the ablation area. Huge rocks rolls down towards lower elevations with the flow of solid ice and snow avalanche from nearby steep high terrain slopes and peaks (Figure 4.6).

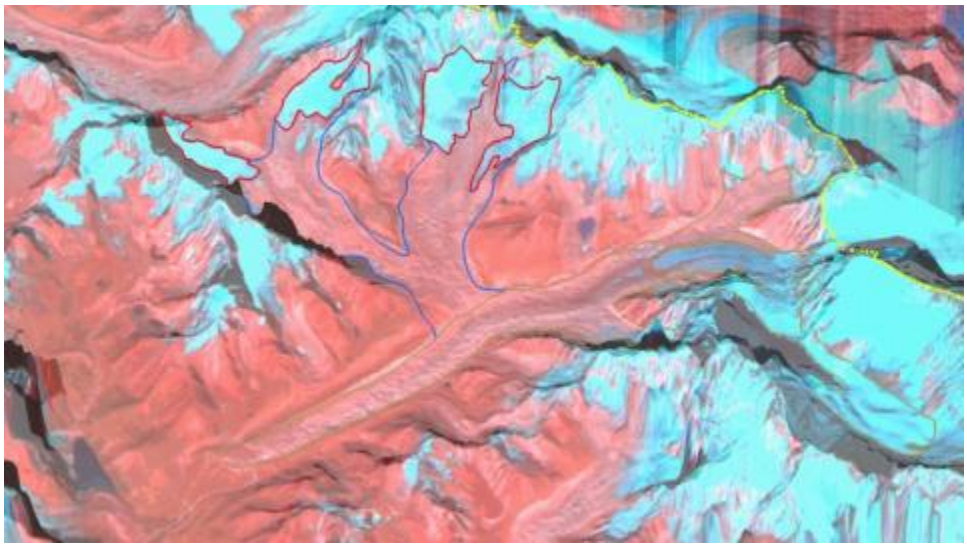

Figure 4.6 Khangri Nup/Shar Glacier

Mass balance of Khangri Nup/ Khangri Shar glacier for common DEM area of 6.939 sq. km (Figure 4.4) for the year 2002-2005 was estimated to be -0.3 ± 0.27 and -1.6 ± 0.25 m.w.e.a-1 for clean ice (accumulation area) and debris covered (ablation area), respectively.

Bolch et al. (2011a) conducted mass balance study in same area from 1970-2007 and 2002-2007 periods. They found specific mass balance of Khangri Nup/Shar glacier for DTM area covered of 6.85 sq. km. to be -0.28 ± 0.08 (m.w.e.a-1) for the period 1970-2007. Whereas, during 2002-2007 period, the mass balance for the same area was -0.29 ± 0.52 m.w.e.a-1. This aforementioned result is for combined accumulation and ablation area. However, two independent sources recorded reduction in mass balance in Khangri Nup/Shar glacier. High resolution image as well as in-situ data would augment in comparison and validation of these results.

At all cross-sections, glacier surface lowered over time clearly indicating reduction in glacier mass in Khangri Shar/Nup glacier.

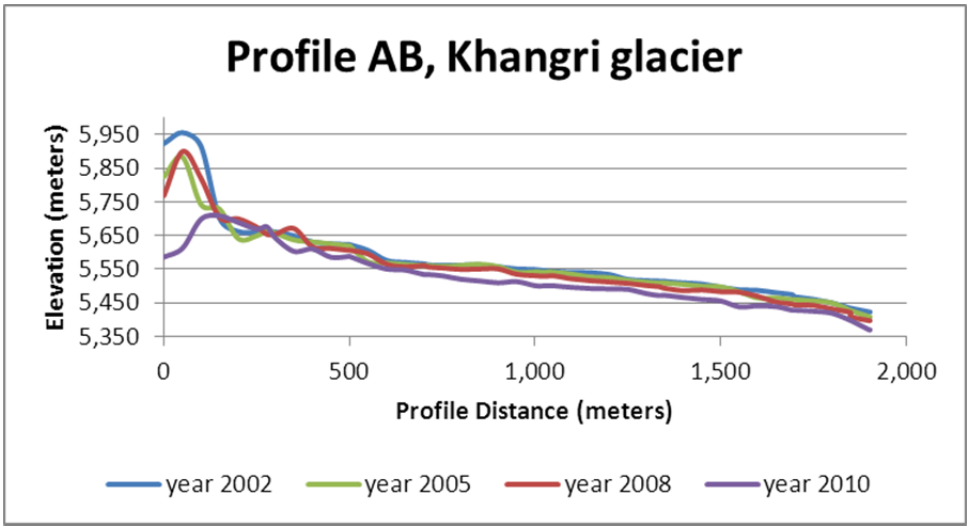

Figure 4.7 Profile AB, Khangri Glacier

The cross section AB (Figure 4.7) of Khangri Nup glacier portrays that there was lower glacier bed elevation in 2008 - 2010 than in 2002 - 2005 and 2005 - 2008 period. There was a sudden decrease in glacier elevation in the AB section from a distance of 0 – 200 m in 2010 than 2002, 2005, 2008 DEM; which could be due to DEM errors or huge ice fall which occurred in 2010. The largest elevation change between the 2008 and 2010 DEMs appeared in the 700 - 1,100 m range.

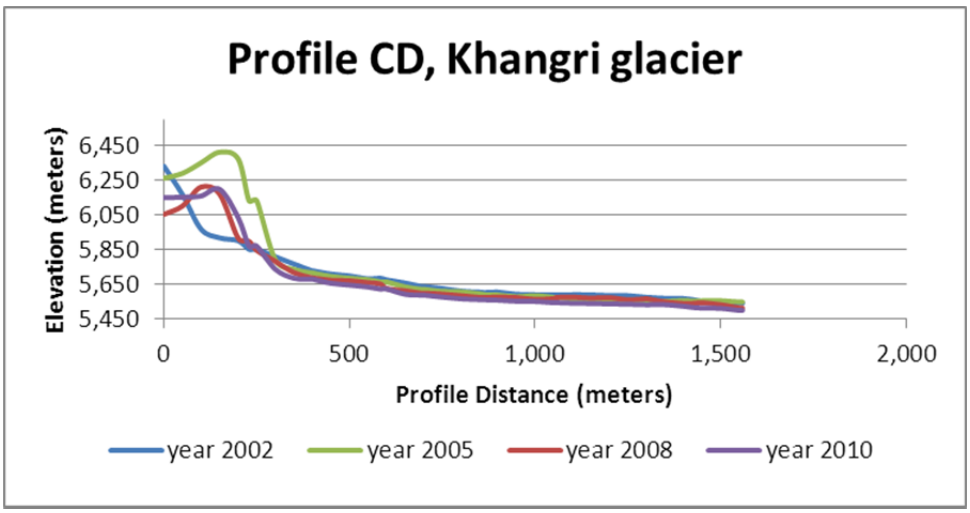

Figure 4.8 Profile CD, Khangri Glacier

The transect CD (Figure 4.8) in accumulation area in Khangri Nup glacier shows a major increase in ice mass in all calendar years after 2002 for 0-300 m section. However, towards the glacier tongue, an overall reduction in elevation was noticed. Except for 0-200 m distance of the glacier, the elevation losses were fairly steady over time.

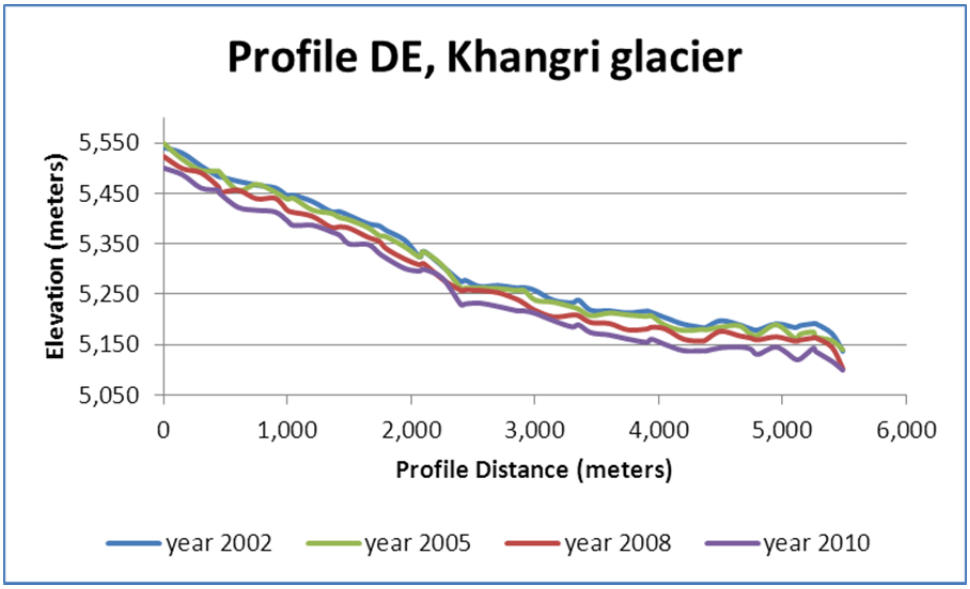

Figure 4.9 Profile DE, Khangri Glacier

The DE (Figure 4.9) transect within the ablation area of Khangri Nup glacier shows a reduction in ablation zone more towards the glacier end at point E. Elevation loss was fairly consistent with time over transect D-E of Khangri Nup glacier.

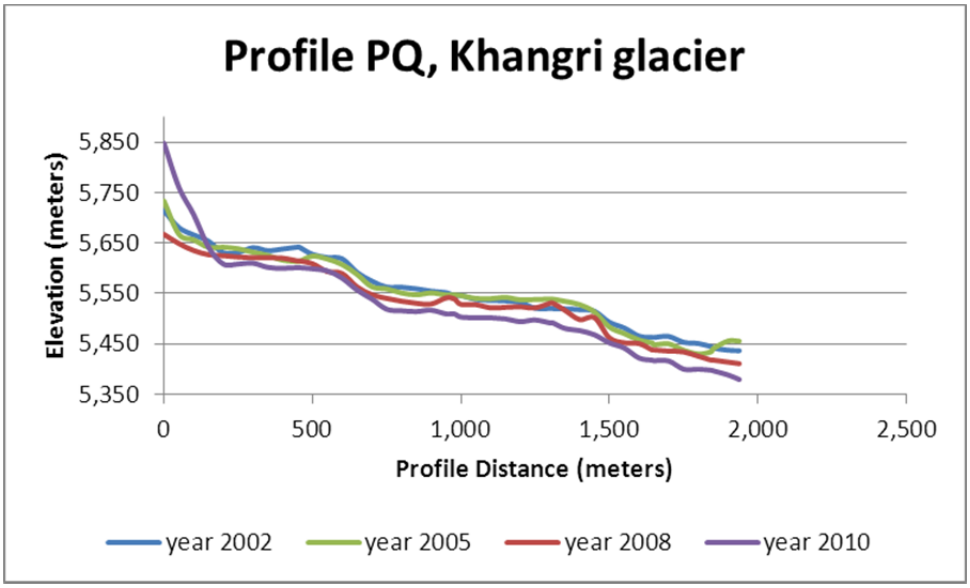

Figure 4.10 Profile PQ, Khangri Glacier

Profile PQ (Figure 4.10) of Khangri Nup glacier shows lowering surface in the accumulation area except in 2010; which might be an error caused due to poor interpolation of ground control points in DEM generation.

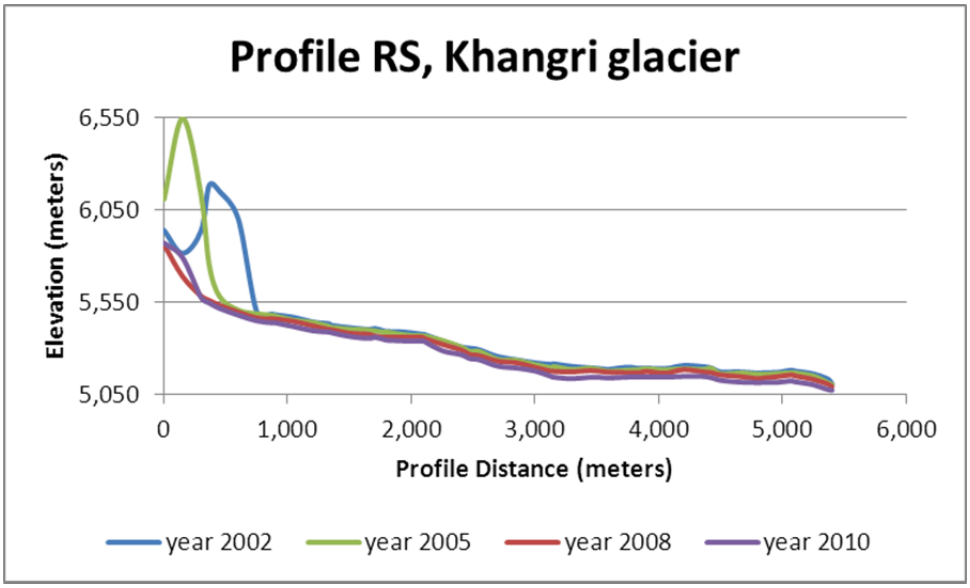

Figure 4.11 Profile RS, Khangri Glacier

Cross section RS (Figure 4.11) of Khangri Shar glacier has lesser elevation changes throughout, except for an increase in glacier mass from 2002 to 2005 in the 0-800m range. However, the aforementioned general trend of lowering glaciers remained the same for the remaining distances of the glacier.

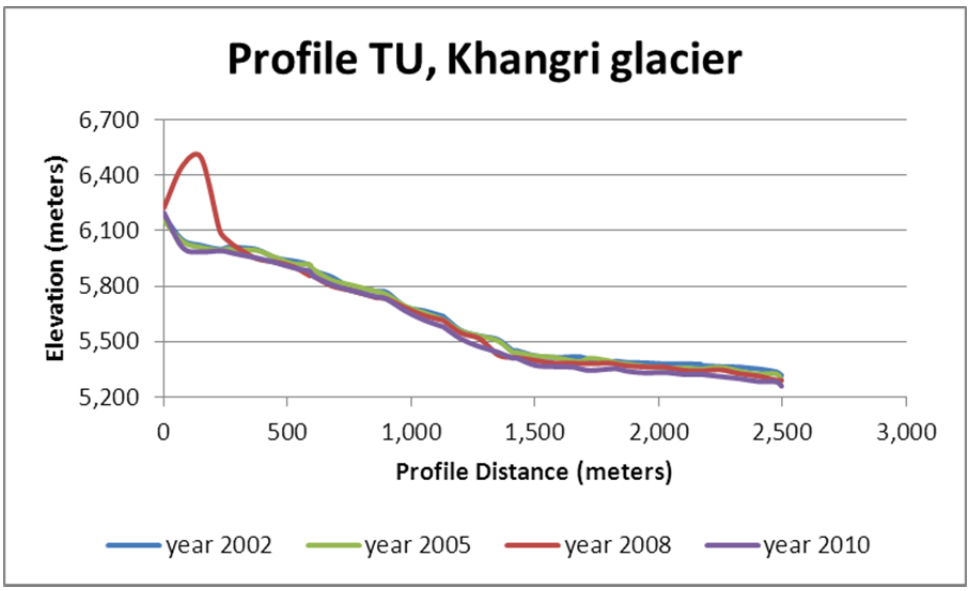

Figure 4.12 Profile TU, Khangri Glacier

Profile TU of Khangri Nup glacier (Figure 4.12) showed fairly steady reduction in glacier elevation throughout time in accumulation zone. The 2008 DEM showed an increase glacier mass from all the previous years within the 0-200m distances; however, this elevation range had a significant decrease in surface elevation in other years.

4.1.2 Khumbu Glacier

Khumbu glacier is the largest glacier in SNP region (Figure 4.13) covering an area 19 sq. km. according to glacier boundary digitized based on ASTER 15m resolution image. The glacier tongue stands at an elevation of ~4,900m and extends up to an elevation of ~7,600m at its glacial head. Khumbu glacier is at the highest elevation of the world (Wessels et al. 2002). The relief difference is almost 2,700m within 18km glacier length which makes it very high steep slope. Khumbu glacier is greatly covered with debris in most of the area because huge rocks rolls down towards lower elevation with

the flow of solid ice and snow avalanche from near-by steep high terrain slopes and peaks (Benn and Owen 2002). Khumbu glacier accumulates snow mass more in summer may till mid-September, than winter showing the characteristics of Himalayan glaciers as summer accumulation type (Benn & Owen, 2002).

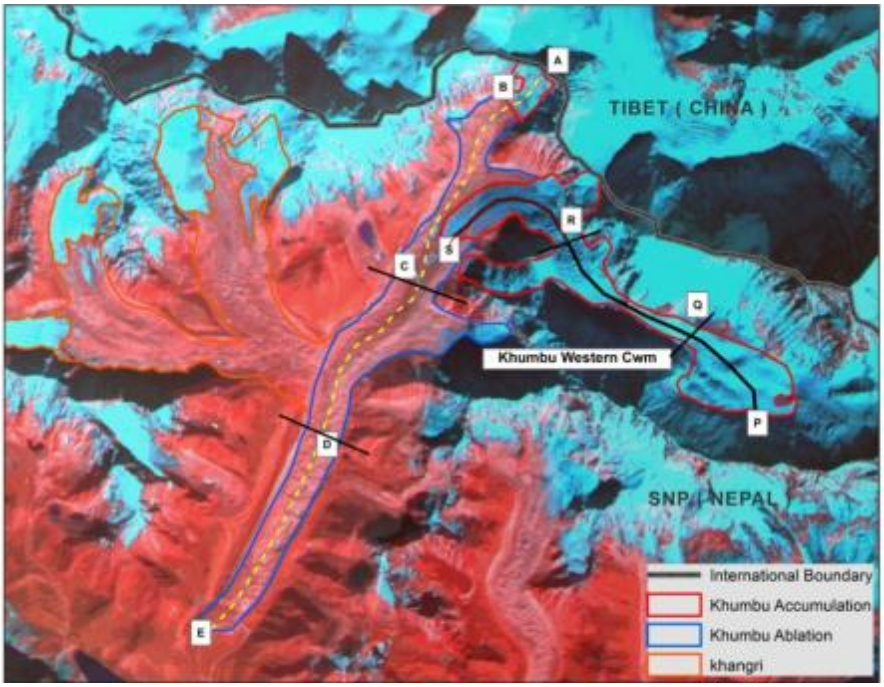

Figure 4.13 Khumbu Glacier with Western CWM Area, SNP region

The mean elevation of Khumbu glacier decreased more in 2005-2008 periods than in 2002-2005 periods (Table 4.6, Figure 4.13), based on common DEMs area on three years image.

Table 4.6 Average elevation difference of Khumbu Glacier

Mean Elevation and Mean Elevation Differences (meters)			
Year	2002	2005	2008
Mean Elevation	5404.92	5390.17	5376.28

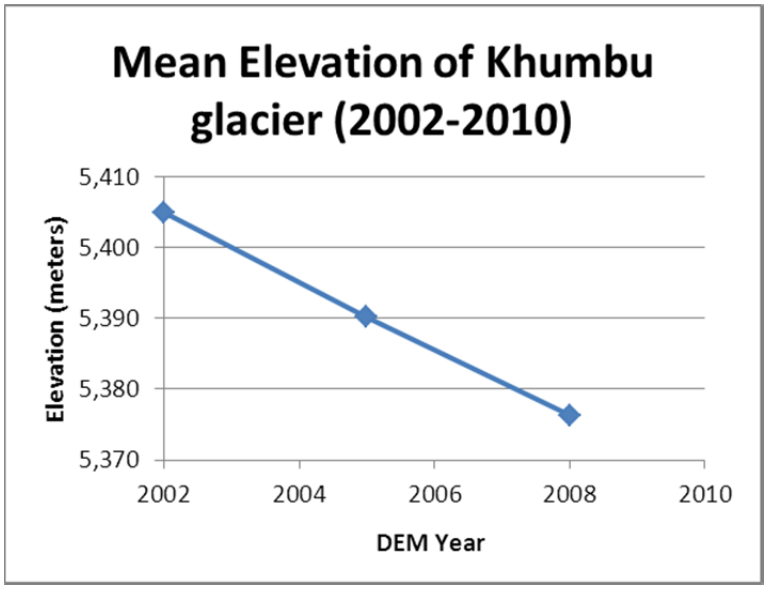

Figure 4.14 Mean Elevation of Khumbu Glacier

Mass balance of Khumbu glacier for the year 2002 - 2005 DEMs was -0.3 ± 0.27 m.w.e.a-1 for clean ice (C-Type) and -1.6 ± 0.25 m.w.e.a-1 for debris covered (D-type) region.

Bolch et al. (2011a) conducted mass balance study in same area from 1970-2007 and 2002-2007 periods. The specific mass balance of Khumbu glacier combined with the accumulation area and ablation area for the period of 1970-2007 is reported as -0.27 ± 0.08 m.w.e.a-1 for digital terrain model (DTM) of area 14.26 sq. km. The period of 2002-2007 also showed negative mass balance of (-0.45 ± 0.52) m.w.e.a-1 for a DTM area coverage of 14.7 sq. km.

Surface elevation profile in accumulation and ablation area as well as in the Khumbu icefall region Khumbu Western Cwm were studied to evaluate the thinning of glaciers at various profiles across the glacier (Figure 4.13) . The results showed surface

lowering in the majority of the evaluated transects, clearly indicating individual and cumulative reduction in surface elevations.

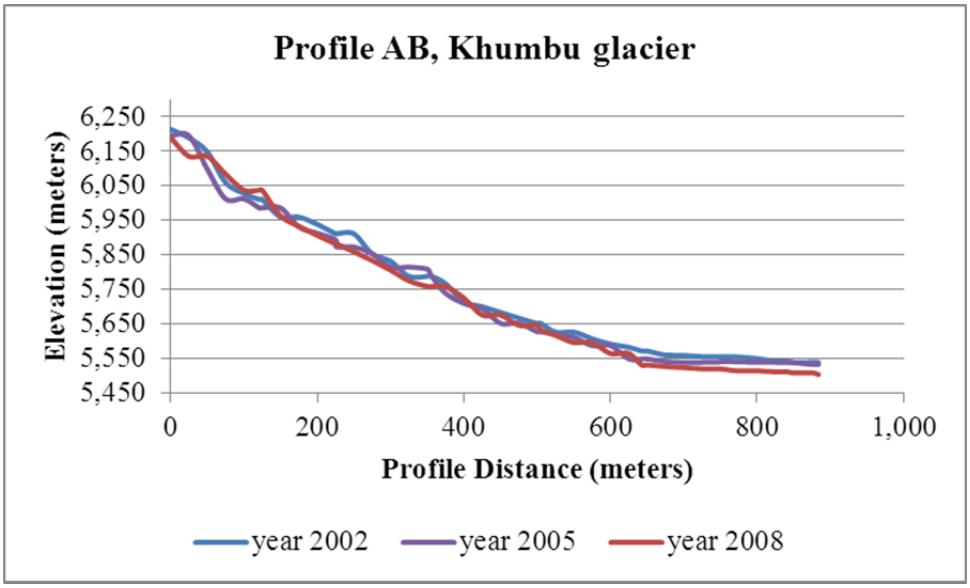

Figure 4.15 Profile AB, Khumbu Glacier

Figure 4.15 represents the surface profile at A-B in the accumulation region, which shows surface change in 2002, 2005, and 2008 DEMs. In 2008 DEM, glacier showed incremental accumulation of ice in the first 150 meters which could be attributed to DEM errors or the real increment. Between the periods 2005 - 2008 substantial net thickness changes of the A-B cross section occurred at cross-sectional distances of 200-850 meters.

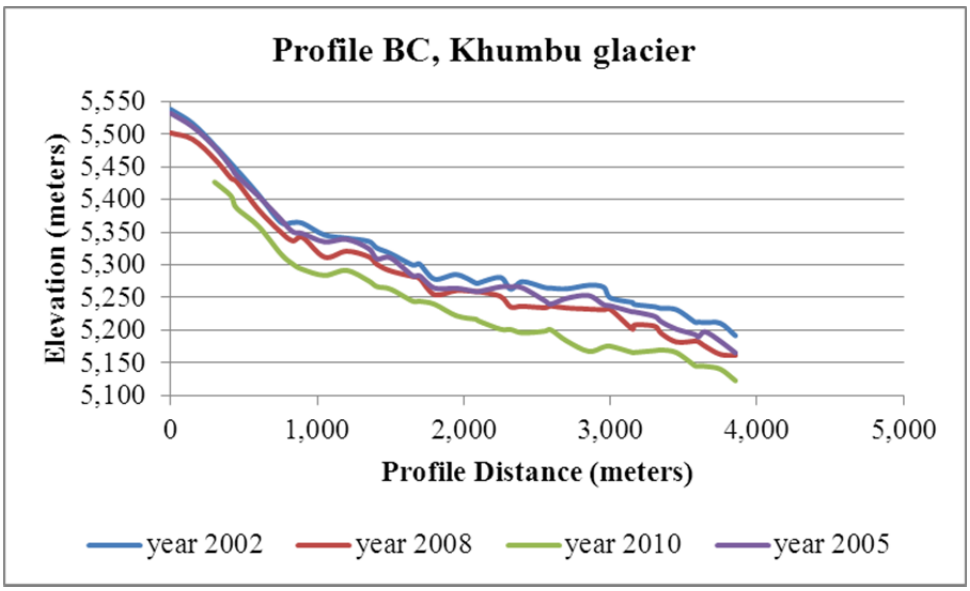

Figure 4.16 Profile BC, Khumbu Glacier

The Upper Ablation profile BC of Khumbu (Figure 4.16) glacier shows consistent surface lowering. The profile BC also portrays lowering in ice thickness heightened with the increase in calendar years. However, the most significant mass losses transpired at 1,000-2,000 meters as well as beyond 2,500 meters to the end of the transect.

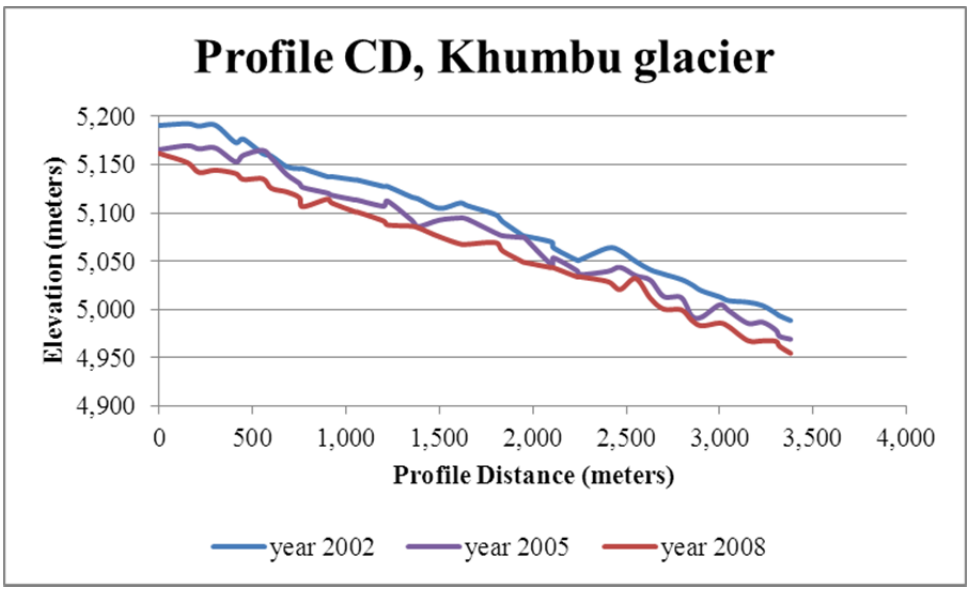

Figure 4.17 Profile CD, Khumbu Glacier

The mid ablation section CD (Figure 4.17) shows steady elevation change rates throughout the elevation profile CD of Khumbu glacier. The largest section of volumetric mass losses in CD profile appeared in 1,500 - 2,000 m ranges and shows an increase at the lower part of the transect.

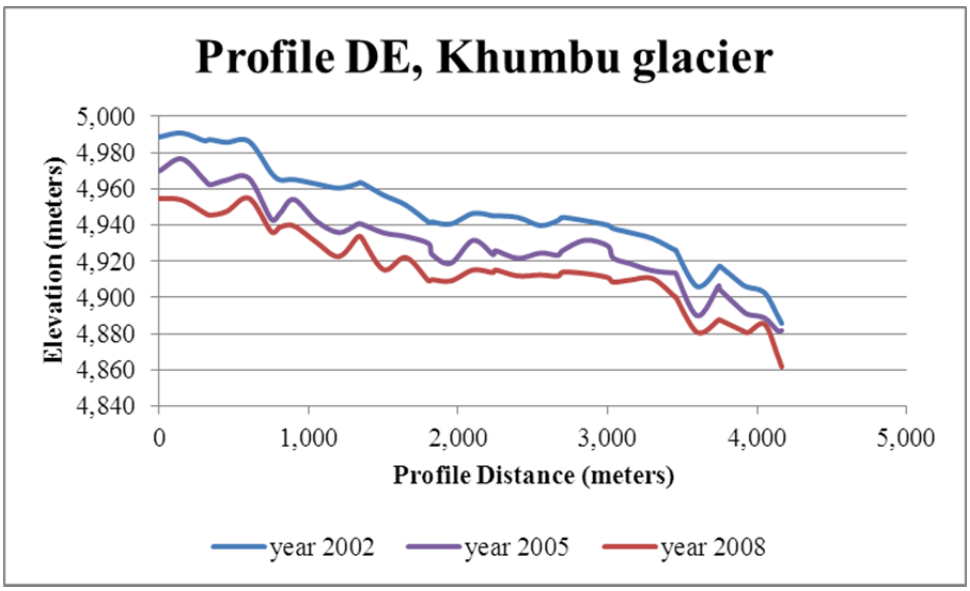

Figure 4.18 Profile DE, Khumbu Glacier

The Lower Ablation of transect DE (Figure 4.18) of Khumbu glacier shows characteristics indicating glacier tongue, as volumetric changes are larger at the beginning of the transect than towards the glacier's terminus at point E. The largest elevation changes were seen in D-E profile during the time period of 2002-2005.

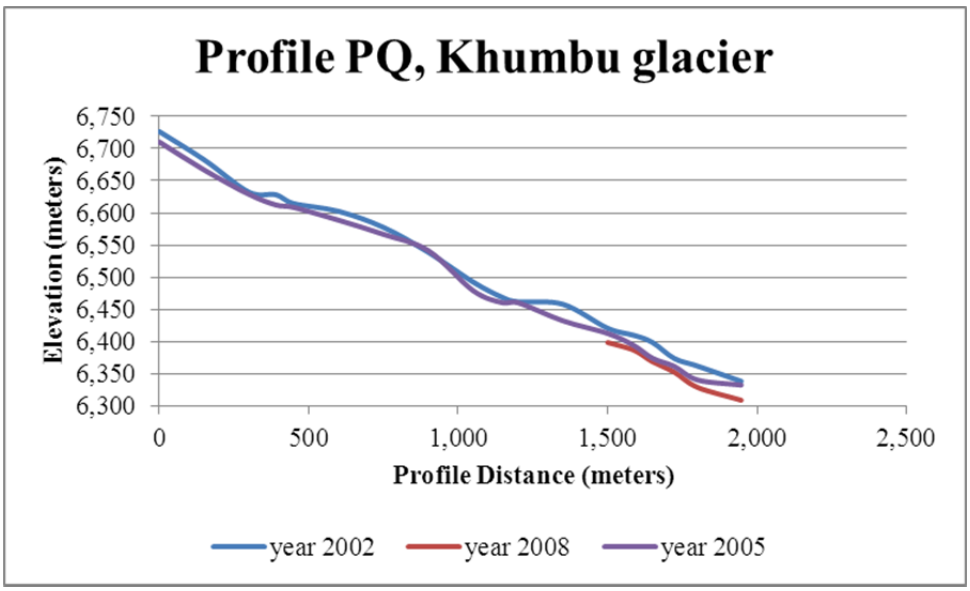

Figure 4.19 Profile PQ, Khumbu Glacier

The PQ transects (Figure 4.19) of Khumbu ice fall, Western Cwm, was not covered in 2008 and 2010 DEM. Hence, the study compared only 2002 and 2005 DEMs for surface elevation changes. Here, the glacier's surface was fairly constant with the largest mass changes occurring at between 1,200m toward the end of transect.

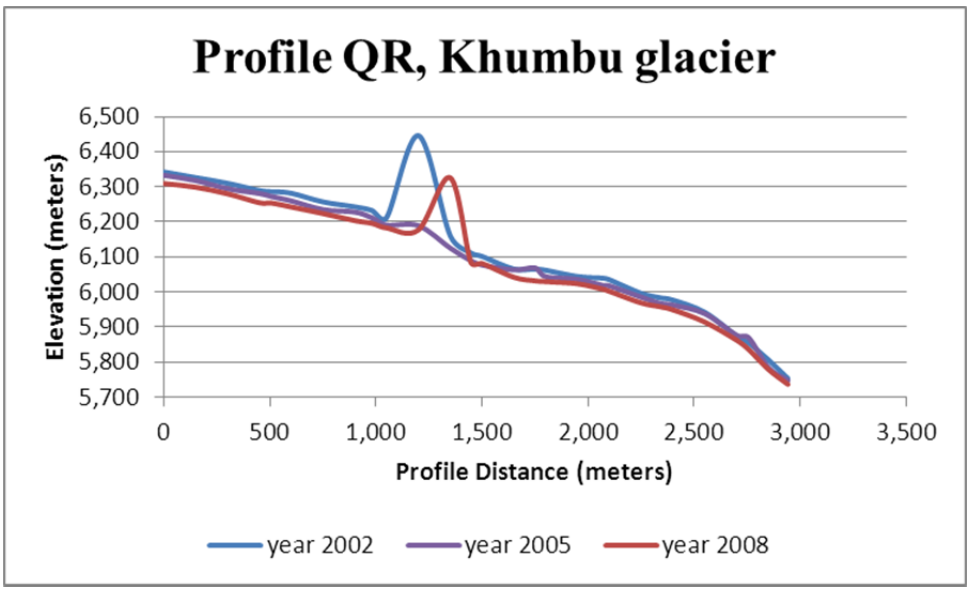

Figure 4.20 Profile QR, Khumbu Glacier

The middle portion of Khumbu Western Cwm profile, QR (Figure 4.20) shows some outliers in 2002 and 2008 DEMs from 1,000-1,500 meters, as that part is covered with shadows (Figure 4.13). The elevation changes are mostly gradual throughout the section, except for the 1,000 - 1,500 m interval.

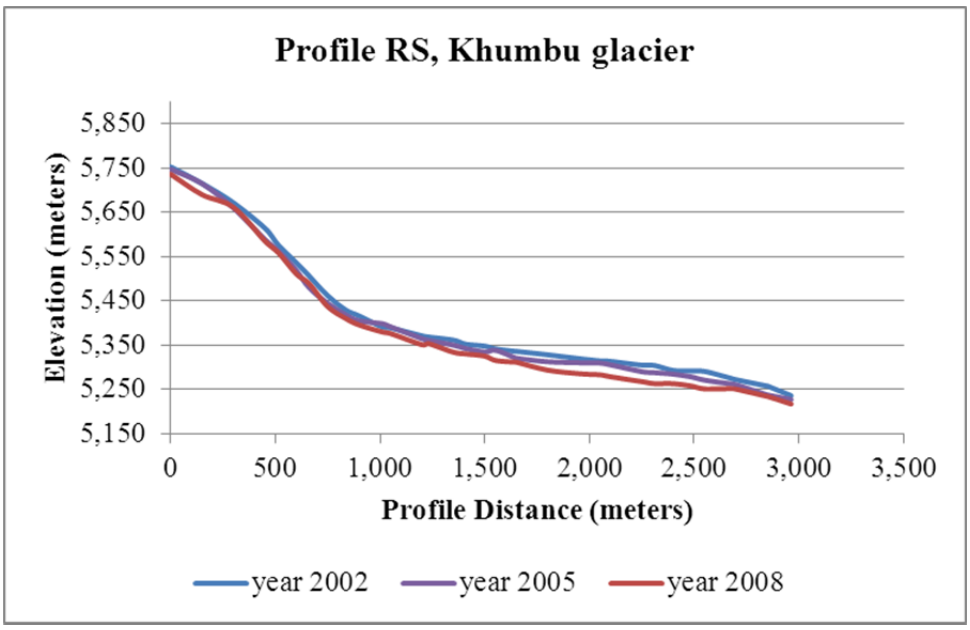

Figure 4.21 Profile RS, Khumbu Glacier

The lowest part of the ice covered glacier of the Khumbu Western Cwm. Cross-section RS (Figure 4.21) shows more mass losses towards the end of the section point. The portion RS is a curved portion and velocity of ice mass should have decreased and accumulated; however, increase in surface temperature might be the cause of melting.

4.1.3 Nojumba Glacier

Nojumba glacier lies in North West part of SNP region (Figure 4.22) covering an area of 14.1246 sq. km. according to glacier boundary digitized based on ASTER 15m resolution image. The glacier tongue stands at an elevation of approximately 4,680 m and extends up to an elevation of approximately 6,200m at its glacial head according to topographic map of 1:50,000 scales published by Department of Survey (DoS), Nepal.

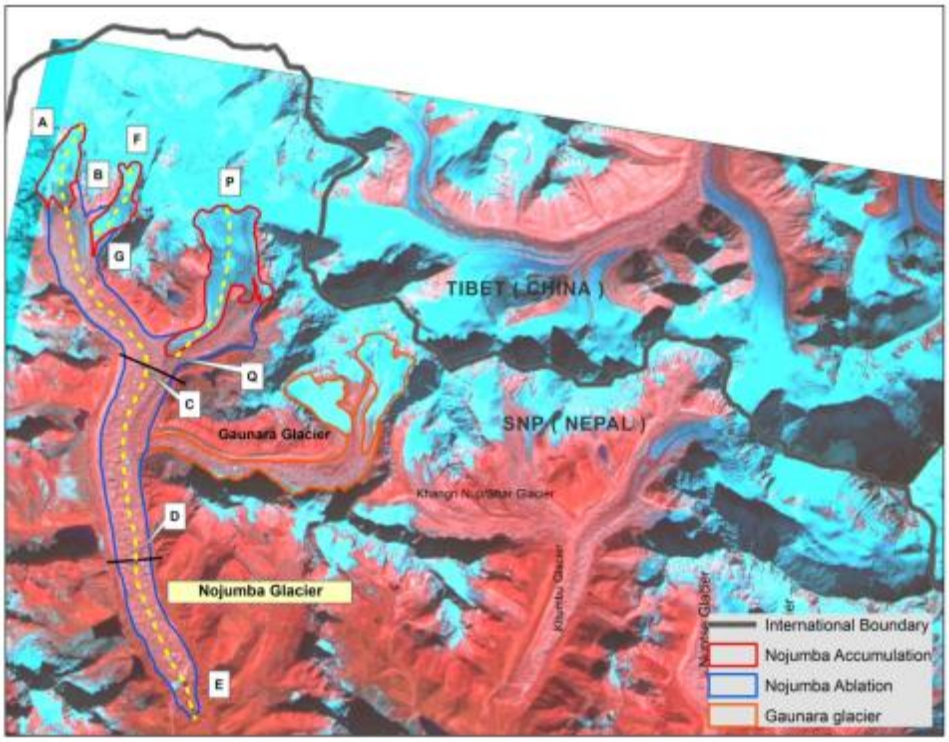

Figure 4.22 Location of Nojumba Glacier in The SNP Region

The mean elevation of Nojumba glacier decreased from 2002 - 2005 whereas it had increased from 2005 - 2008 (Table 4.7, Figure 4.23).

Table 4.7 Mean Elevation Nojumba Glacier

Mean Elevation (meters)				
Year	2002	2005	2008	2010
Mean Elevation	5098.4	5091.68	5095.94	5091.7

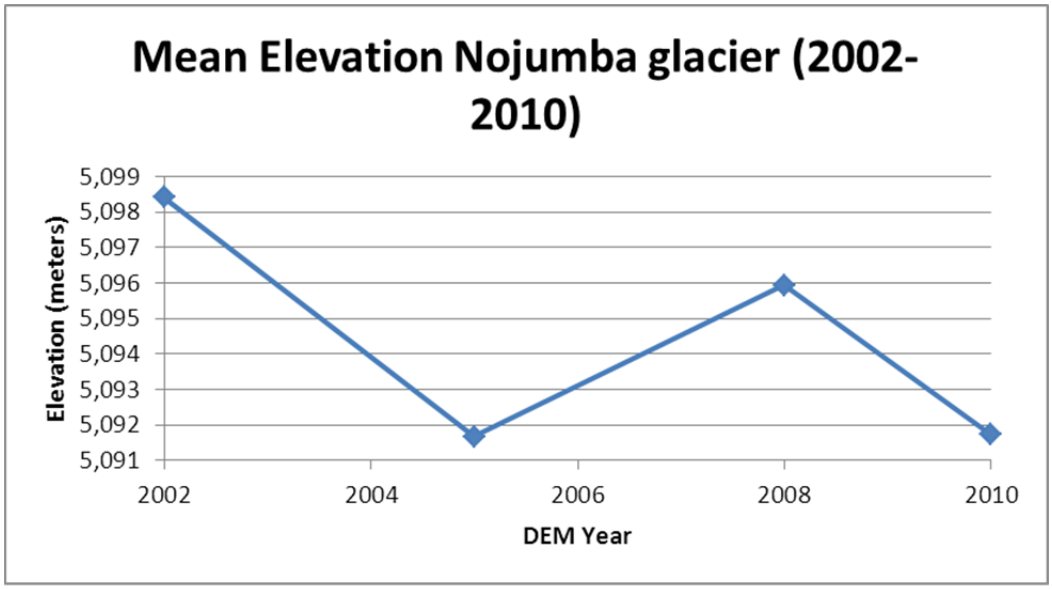

Figure 4.23 Mean Elevation of Nojumba Glacier

Mass balance of Nojumba glacier for the year 2002 - 2005 DEMs was -0.3 ± 0.27 m.w.e.a-1 for clean ice (C-Type) and -1.6 ± 0.25 m.w.e.a-1 for debris covered (D-type). Previous study on mass balance of this glacier could not be found hence could not compare with other result. However, comparing with other glaciers result in SNP region itself is significant.

Surface elevation profile in accumulation and ablation in the Nojumba were studied to evaluate the glacier melt at various profiles across the glacier. The results showed surface lowering in most of transects of Nojumba glacier clearly indicating individual and cumulative reduction in surface elevations.

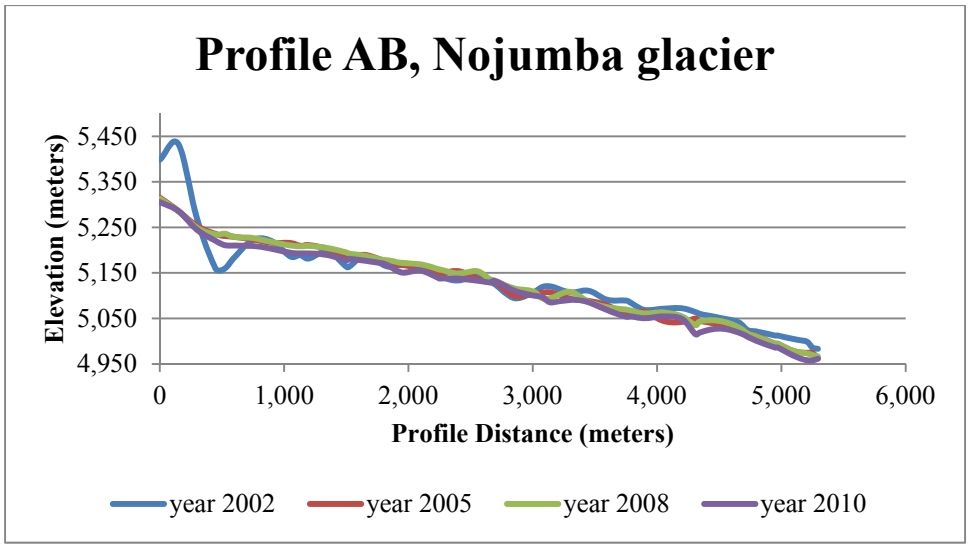

Figure 4.24 Profile AB, Nojumba Glacier

The transect AB of Nojumba glacier (Figure 4.24) showed loss of volumetric mass in the accumulation area but an increase in glacier mass in the ablation region from 2002-2008. The most important volumetric glacier mass losses happened between 2002 and 2005 DEMs within the distances of 200-900m. Additional glacier mass losses appeared in the 2005 and 2008 DEMs portrayed at 500-700m. From 1,200-1,600m the glacier exhibited an increase in glacier mass as shown in the 2002, 2005, and 2008 DEMs.

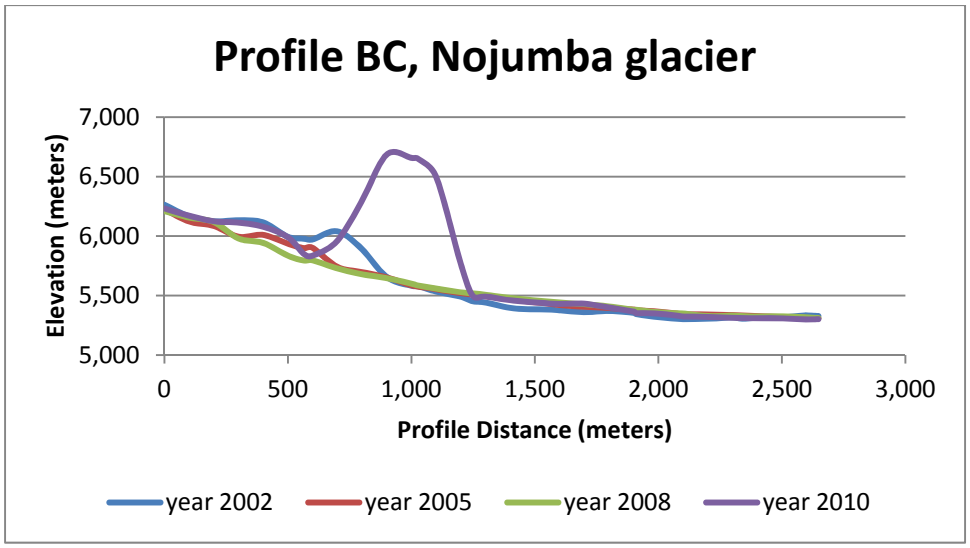

Figure 4.25 Profile BC, Nojumba Glacier

Nojumba glacier's cross-section BC (Figure 4.25) showed a volumetric mass increase in the accumulation region and a decrease of volumetric mass in the ablation region within the time period studied. Cross-section BC had a decrease in volumetric masses from 0-500 m in the 2002, 2005, and 2008 DEMS. However, within the glaciers distance of 1,000-2,400 meters there was an accumulation of glacier mass with time. There was a decrease in glacier mass from 3,000-5,200 meters in between the 2002 and 2005 DEMS but a slight increase in mass in 3,500-4,700m between the 2005 and 2008 DEMs.

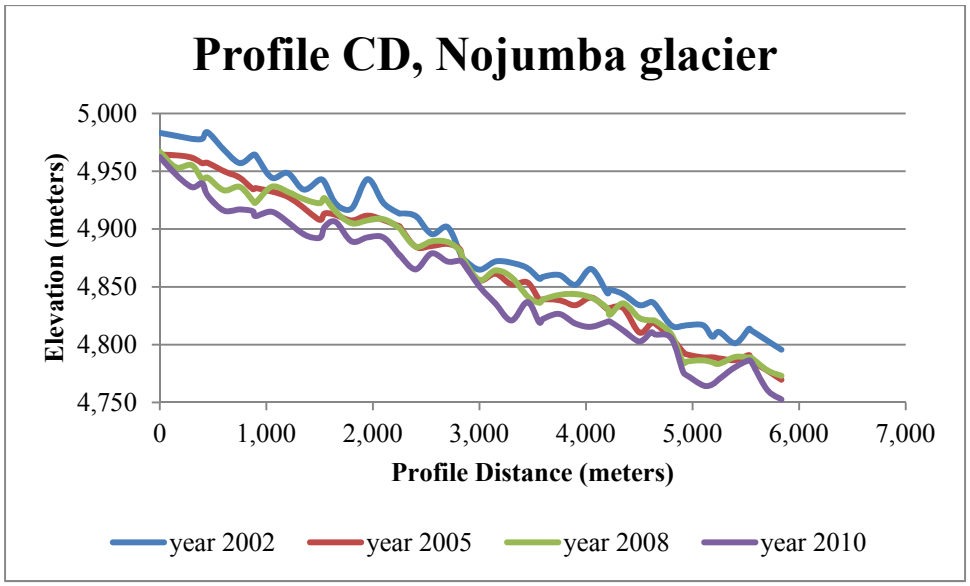

Figure 4.26 Profile CD, Nojumba Glacier

Profile CD of Nojumba glacier (Figure 4.26) exhibited a constant trend of volumetric glacier mass losses from the 2002 and 2005 DEMs. The 2005 and 2008 DEMs had decreases in glacier masses between 0-1,000m as well as from 4,500-5,300m.

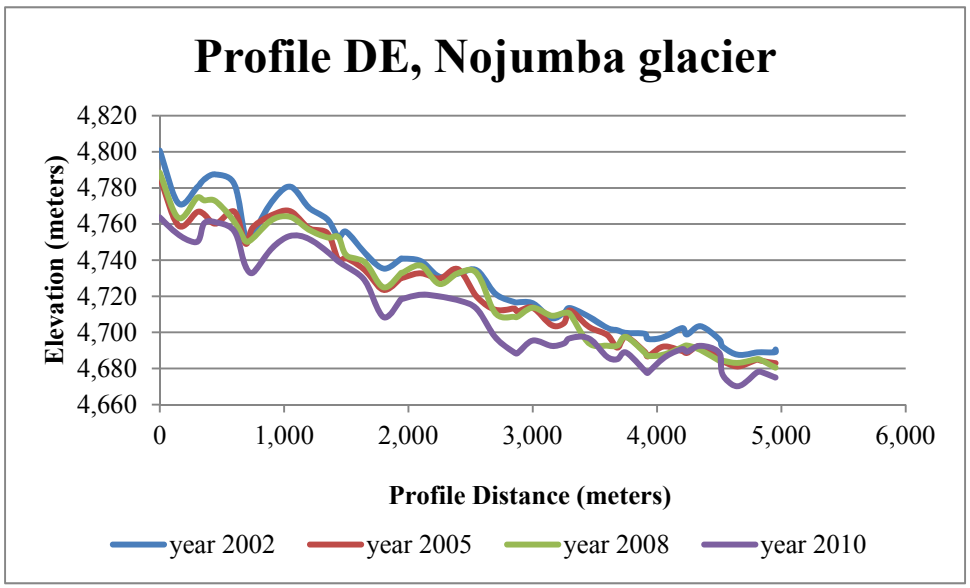

Figure 4.27 Profile DE, Nojumba Glacier

The cross-section DE of Nojumba glacier (Figure 4.27) experienced losses in glacier masses in regards to the increase during the period of study. Significant volumetric losses transpired between the years of 2002 to 2005. There was a predominant trend of glacier mass increase from 2005 to 2008 with the main areas being significantly reduced in the accumulation glacier region while the ablation area had lesser volumetric increases.

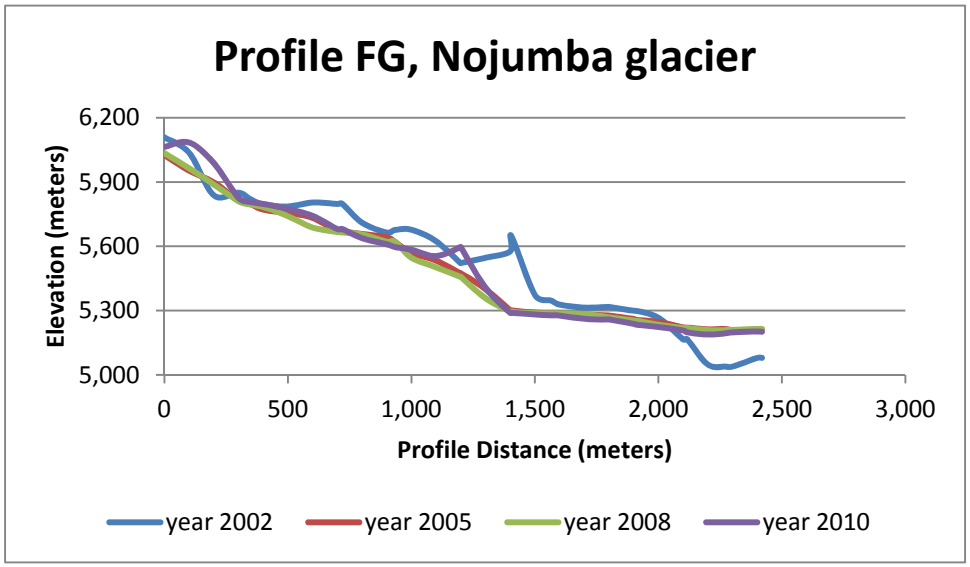

Figure 4.28 Profile FG, Nojumba Glacier

Profile FG of Nojumba glacier (Figure 4.28) showed significant losses in volumetric glacier masses in its middle section between 600-1,760m between 2002 and 2005. There was an increase in glacier masses in the glacier from 2,200 -2,400m from 2002 - 2005 DEMs. The 2002 and 2005 DEMs showed the same general trend of glacier masses except 2002 had slightly higher glacier masses during the study.

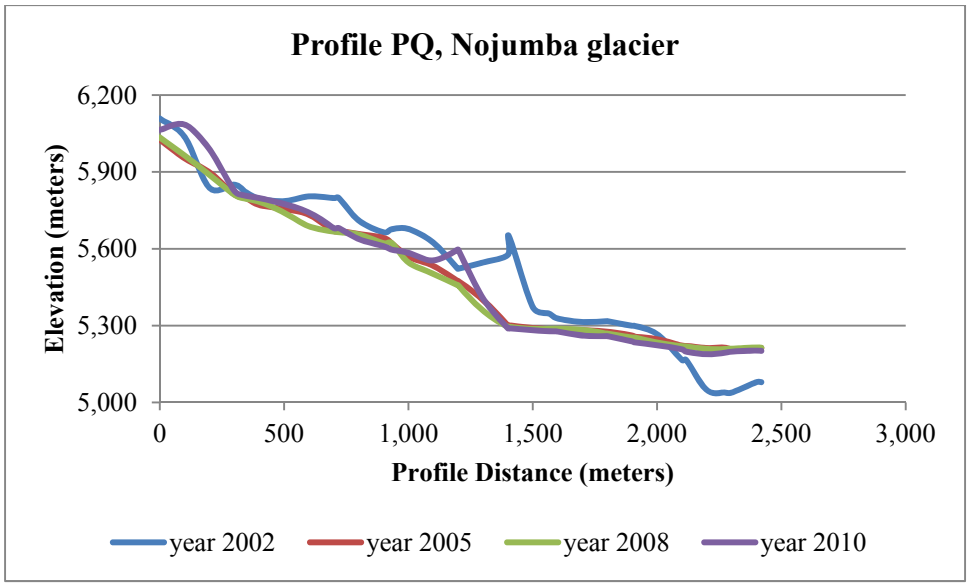

Figure 4.29 Profile PQ, Nojumba Glacier

Nojumba glaciers transect PQ (Figure 4.29) for DEMs 2002, 2005, and 2008 showed a trend of decreasing glacier mass with increased time. The most sizeable mass changes were within the glacier ablation area of 4,500 - 5,100m as shown in the lines illustrating the reprojection of 2002 and 2005 DEMs

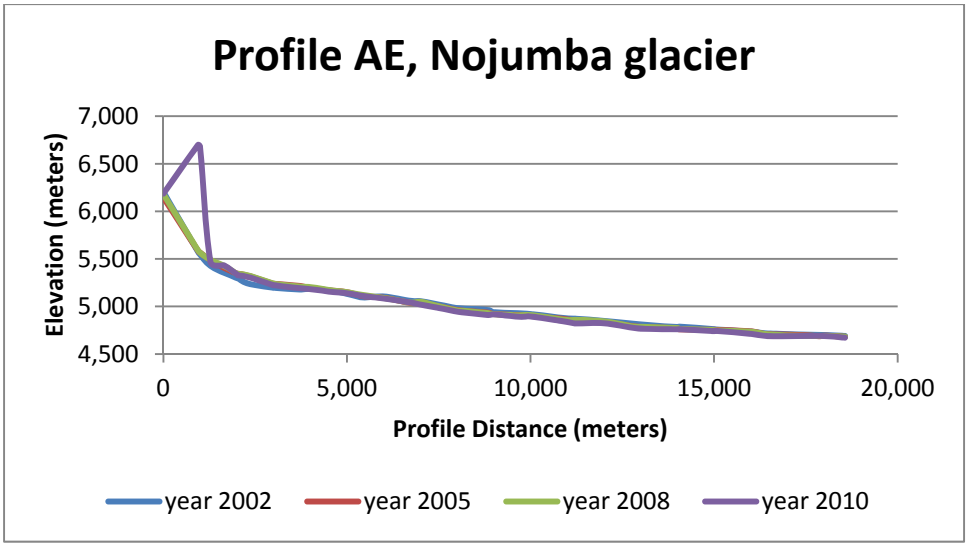

Figure 4.30 Profile AE, Nojumba Glacier

4.1.4 Gaunara Glacier

Gaunara glacier serves as a tributary for Nojumba glacier (Figure 4.31) covering an area 9.394 sq. km. according to glacier boundary digitized based on ASTER 15m resolution image. The glacier tongue stands at an elevation of approximately 4,930m and extends up to an elevation of approximately 6,000m at its glacial head according to topographic map of 1:50,000 scale published by DoS, Nepal.

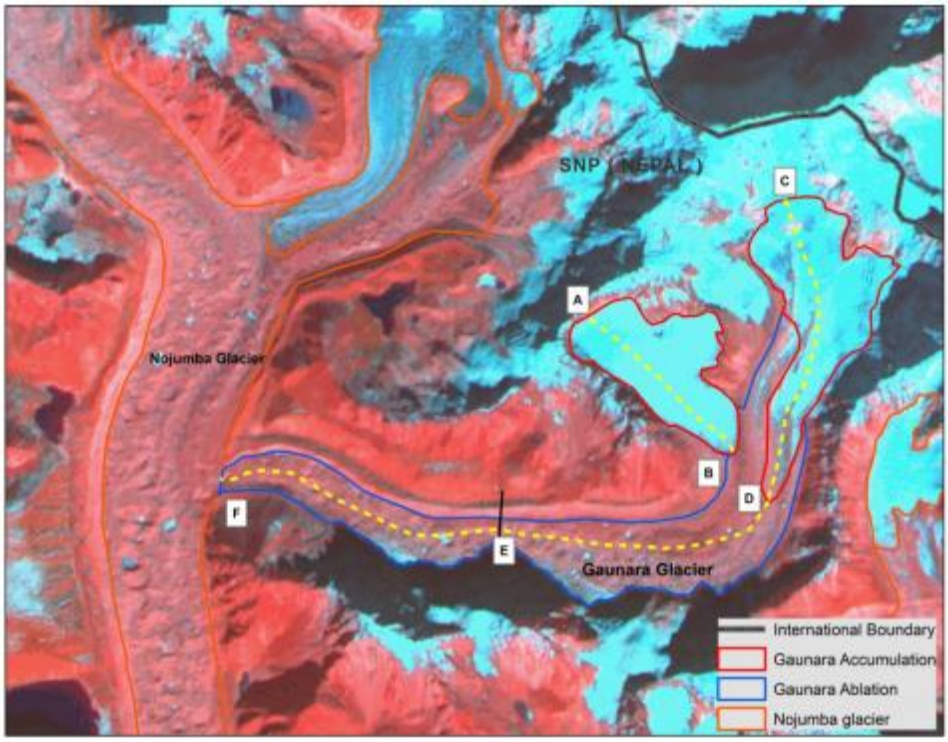

Figure 4.31 Location of Gaunara Glacier in The SNP Region

The mean elevation of Gaunara glacier for each individual year evaluated is provided (Table 4.8, Figure 4.32).

Table 4.8 Elevation Difference of Gaunara Glacier

Mean Elevation (meters)				
Year	2002	2005	2008	2010
Mean Elevation	5415.6	5408.6	5402.6	5386.5

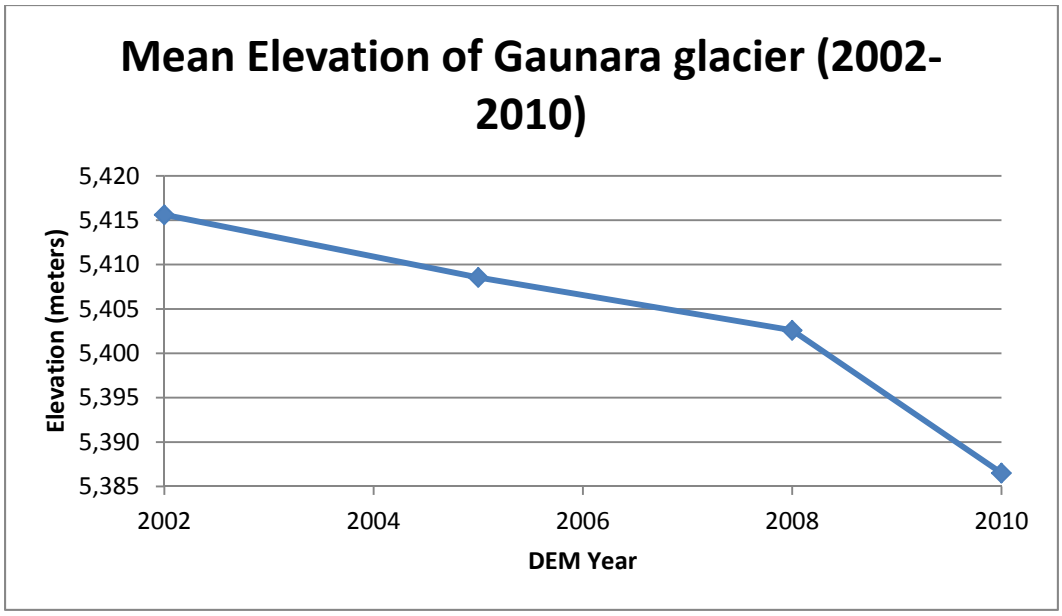

Figure 4.32 Mean Elevation of Gaunara Glacier

Mass balance of Gaunara glacier for the year 2002-2005 DEMs was -0.3 ± 0.27 m.w.e.a-1 for clean ice (C-Type) and -1.6 ± 0.25 m.w.e.a-1 for debris covered (D-type).

Surface elevation profile in accumulation and ablation in the Gaunara glacier were studied to evaluate mass balance changes of glaciers at various profiles across the glacier. The analyses results indicated surface lowering in most transects, clearly indicating individual and cumulative reduction in surface elevation.

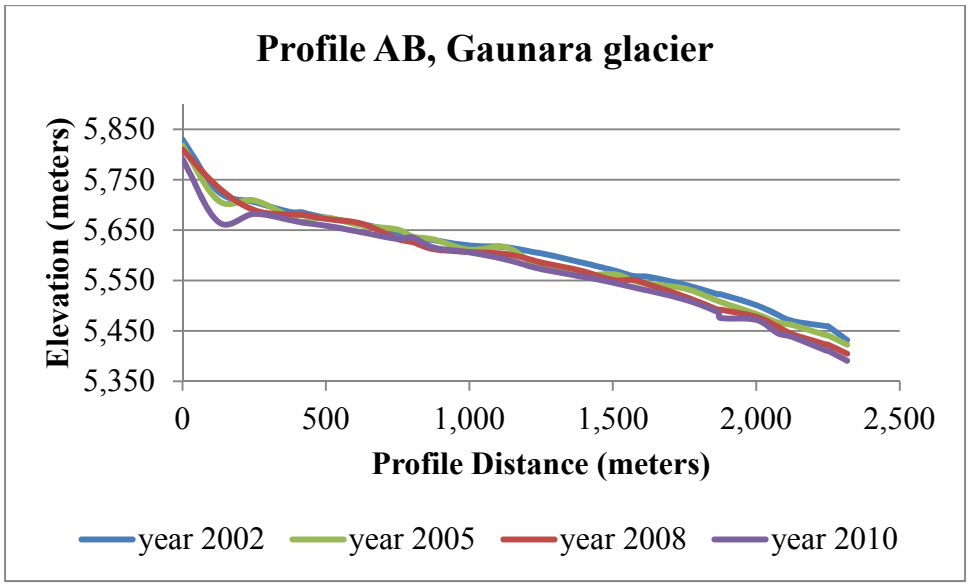

Figure 4.33 Profile AB, Gaunara Glacier

Gaunara glacier profile AB (Figure 4.33) had a general trend of glacier mass increase from 0-150m while the volumetric masses decreased within this glacier from 150m - 600m from 2002 - 2008. The most notable glacier melt occurred from 200m - 280m.

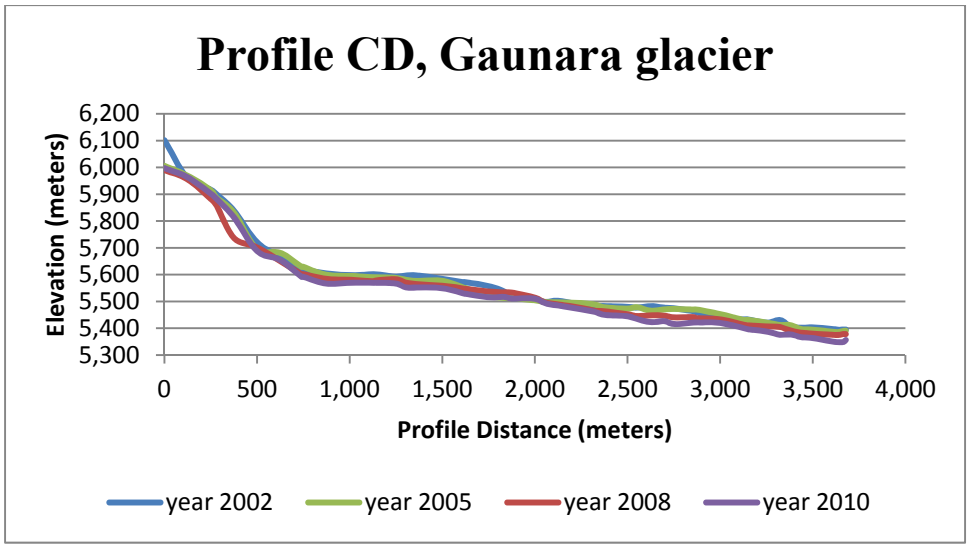

Figure 4.34 Profile CD, Gaunara Glacier

Gaunara glacier transect CD (Figure 4.34) portrayed glacier melting which transpired from 2002 - 2005. Sizeable glacier melt occurred in the accumulation range from 0 - 200m as shown in the elevation differences of 2002 and 2005 DEMs.

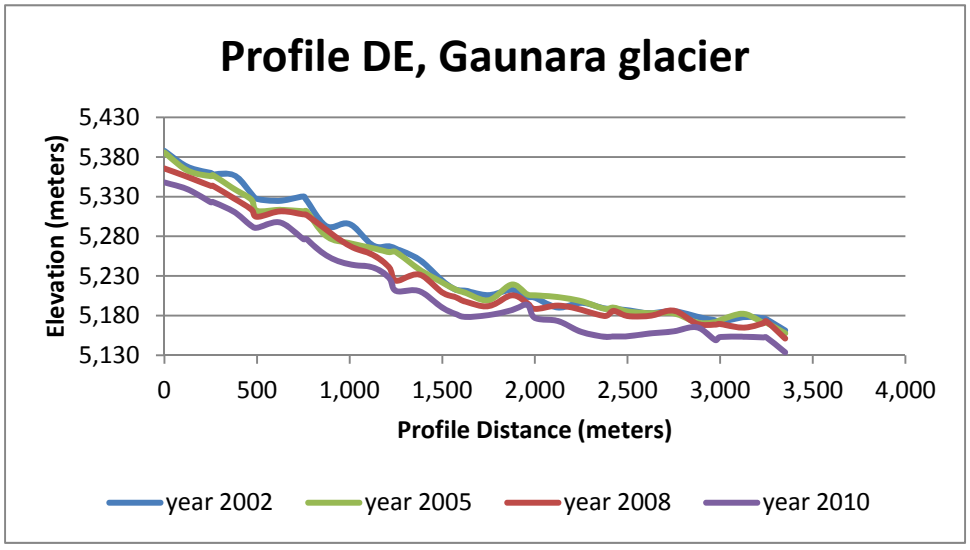

Figure 4.35 Profile DE, Gaunara Glacier

Gaunara glacier profile DE (Figure 4.35) established a general trend of glacier melt from the period of study from 2002-2005. Comparison of the 2002 and 2005 DEMs showed the most significant elevation changes which occurred at distances of 400-700m. Notable glacier mass losses from the evaluation of 2005 and 2008 DEMs appeared at distances of 480-500m and 1,200-1,400m.

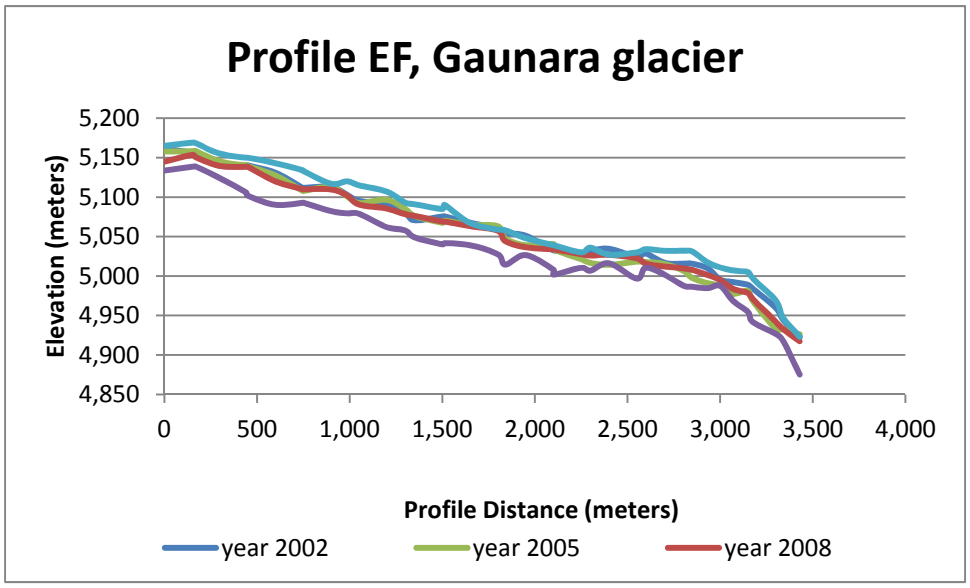

Figure 4.36 Profile EF, Gaunara glacier

The cross section EF (Figure 4.36) of Gaunara glacier showed a general trend of glacier melt that transpired from 2002-2008. Largest volumetric mass losses occurred at the accumulation region 0 - 900m and at the ablation area from 2,200m - 3,500m.

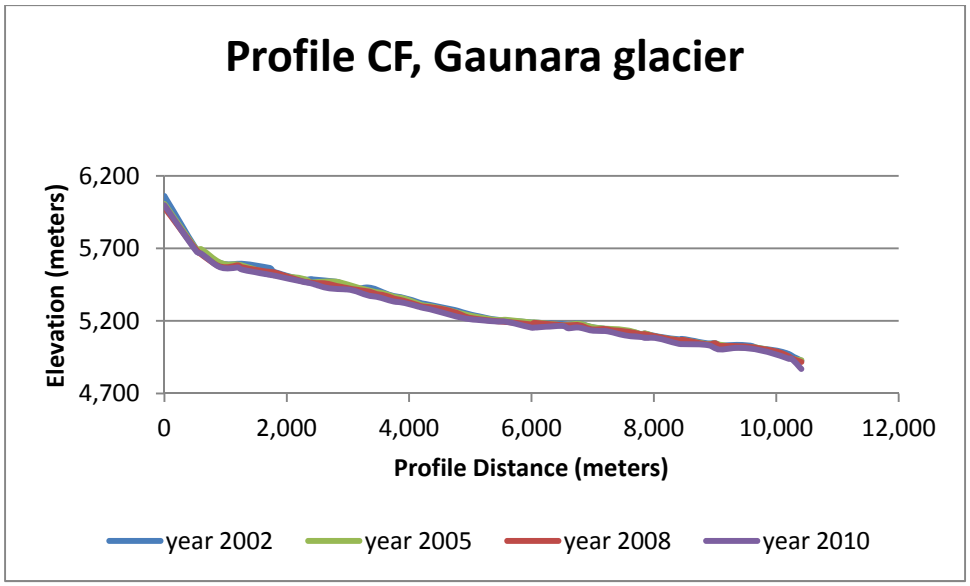

Figure 4.37 Profile CF, Gaunara Glacier

4.1.5 Nuptse Glacier

Nuptse glacier flows at the base of Nuptse Peak (7,864m) (Figure 4.38) covering an area 4.84 sq. km. according to glacier boundary digitized based on ASTER 15m resolution image. The glacier tongue stands at an elevation of approximately 4,900m and extends up to an elevation of approximately 6,000 m at its glacial head according to topographic map scale of 1:50,000 published by DoS, Nepal.

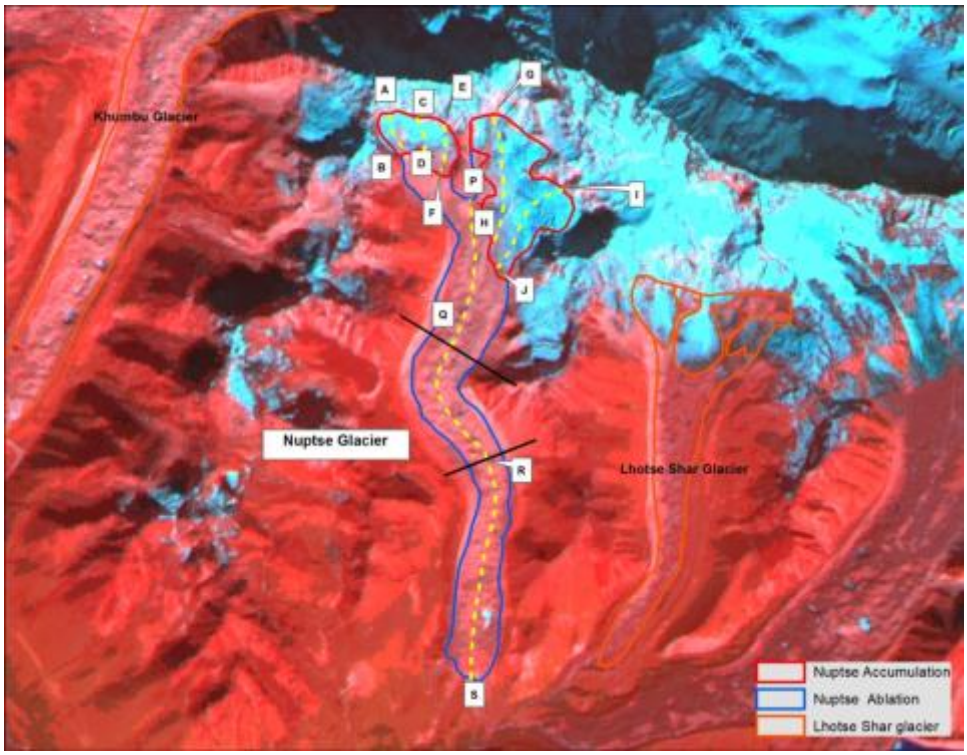

Figure 4.38 Location of Nuptse Glacier in SNP region

The mean elevation of Nuptse glacier in individual year is provided (Table 4.9, Figure 4.39).

Table 4.9 Differences in Elevation of Nuptse Glacier

Mean Elevation (meters)			
Year	2002	2005	2008
Mean Elevation	5382	5354.1	5315.5

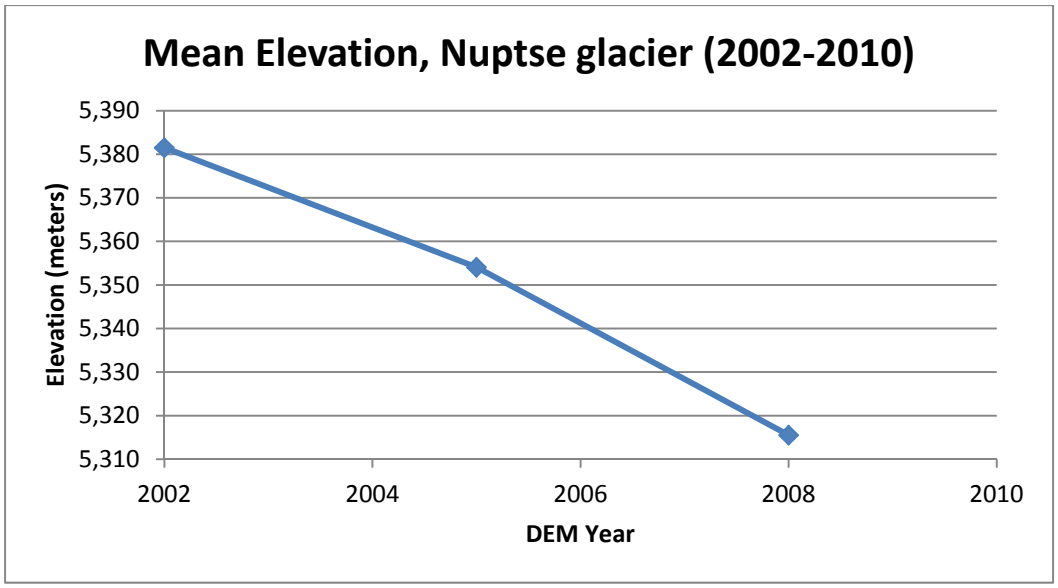

Figure 4.39 Mean elevation of Nuptse Glacier

Mass balance of Nuptse glacier for the year 2002-2005 DEMs was (-0.2 ± 0.61) m.w.e.a-1 for clean ice (C-Type) and -0.5 ± 0.42 m.w.e.a-1 for debris covered (D-type).

Bolch et al. (2011a) conducted mass balance study in same area from 1970 - 2007 and 2002 - 2007 periods. The specific mass balance of Nuptse glacier and the combined accumulation area and ablation area for the period of 1970-2007 is reported as -0.25 ± 0.08 m.w.e.a-1 for DTM area of 3.45 sq. km. The period 2002 - 2007 also showed negative mass balance of (-0.40 ± 0.53) m.w.e.a-1 for a DTM area coverage of 3.52 sq. km. Surface elevation profile in accumulation and ablation in the Nuptse glacier were studied to evaluate the thinning of glaciers at various profile across the glacier and the results showed surface lowering in most transect clearly indicating individual and cumulative reduction in surface elevation.

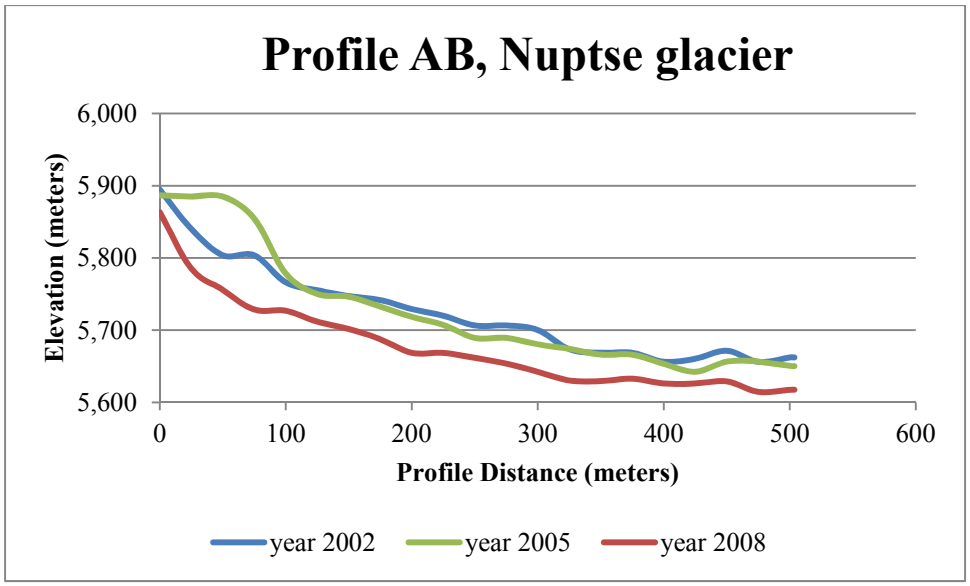

Figure 4.40 Profile AB, Nuptse Glacier

Cross-section AB (Figure 4.40) of Nuptse glacier showed a continuous trend of glacier melting from 2002 - 2008. The 2005 DEM showed increases in glacier masses in transect AB from the 0 - 100m in comparison to the 2005 and 2008 DEMs. Sizeable volumetric mass losses occurred in cross section AB at 80m as depicted in the 2005 and 2008 DEMs.

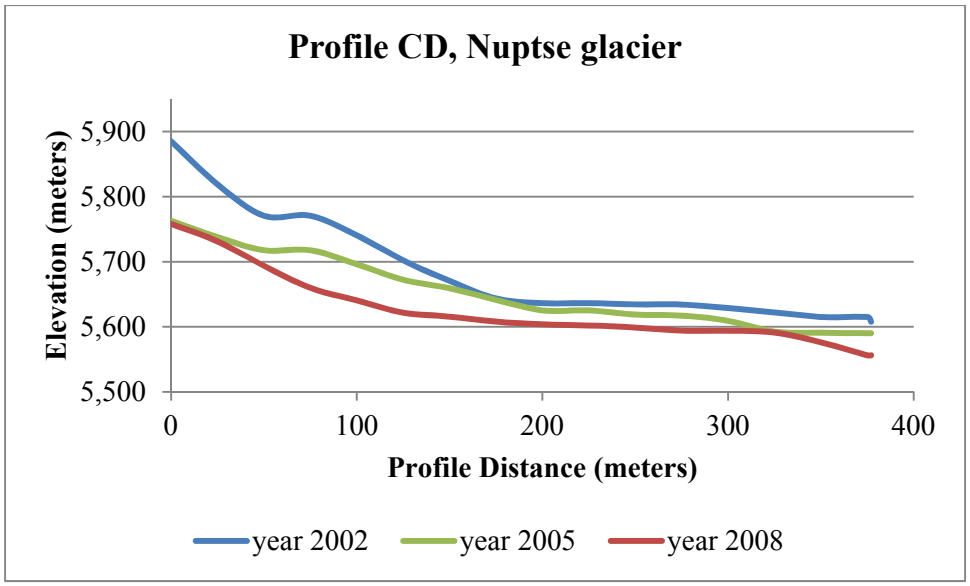

Figure 4.41 Profile CD, Nuptse Glacier

Nuptse Glacier profile CD (Figure 4.41) showed Glacier mass accumulation from 2002 DEM to the 2005 DEM. However, the increased volumetric mass had a significant decrease from 2005 - 2008 so much that it provided evidence of Glacier melting processes in cross section CD.

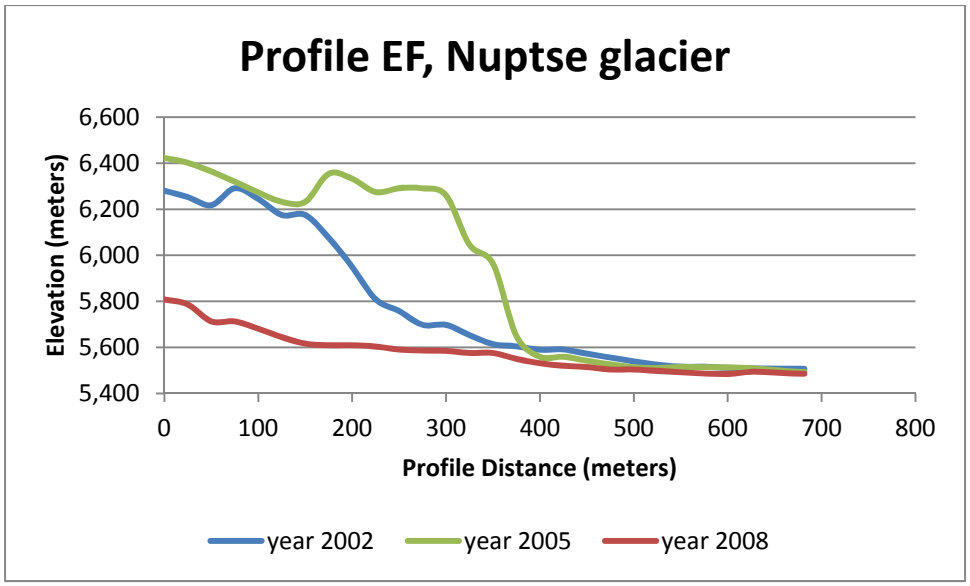

Figure 4.42 Profile EF, Nuptse Glacier

Transect EF (Figure 4.42) of Nuptse glacier showed a significant increase in mass balance from 200m - 400m between 2002 - 2005. Notable glacier mass losses occurred from profile distance 0 - 400m amongst the 2005 and 2008 DEMs which offset the previous mass balance accumulation. From 400m to the end, glacier mass balance decreased in accordance to the increase of the calendar years.

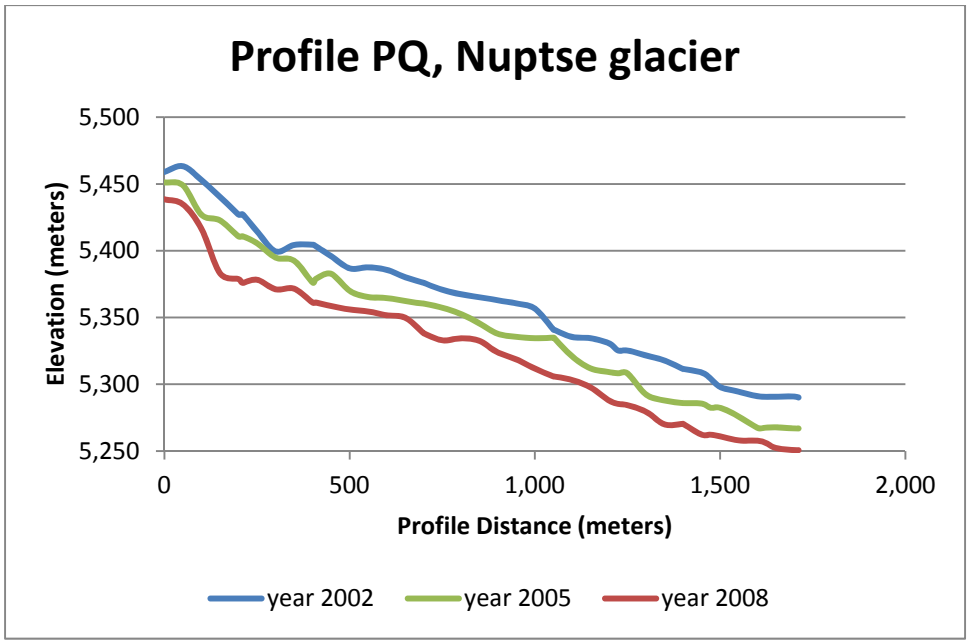

Figure 4.43 Profile PQ, Nuptse Glacier

PQ (Figure 4.43) profile of Nuptse glacier had a general trend of glacier melt occur from 2002 to 2008. The largest elevation changes of transect PQ occurred at 200m between the years of 2005 and 2008.

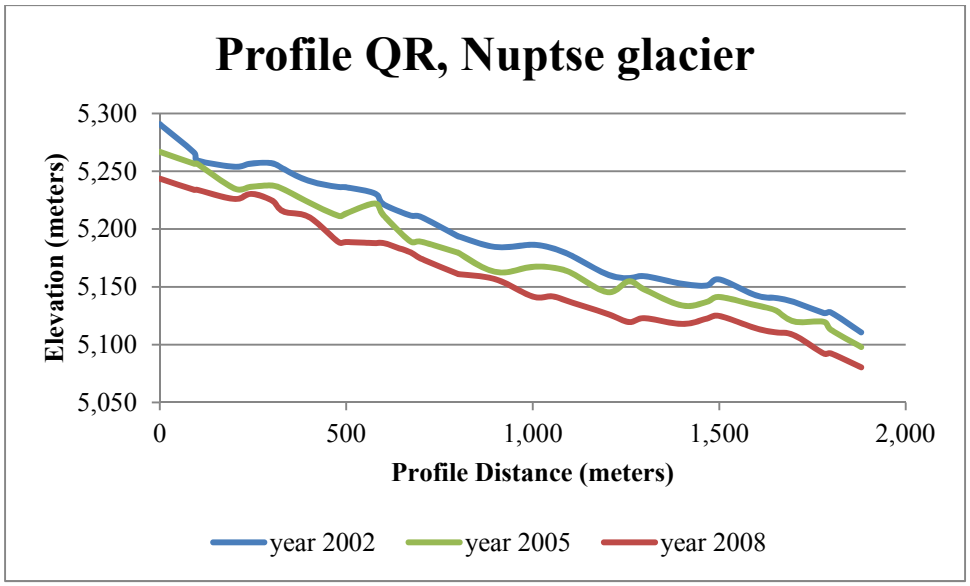

Figure 4.44 Profile QR, Nuptse Glacier

Nuptse glacier transect QR (Figure 4.44) showed glacier melt occurring in quantifiable amounts from 2002 to 2008 with the exception of similar elevations between the 2005 and 2008 DEMs at 400m.

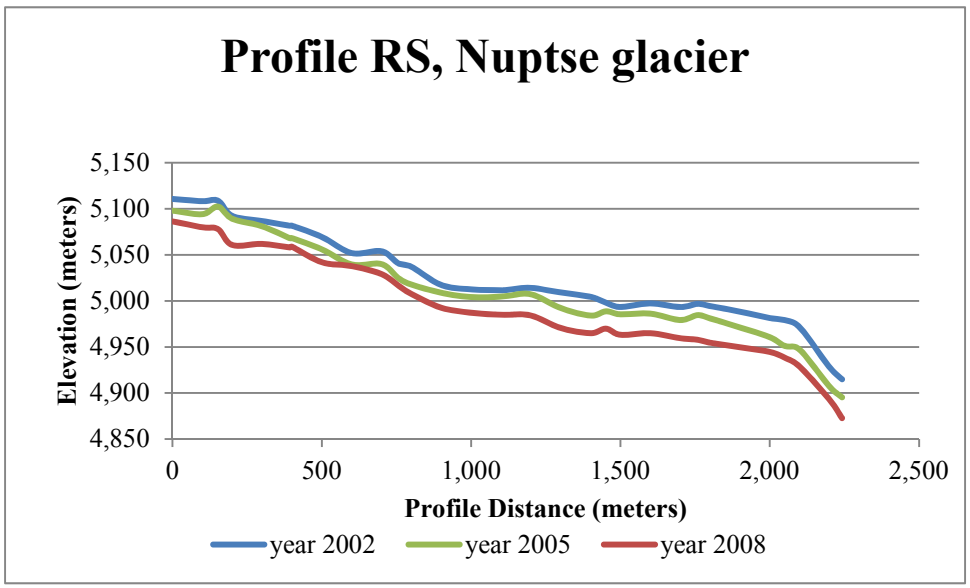

Figure 4.45 Profile RS, Nuptse Glacier

Profile RS (Figure 4.45) of Nuptse glacier illustrated continued glacier mass losses from the years 2002 to 2008. The most notable elevation changes transpired at approximately 1,800m between the 2005 and 2008 DEMs.

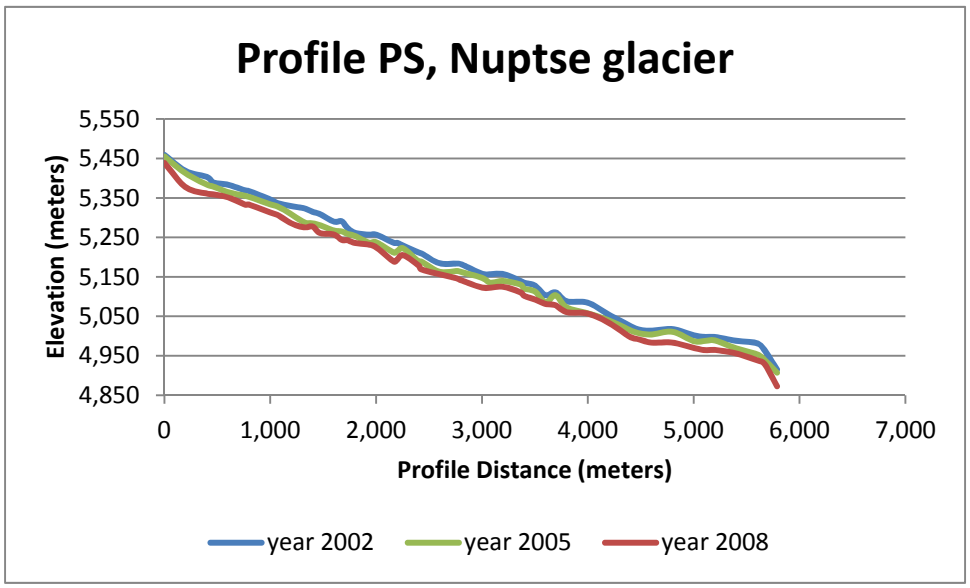

Figure 4.46 Profile PS, Nuptse Glacier

Cross section PS (Figure 4.46) of Nuptse glacier showed continual linear mass balance losses that occurred from with the increase of calendar years from 2002 - 2008.

4.1.6 Lhotse Nup Glacier

Lhotse Nup glacier lies in between Nuptse and Lhotse glaciers (Figure 4.47) covering an area 2.73 sq. km, according to glacier boundary digitized based on ASTER 15m resolution image. The glacier tongue stands at an elevation of approximately 5,000m and extends up to an elevation of 6,200m at its glacial head according to topographic map scale of 1:50,000 published by DoS, Nepal.

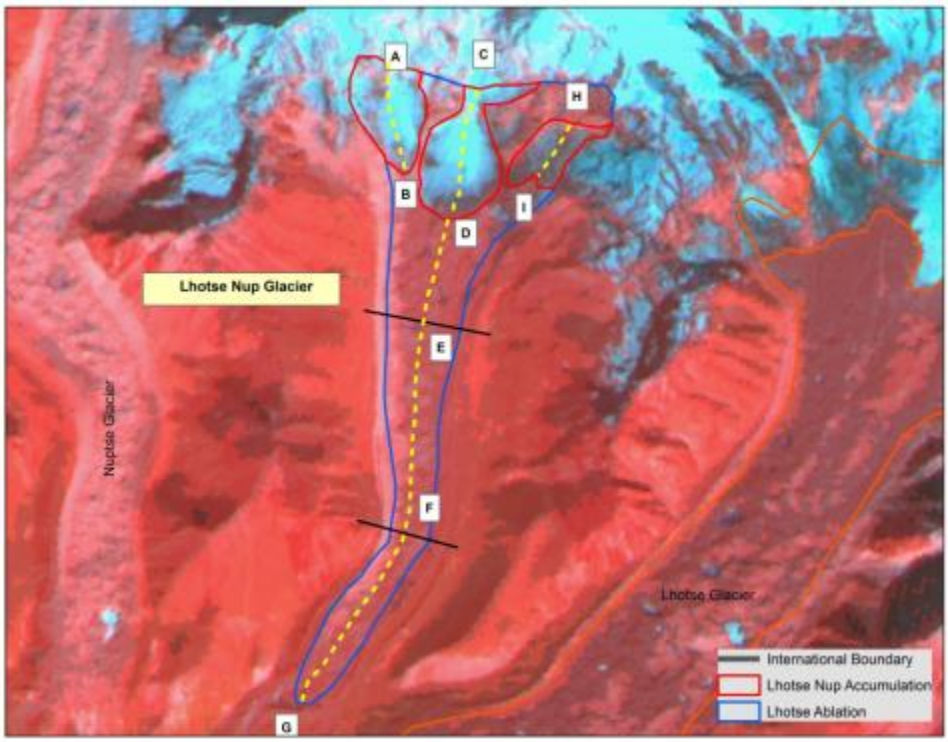

Figure 4.47 Location of Lhotse Nup Glacier in SNP region

The mean elevation of Lhotse Nup glacier in individual year is provided (Table 4.10, Figure 4.48).

Table 4.10 Mean Elevation difference of Lhotse Nup Glacier

Mean Elevation (meters)		
Year	2002	2005
Mean Elevation	5395.3	5285.1

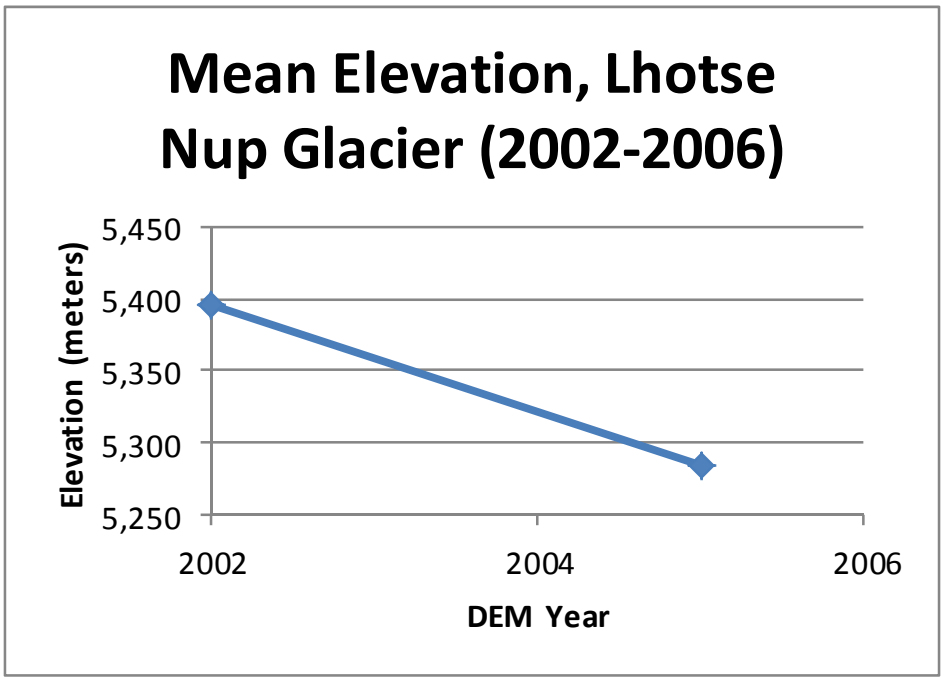

Figure 4.48 Mean elevation of Lhotse Nup Glacier

Mass balance of Lhotse Nup glacier for the year 2002-2005 DEMs was -2.8 ± 0.89 m.w.e.a-1 for clean ice (C-Type) and -1.2 ± 0.61 m.w.e.a-1 for debris covered (D-type).

Bolch et al. (2011) conducted mass balance study in the same area from 1970-2007 and 2002-2007 periods. The specific mass balance of Lhotse Nup glacier combined accumulation area and ablation area for the period of 1970-2007 is reported as -0.18 ± 0.07 m.w.e.a-1 for DTM area of 1.86 sq. km. The period 2002-2007 also showed negative mass balance of (-1.03 ± 0.51) m.w.e.a-1 for a DTM area coverage of 1.86 sq. km.

Surface elevation profile in accumulation and ablation in the Lhotse Nup glacier were studied to evaluate the mass balance changes at various profile across the glacier

(Figure 4.48). This study provided quantification of mass balance changes indicating surface lowering in most transects while clearly portraying individual and cumulative reduction in surface elevation.

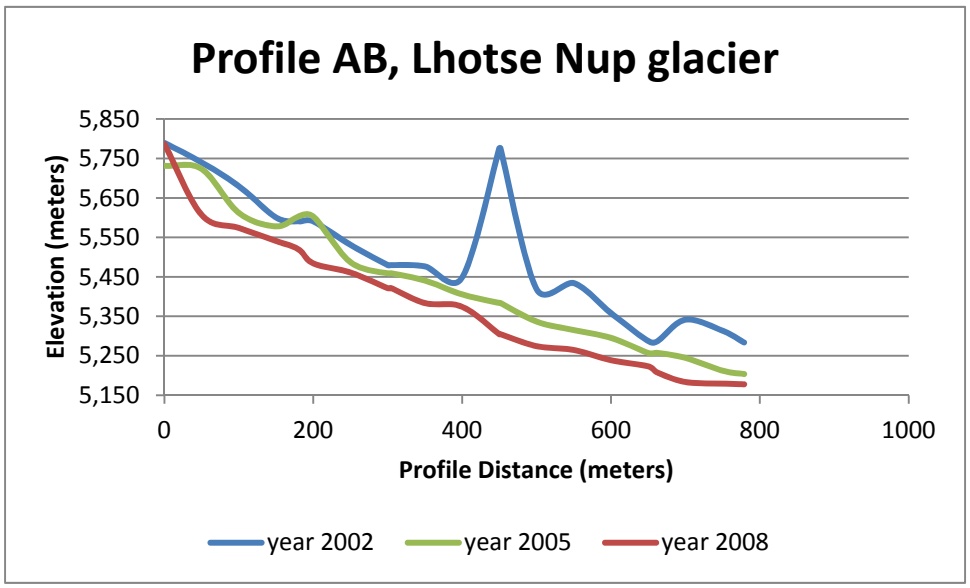

Figure 4.49 Profile AB, Lhotse Nup Glacier

Lhotse Nup glacier profile of AB (Figure 4.49) illustrates measurable glacier mass losses that appeared from 2002-2005. The most volumetric changes were observed in the glacier ablation area from 400-750m.

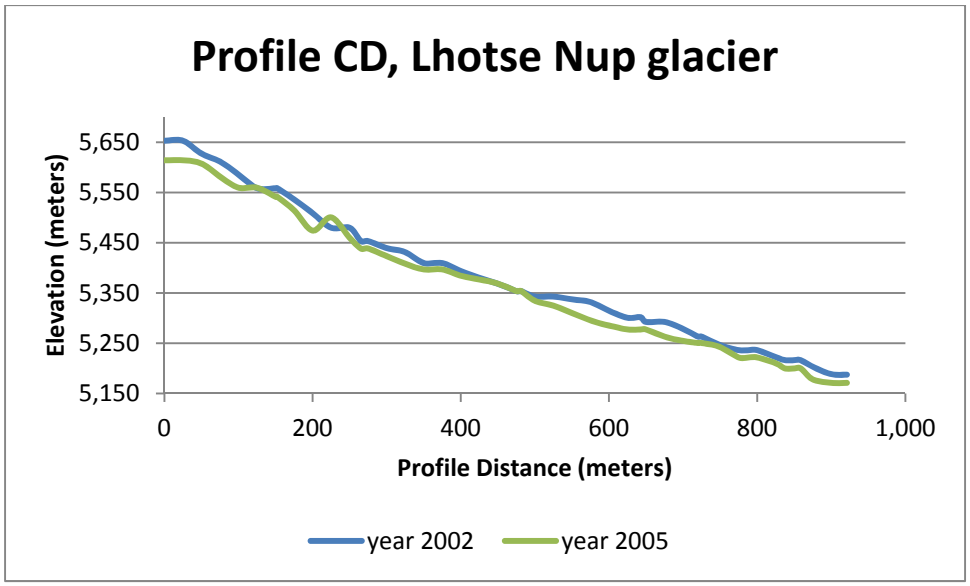

Figure 4.50 Profile CD, Lhotse Nup Glacier

Cross section CD (Figure 4.50) of Lhotse Nup glacier depicts volumetric mass losses that have developed from 2002 - 2005. Despite the area of the glacier evaluated mass losses in cross section BC remained fairly constant except for a distance of 300m where there were no observable mass changes.

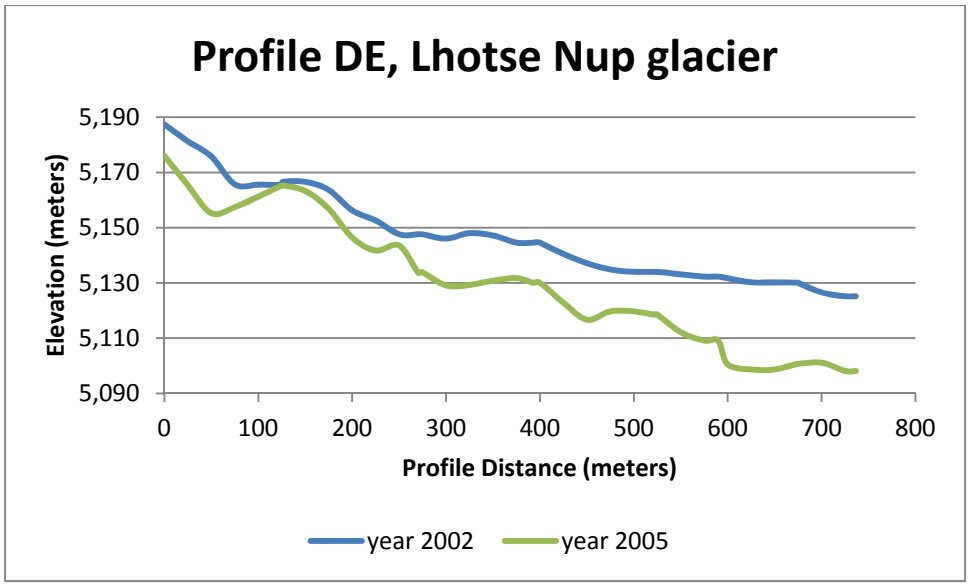

Figure 4.51 Profile DE, Lhotse Nup Glacier

The comparison of DEMs from 2002-2005 of Lhotse Nup glacier transect DE (Figure 4.51) of Lhotse Nup glacier quantifies significant glacier mass losses with increased time. Considerable shrinkage of glacier masses occurred at distances of 300m - 720m.

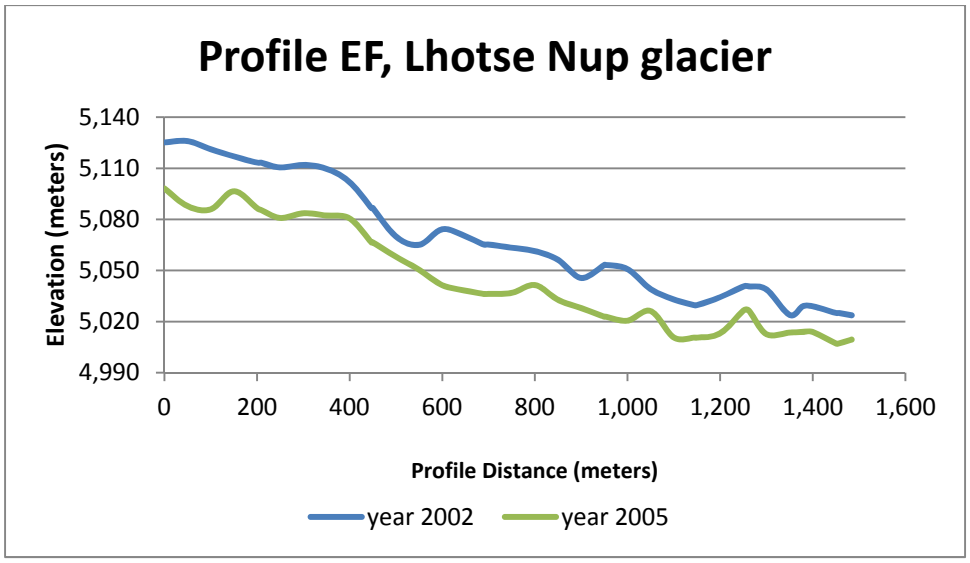

Figure 4.52 Profile EF, Lhotse Nup Glacier

Profile EF (Figure 4.52) of Lhotse Nup glacier presents a constant trend of glacier elevation reductions from 2002 to 2008. Reductions in glacier mass in profile EF were significant at all distances in the study except at 1,400m.

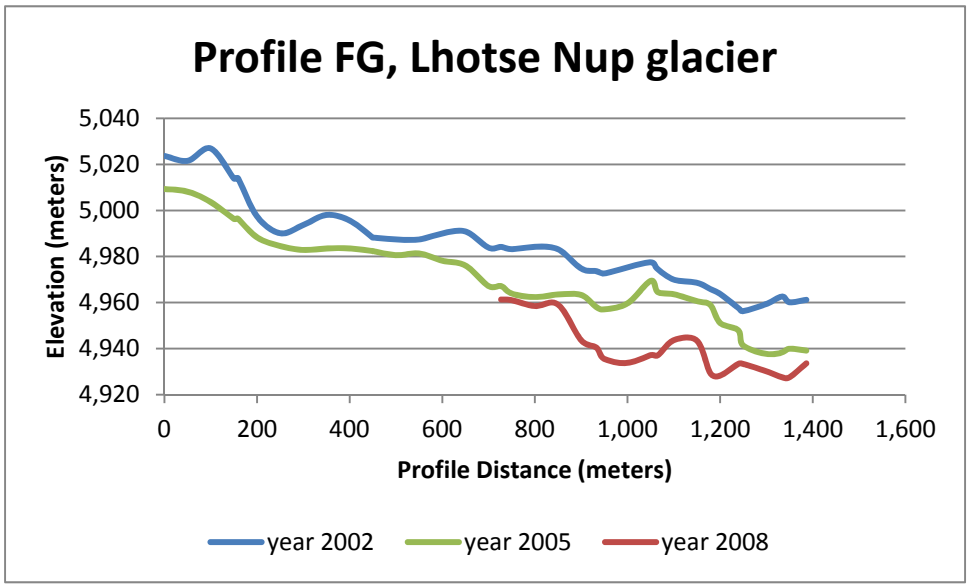

Figure 4.53 Profile FG, Lhotse Nup Glacier

Evaluation of 2002 and 2005 DEMs of Lhotse Nup glacier transect FG (Figure 4.53) revealed volumetric mass losses. Sizeable changes in glacier masses transpired at distances of 80m, 600m -1,000m, and 1,260m -1,280m.

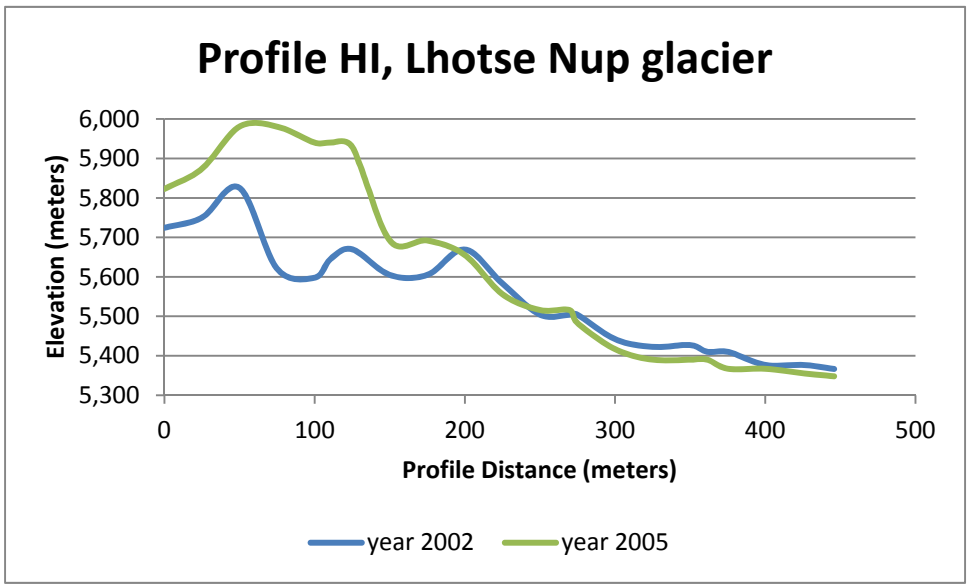

Figure 4.54 Profile HI, Lhotse Nup Glacier

Cross section HI (Figure 4.54) of Lhotse Nup glacier showed an increase in glacier mass in the accumulation area as well as a mass decrease in the glacier's ablation region from 2002 to 2005. The 2005 DEM of cross section HI depicted a considerable increase in glacier masses from 0 - 150m.

4.1.7 Lhotse Glacier

Lhotse glacier flows at the base of Lhotse Peak (8,386m) (Figure 4.55) covering an area 7.155 sq. km according to glacier boundary digitized based on ASTER 15m resolution image. The glacier tongue stands at an elevation of approximately 4,750m and

extends up to an elevation of 5,600m at its glacial head according to topographic map scale of 1:50,000 published by DoS, Nepal.

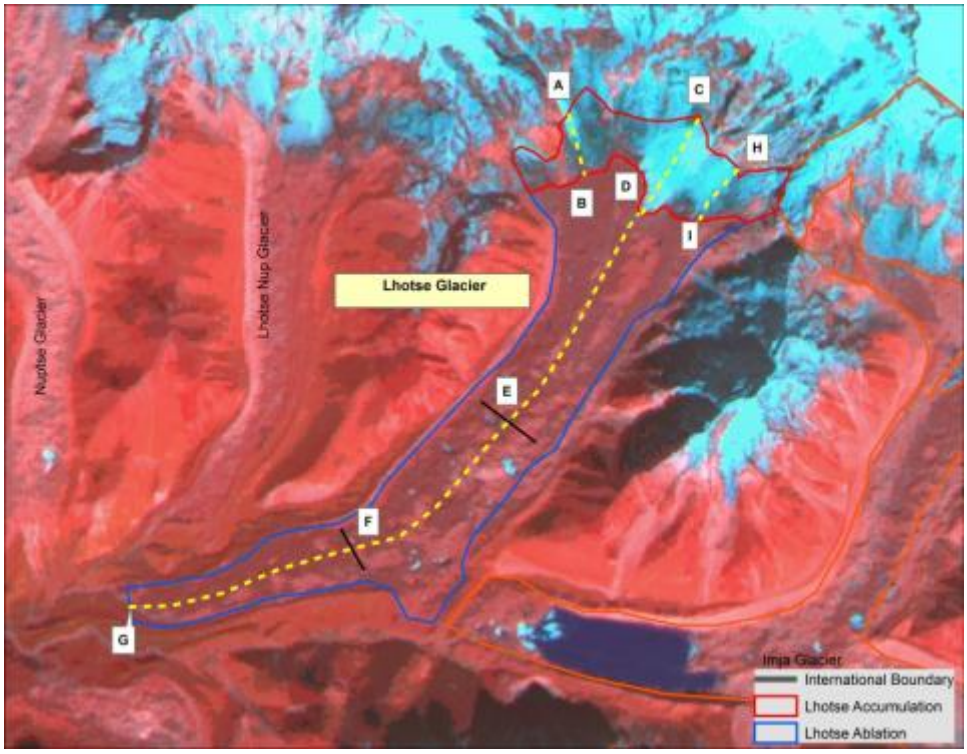

Figure 4.55 Location of Lhotse Glacier in SNP Region

The mean elevation of Lhotse glacier in individual year is provided (Table 4.11, Figure 4.56).

Table 4.11 Mean Elevation Differences of Lhotse Glacier

Mean Elevation (meters)		
Year	2002	2005
Mean Elevation	5129.4	5111.3

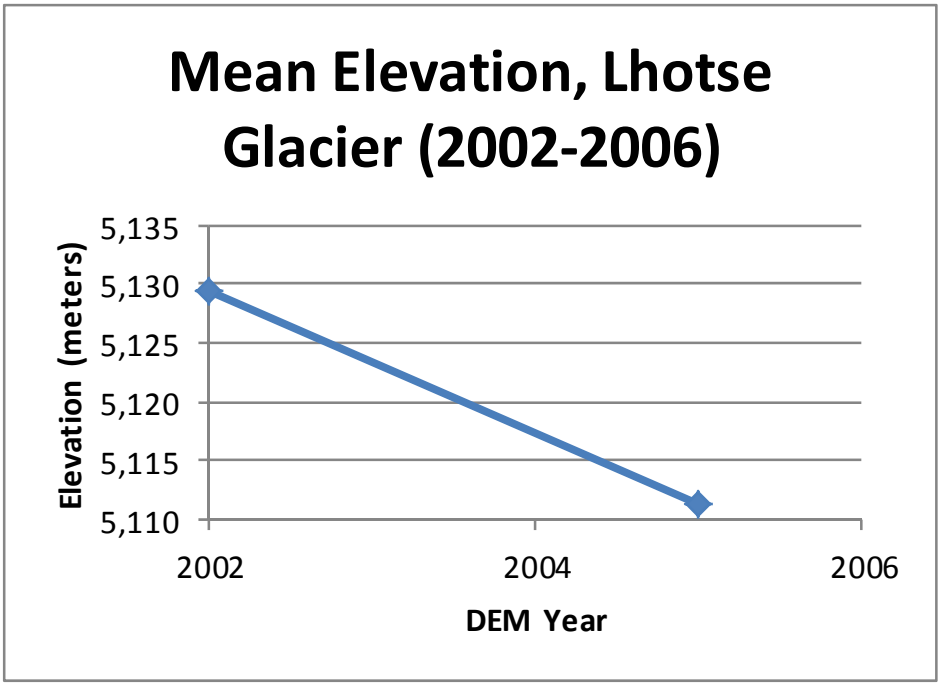

Figure 4.56 Mean Elevation of Lhotse Glacier

Mass balance of Lhotse glacier for the year 2002-2005 DEMs was -2.8 ± 0.57 m.w.e.a-1 for clean ice (C-Type) and -1.1 ± 0.29 m.w.e.a-1 for debris covered (D-type).

Bolch et al. (2011a) conducted mass balance study in same area from 1970-2007 and 2002-2007 periods. The specific mass balance of Lhotse glacier combined with accumulation area and ablation area for the period of 1970-2007 is reported as -0.26 ± 0.08 m.w.e.a-1 for DTM area of 6.71 sq. km. The period 2002-2007 also showed negative mass balance of (-1.10 ± 0.52) m.w.e.a-1 for a DTM area coverage of 6.71 sq. km.

Surface elevation profile in accumulation and ablation in the Lhotse glacier were studied to evaluate the thinning of glaciers at various profile across the glacier (Figure 4.55).

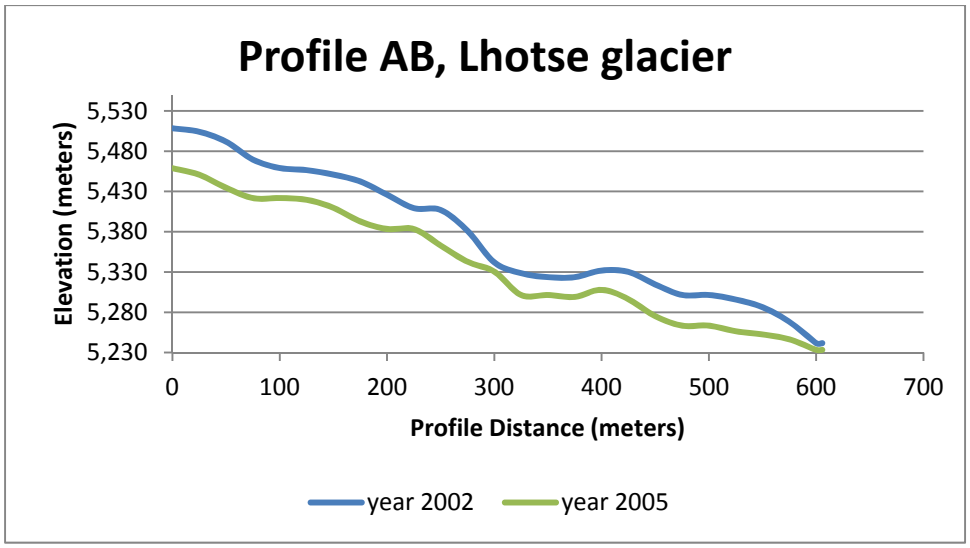

Figure 4.57 Profile AB, Lhotse Glacier

Lhotse glacier profile AB (Figure 4.57) showed a mostly linear relationship of glacier mass decreases from 2002 to 2005. During this time period the glacier mass had a constant rate of mass decreases from 0-550m.

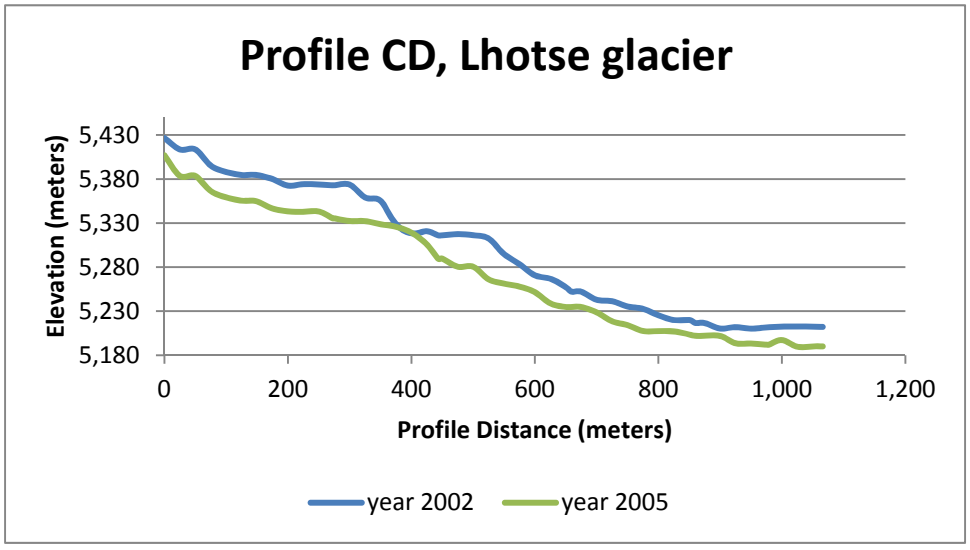

Figure 4.58 Profile CD, Lhotse Glacier

Transect CD (Figure 4.58) of Lhotse glacier provides evidence of glacier melting as shown in the elevation changes which appeared in 2002-2005 intervals.

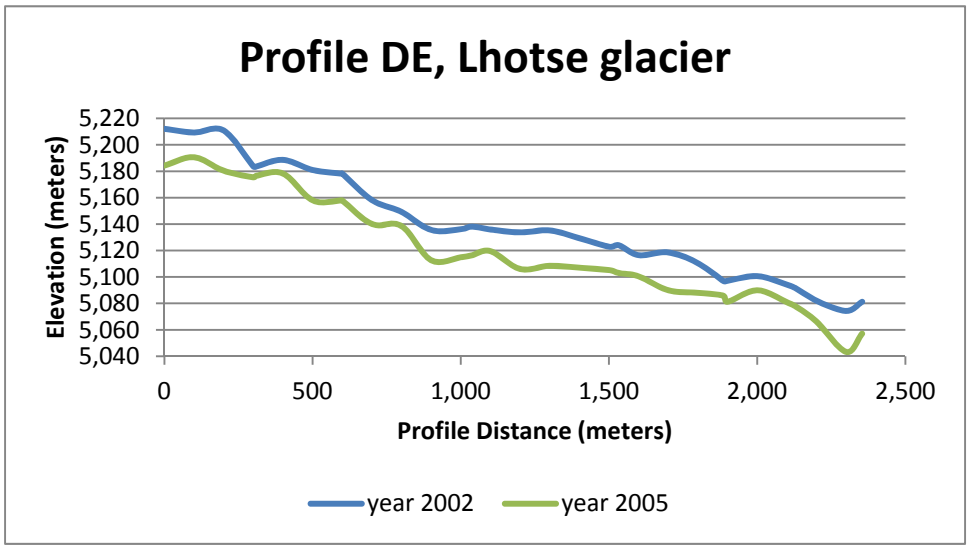

Figure 4.59 Profile DE, Lhotse Glacier

Lhotse glacier profile DE (Figure 4.59) portrays similar constant glacier mass losses except for distances of 2,040-2,200m from 2002 to 2005.

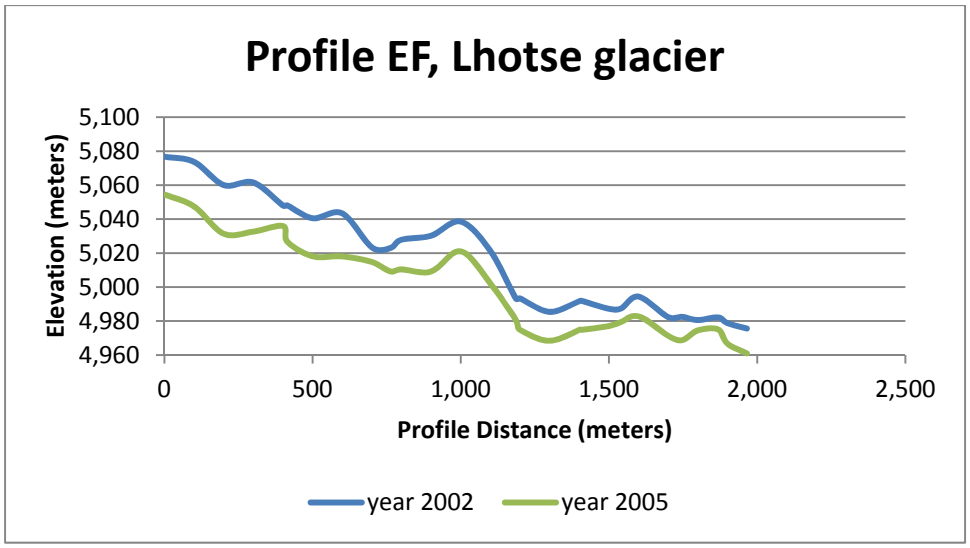

Figure 4.60 Profile EF, Lhotse Glacier

Evaluation of cross section EF (Figure 4.60) of Lhotse glacier 2002 and 2005 DEMs shows dissipation of glacier masses within time period evaluated. The largest volumetric changes appeared within distance of the glacier 0 - 600m and this was a fairly constant trend.

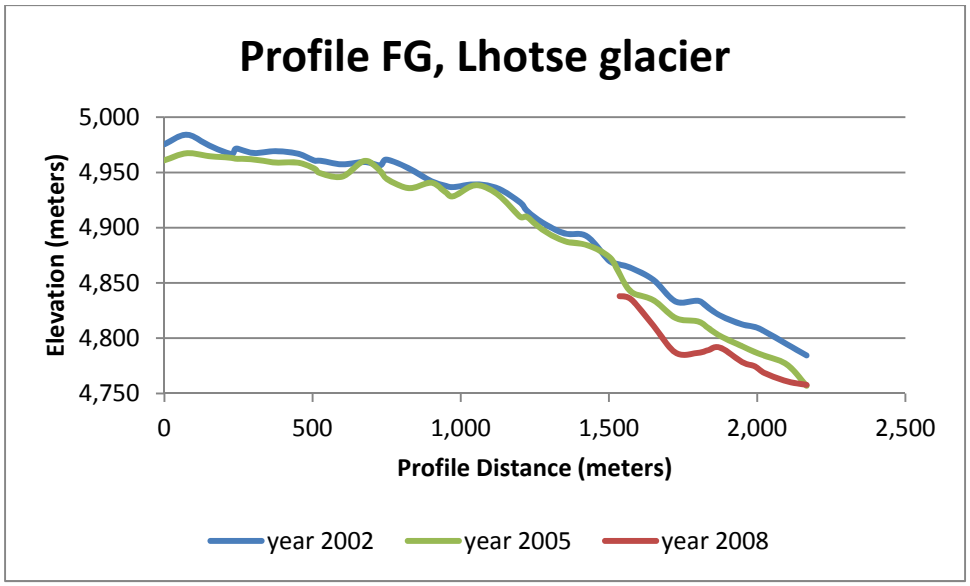

Figure 4.61 Profile FG, Lhotse Glacier

Lhotse glacier's profile FG (Figure 4.61) shows glacier melting which occurred from 2002 - 2005. The largest mass changes of profile FG occurred at distances of 1,480-2,200m.

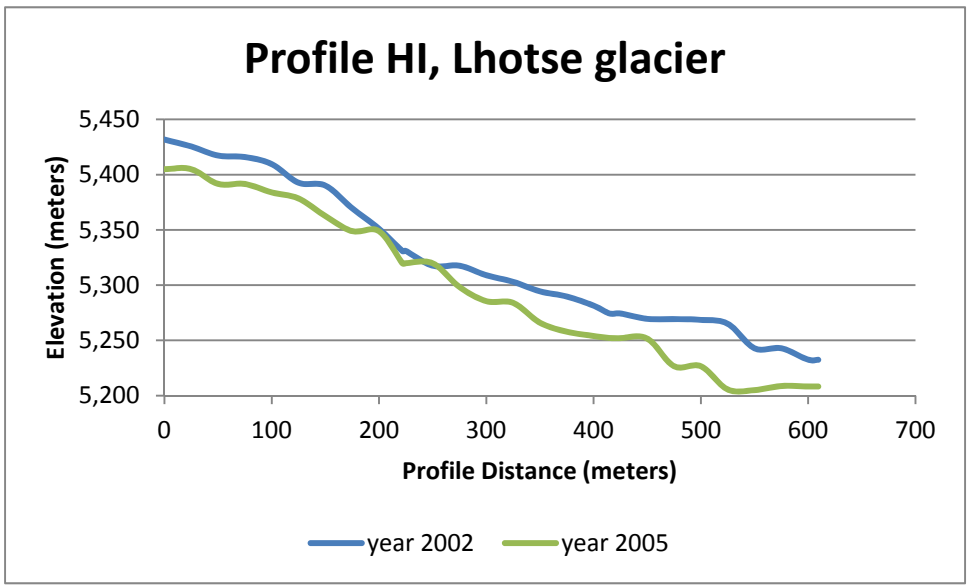

Figure 4.62 Profile HI, Lhotse Glacier

Transect HI (Figure 4.62) of Lhotse glacier's profile FG shows quantifies a linear correlation of glacier mass losses which was observed from 2002-2005. The largest transect FG glacier changes occurred at 500m distance.

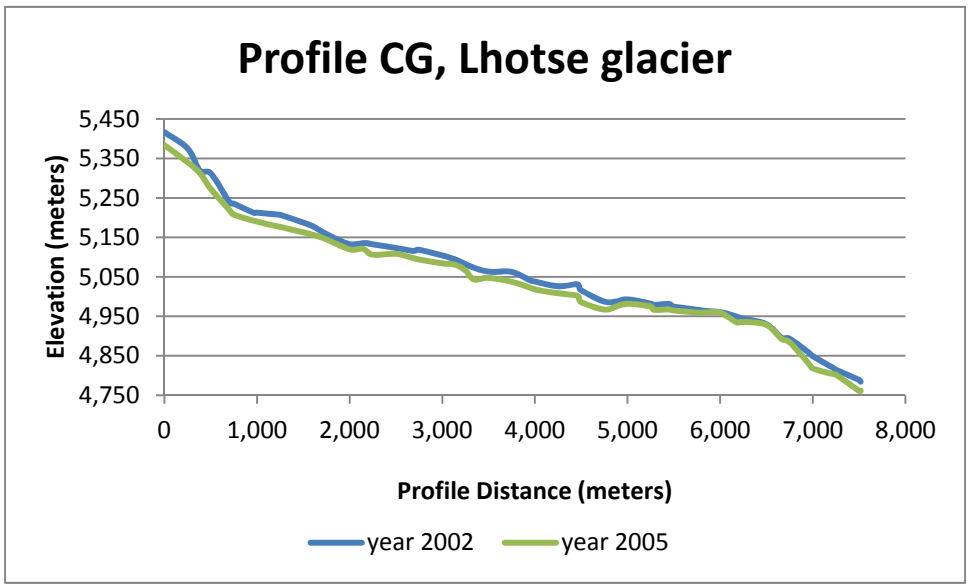

Figure 4.63 Profile CG, Lhotse Glacier

4.1.8 Imja Glacier

Imja glacier (Figure 4.64) covers an area 14.07 sq. km according to glacier boundary digitized based on ASTER 15m resolution image. The glacier tongue stands at an elevation of 5,000m and extends up to an elevation of 6,170 m at its glacial head. Imja glacier stands at the south east base of Mt. Everest. Lhotse Shar and Ambulpacha glaciers are the two tributaries that join Imja glacier. All of the melt products from these three glaciers drains into Dudh Koshi Basin and finally to Ganges River into the Indian Ocean. The relief difference is almost 1,200m within 9km which makes it a steep slope. The Imja

Tsho normally called Imja Pro-Glacial Lake stands at the base of Imja glacier at an elevation of 5,000m. As being part of Himalayan glacier it accumulates snow mass in through summer accumulation rather than winter precipitation through May till mid-September (Benn & Owen, 2002).

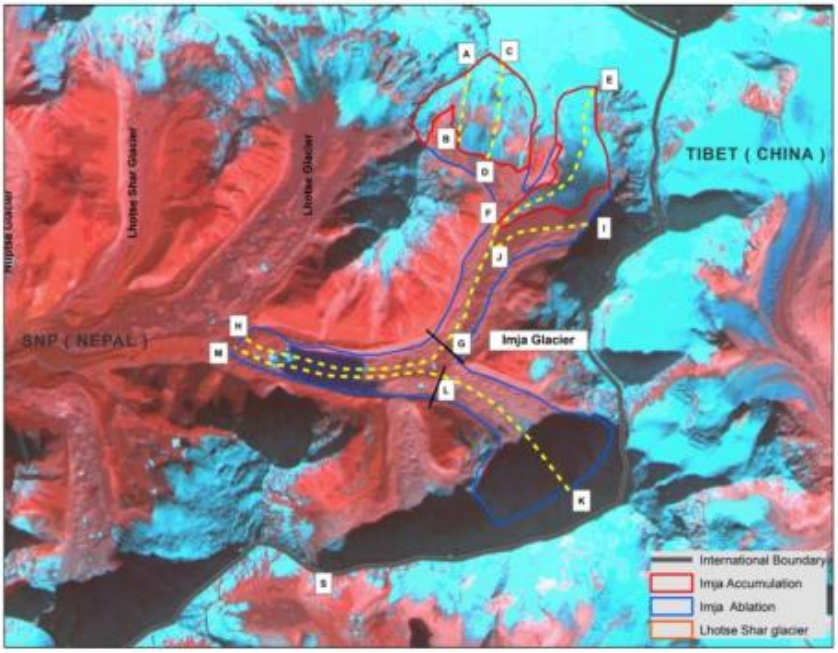

Figure 4.64 Location of Imja Glacier in SNP region

The mean elevation of Imja glacier decreased in 2005 compared to (Table 4.12) based on the DEMs created. Imja glacier was covered only in 2002 and 2005 DEMs; hence data from 2008 and 2010 DEMs could not be extracted.

Table 4.12 Mean Elevation of Imja Glacier in meters

Mean elevation of Imja glacier (meters)		
glacier Year	2002	2005
Imja	5444.47	5428.026

Mass balance of Imja glacier for the year 2002-2005 DEMs was -3.4 ± 0.31 m.w.e.a-1 for clean ice (C-Type) and -3.1 ± 0.27 m.w.e.a-1 for debris covered (D-type). Bolch et al. (2011a) found a combined Lhotse Shar/Imja glacier mass balance -0.50± 0.09 m.w.e.a-1 for the period of 1970-2007 based on glacier area covered by DTM of 8.65 sq. km.; however, the glacier size was reported as 10.7 sq. km. Similarly, mass balance for the same combined glacier reported was -1.45 ± 0.52 m.w.e.a-1 for the period of 2002-2007 for common area of 8.87 sq. km in DEMs. However, this result cannot be compared, as Bolch et al. (2011a), combined Lhotse Shar/Imja glaciers together, whereas this study results is only for Imja glacier. Both independent studies have shown negative mass balance over the same period signifying glacier mass melt in Imja glacier and its tributaries glacier.

Surface elevation profile in accumulation and ablation area was studied to evaluate the volumetric changes of glaciers at various profiles across the Imja glacier. The study demonstrated surface lowering in the majority of Imja glacier transects which clearly indicates individual and cumulative reduction in glacier mass.

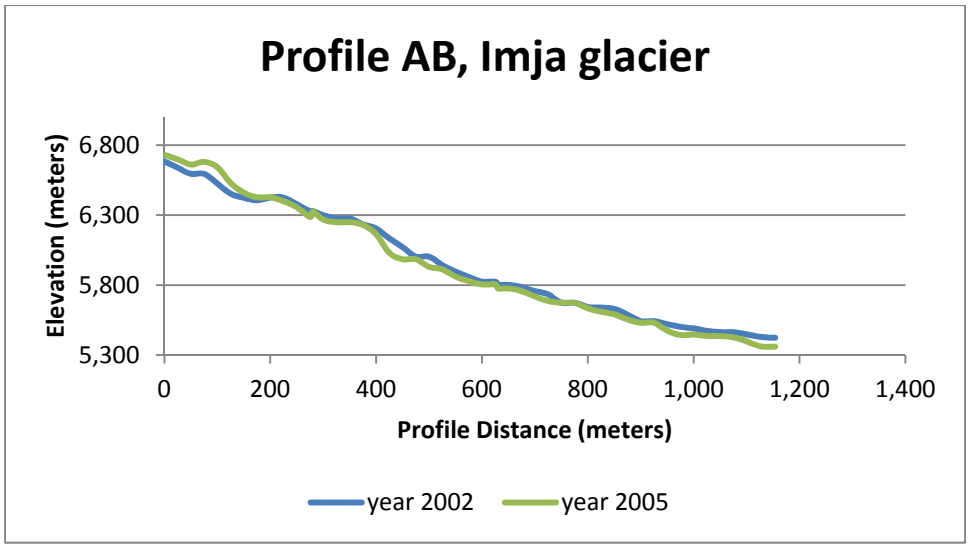

Figure 4.65 Profile AB, Imja Glacier

Cross section AB of Imja glacier (Figure 4.65) showed slight glacier mass increases in the 0 - 200m accumulation area of the glacier and volumetric decreases for the remaining portion of the glacier with distances of 200m - 1,100m for the years 2002 and 2005.

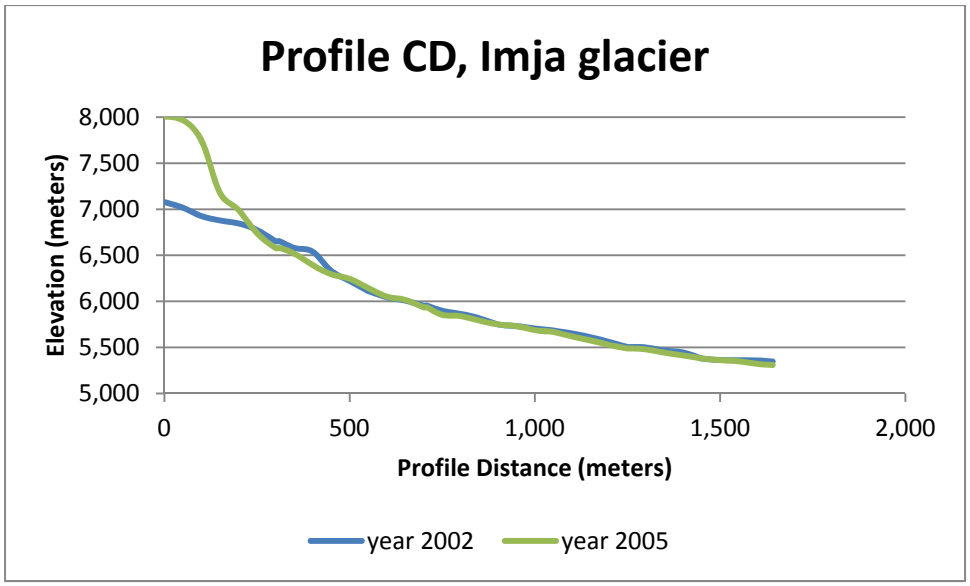

Figure 4.66 Profile CD, Imja Glacier

Imja glacier transect CD(Figure 4.66) exhibited sizeable glacier mass increases from 0 - 200m within the ablation region, quantifiable glacier melt at distances 320-580m, and limited elevation changes within the glacier from 1,800m - 1,640m from 2002 to 2005.

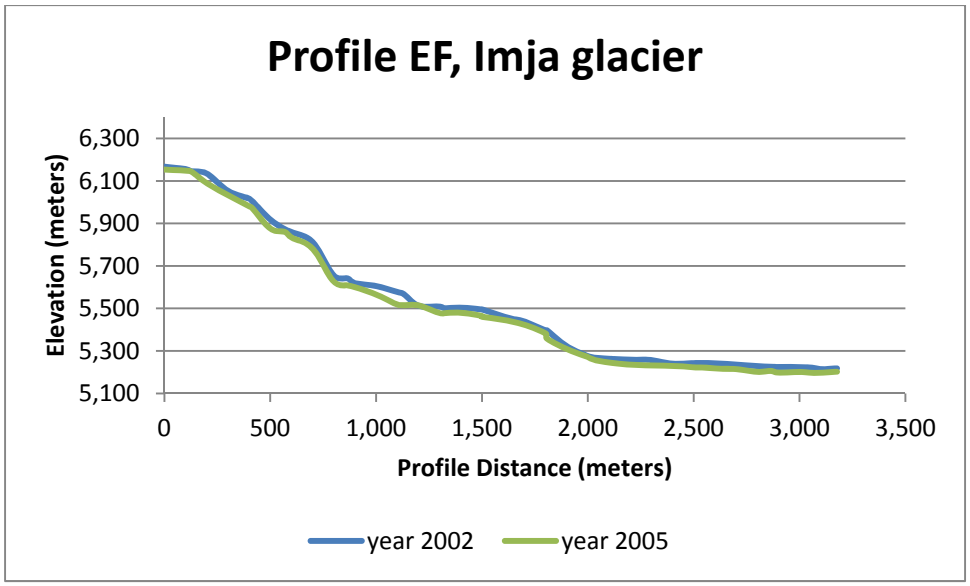

Figure 4.67 Profile EF, Imja Glacier

Analysis of Imja glacier profile EF(Figure 4.67) employing 2002 and 2005 DEMs established almost consistent volumetric mass losses which occurred during this time with the only exception being at 1,200m where there was a slight increase in glacier mass.

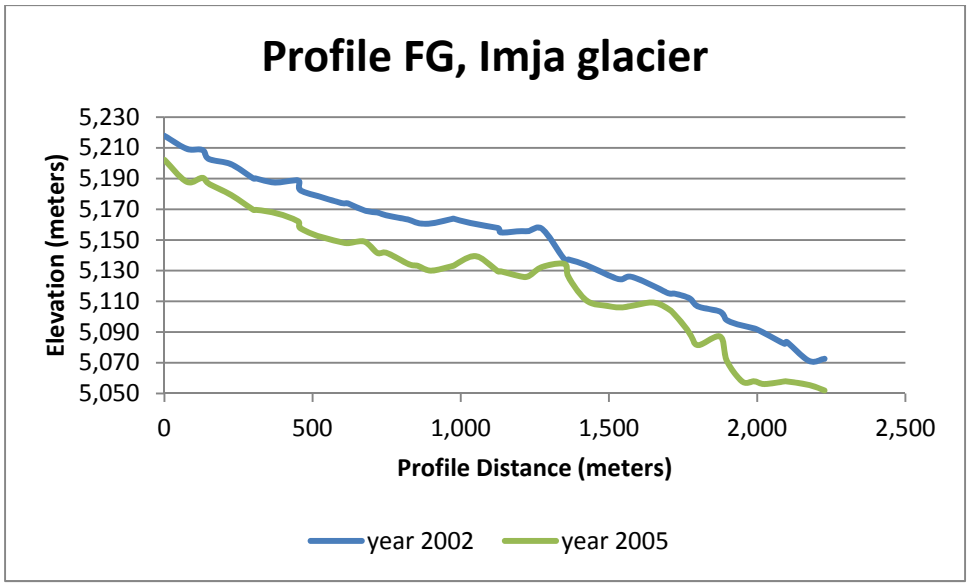

Figure 4.68 Profile FG, Imja Glacier

Cross section FG (Figure 4.68) of Imja glacier showed measurable volumetric mass losses that occurred from 2002 - 2005. The most significant mass losses occurred at 2,000m within the glacier with elevation changes of 50m.

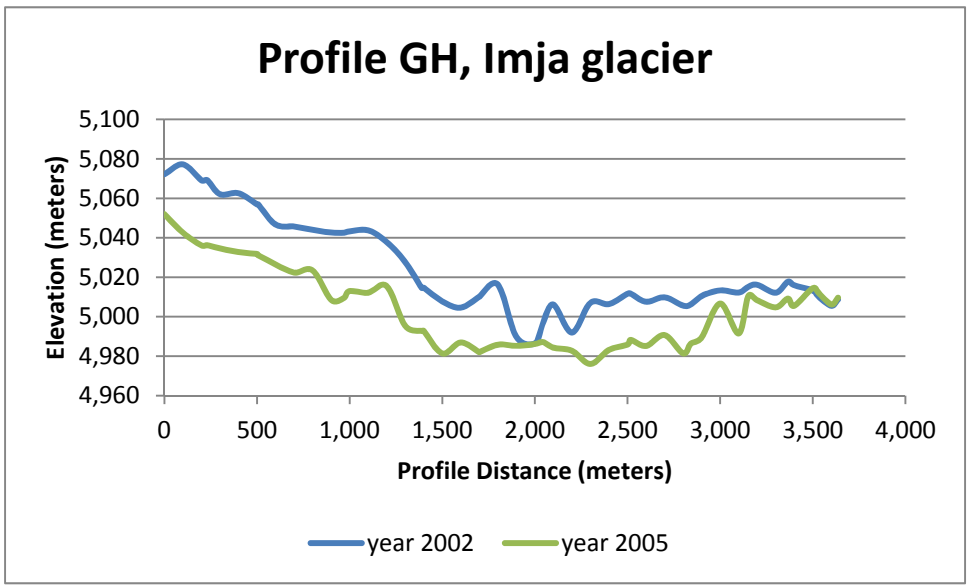

Figure 4.69 Profile GH, Imja Glacier

There was a general trend of glacier melt that appeared in profile GH (Figure 4.69) of Imja glacier for all distances except near 2,000m. This exception at 2,000m is an outlier in the DEMs.

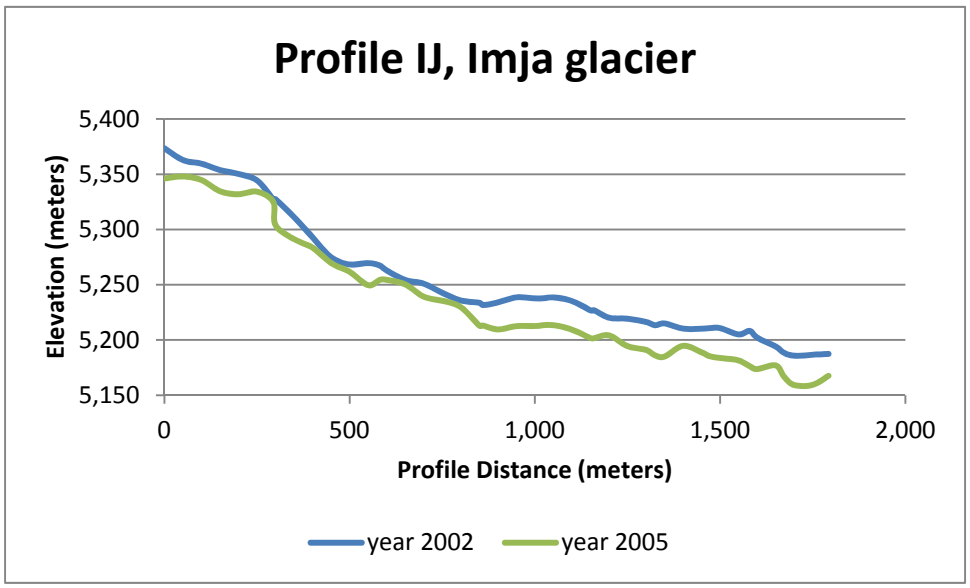

Figure 4.70 Profile IJ, Imja Glacier

Imja glacier transect IJ (Figure 4.70) illustrated a general trend of glacier melting from 2002 - 2005. The largest mass losses within this glacier occurred at distances of 0 - 200m.

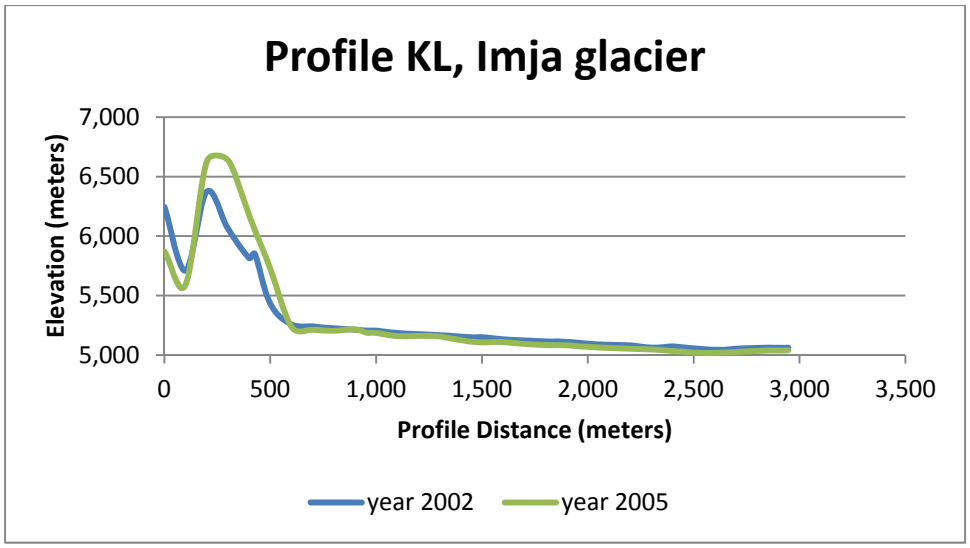

Figure 4.71 Profile KL, Imja Glacier

Profile KL (Figure 4.71) of Imja glacier exhibited an accumulation of snow from an estimated 250 – 500m from 2002 to 2005. From the 500-3,000m range there was a slight reduction in mass balance with an increase in calendar years from 2002 to 2005.

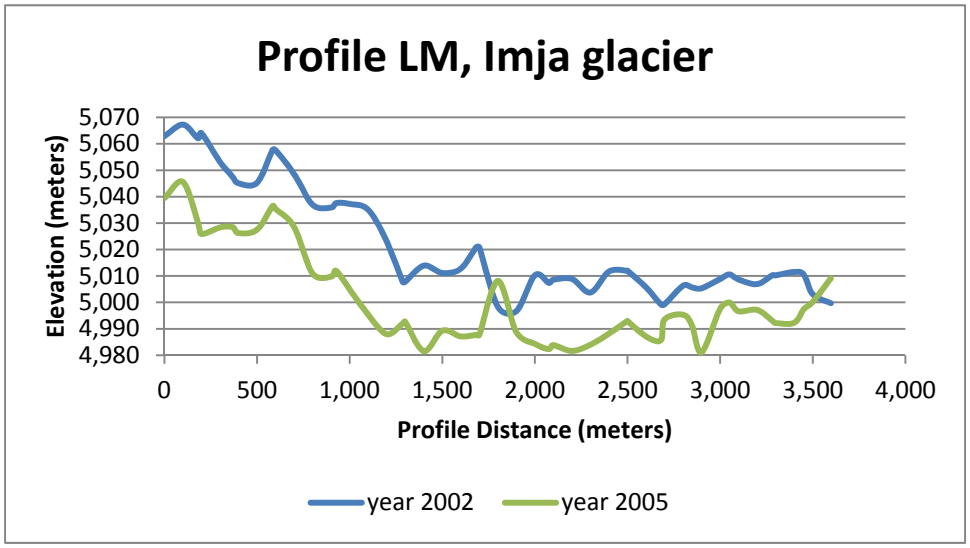

Figure 4.72 Profile LM, Imja Glacier

Significant volumetric losses in transect LM (Figure 4.72) of Imja glacier occurred throughout the entire glacier except at 3600m distance which experienced some accumulation.

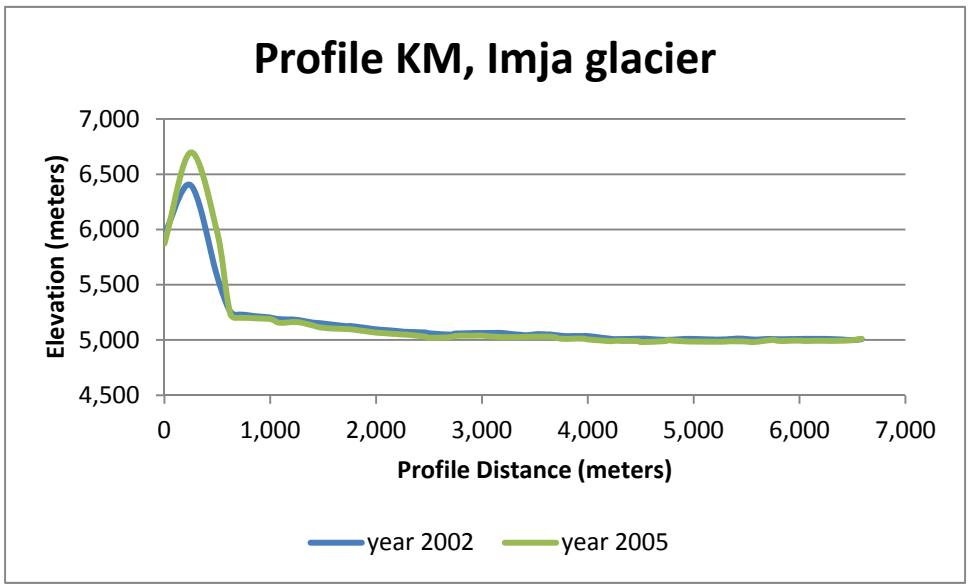

Figure 4.73 Profile KM, Imja Glacier

The glacier transect KM (Figure 4.73) exhibited an increase in snow from 0 - 900m from 2002 to 2005 (Figure 4.74). The mass balance of cross section KM remained fairly constant from 1,000 – 6,500m during 2002 to 2005 and showed no significant changes.

4.1.9 Results and discussion objective 1

I reject the first hypothesis, because there was a general reduction in glacier mass balance in the study area. Figure 4.1, which compared elevations of all the DEMS with AGDEM produced from NASA demonstrated that these DEMS were within acceptable

ranges to be further utilized in mass balance estimations. Additionally, the comparisons of the surface lowering of the studied glaciers within the Himalayas correlated with results found by other researchers within the Himalayan mountain range (Bolch et al. 2011a).

4.2 Planimetric changes in Imja glacial Lake

The research showed that within the last three decades (1975-2010), the Imja glacier lake increased in surface area by about 268% (Table 4.13, Figure 4.75, Figure 4.75) and estimation from five September images (1992-2009) incline to be 58% (Figure 4.76) indicating glacier melt around the lake area showing sign of glacier retreat in SNP region. During image analysis many small lakes were found and earlier small lakes merged to form larger ones indicating a future sign of forming numerous potential GLOFs hazard lakes.

Table 4.13 Data Acquisition Date and Area Change of Imja Glacier Lake

Acquisition Date	Area (sq.km)	Change (sq.km)/yr		Acquisition Date	Area (sq.km)	Change (sq.km)/yr
12 March, 1975	0.286	0		05 Jan, 2002	0.867	0.035
20 March, 1977	0.336	0.05		02 Nov, 2004	0.905	0.039
06 Jan, 1979	0.421	0.085		16 Nov, 2006	0.913	0.008
17 Jan, 1989	0.507	0.086		06 Jan, 2008	0.94	0.027
22 Sept, 1992	0.636	0.129		15 Oct, 2009	1.03	0.09
28 Sept, 2000	0.832	0.196		25 April, 2010	1.053	0.023

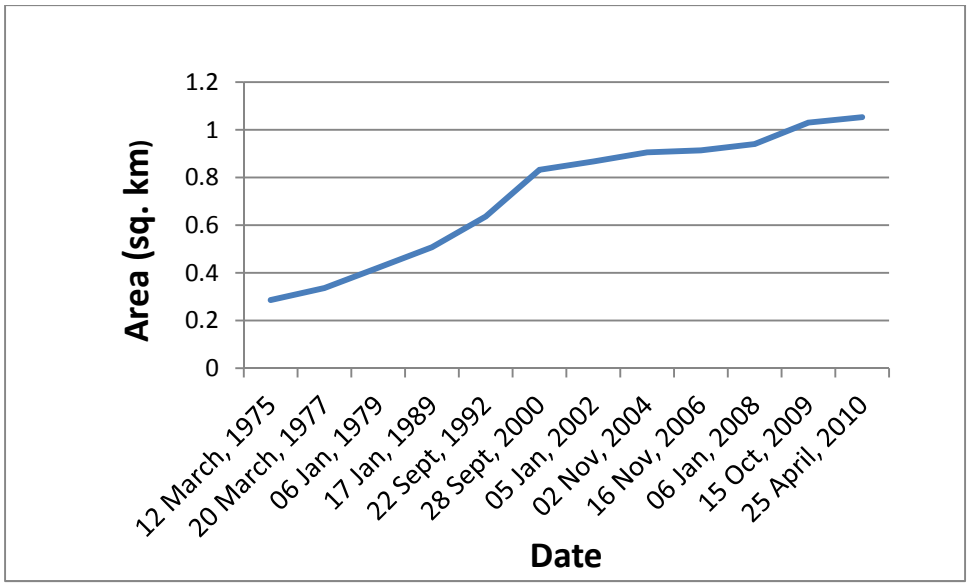

Figure 4.74 Surface Area of Imja Glacial Lake Increase (1975 - 2010)

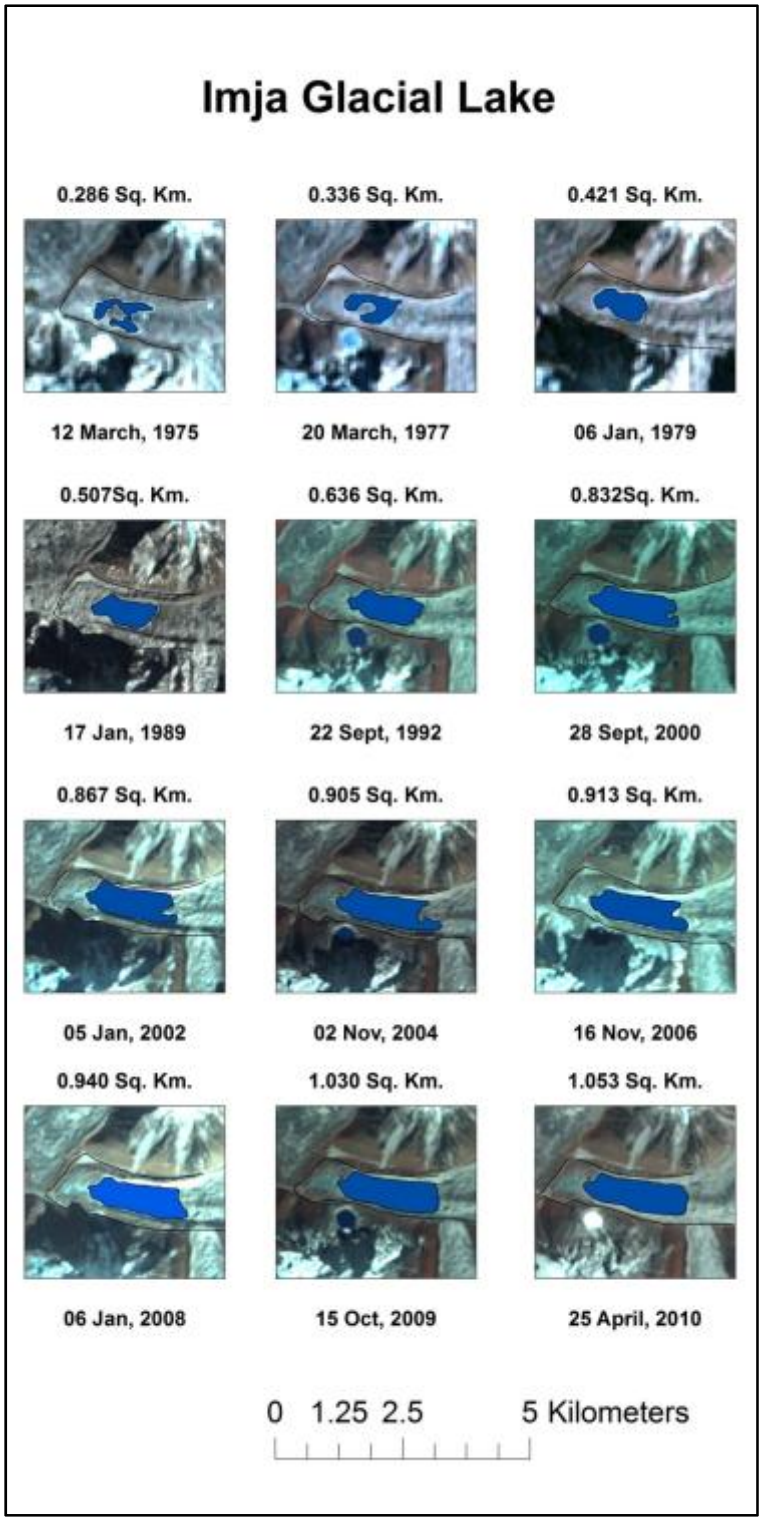

Figure 4.75 Imja Lake surface area change 1975-2010 period

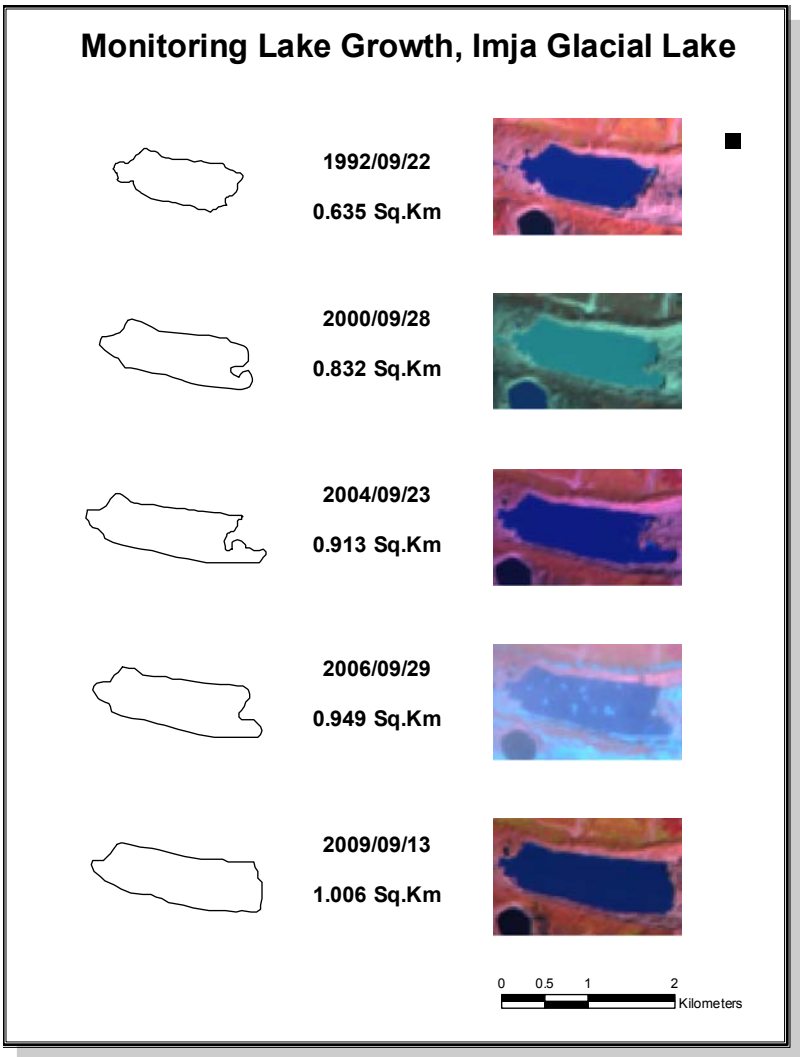

Figure 4.76 Area of Imja Glacier in September Images - 1992-2009

This study, however, has its own inherent limitations. A 30m Landsat image, which is a medium resolution image, was utilized in this study. Higher resolution data will facilitate a more precise demarcation of the glacial lakes and more accurate results can be expected.

The results from the study show that the Himalayan glaciers are continuously melting causing the development and expansion of glacial lakes. The Imja glacial lake in

Nepal is an example for impact of glacial retreat in the form of development of glacial lakes. ICIMOD study prevails only in Nepal and twenty of such potential GLOFs hazard lakes (Figure 4.77) that can trigger at any time in future.

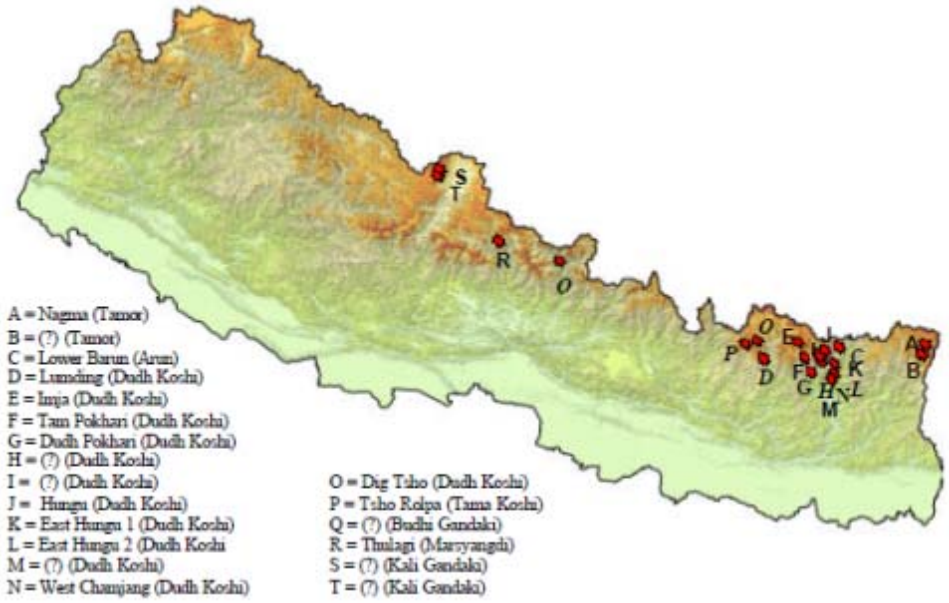

Figure 4.77 Location of Potential GLOFs Hazard Lake

Source: ICIMOD

The surface area of the Imja Lake expanded about 268% between 1975 and 2010. As this lake is located in one of the toughest and rugged landscapes, repeated field visits to the lake is very expensive and time consuming. Therefore, monitoring such lake through satellite images will be a more cost efficient approach to track these glacier retreat changes that can affect local livelihoods. However, to improve the accuracy of the measurements, high resolution satellite images may be more appropriate than medium resolution Landsat data. Monitoring of glacial lakes will thus provide information to

properly develop hazard mitigation plans to protect the lives of people, infrastructure, and the natural resources.

The glacial mass loss in the Imja glacier is linked with the increase in area and volume of Imja glacial lake. This lakes existence was unknown before 1962 (Fujita et al.2009). The lake area increased from 0.08 sq. km. in 1957 to 0.3 sq. km. in 1975, whereas the area in 1997 was 0.6 sq. km and increased to 0.9 sq. km. in 2007 (Bajracharya et al. 2009). This linear increase in lake area over the years supports the perceived information that the Imja glacier is retreating and provides evidence that this impact is also affecting other glaciers in the same area.

4.3 Results and discussion objective 2

I reject the 2nd hypothesis because area of Imja glacial lake has increased during the study period. The second hypothesis of this research which stated the implementation of remote sensing method will augment monitoring of glacial lake formations that can create glacial lake outburst floods was proven in this research. Figure 4.75, Figure 4.76 and Table 4.13 illustrate that the increase in Imja glacial lake surface areas doubled in size from 1989 - 2010. Several lakes within the Himalayan range have formed glacial lakes as a result of glacial melt which subsequently caused glacial lake outbursts as discussed in the Chapter 2, Literature Review. This thesis research has proven that Imja Lake currently threatens the down valley area with the possibility of a glacial outburst.

4.4 Study the temperature variation in the study area

Quantify temperature variations in the study area using Moderate Resolution Imaging Spectroradiometer (MODIS), Land Surface Temperature and Emissivity 8-Day L3 Global Satellite (MOD11A2) images with 1km resolution.

The average summer mean temperature for the last decades (2000-2010), around SNP area was measured using MODIS MOD1A product (Figure 4.78). There was no significant change in temperature during the period. However, the increase in global temperature and its effects have been shown locally and the melting of glacier causes the formation of glacier lake (Campbell 2005; Dyurgerov and Meier 2000). The study showed some slight increase in various months (Table 4.14, 0, Figure 4.78). 2002 - 2005 periods consist of most of the glacier present in both years DEMs, and in this period, the temperature rise can be seen in later years (Figure 4.79).

Table 4.14 Average Maximum Temperature of The Study Area using MODIS Image from 2000-2011

	Jan	Feb	Mar	Apr	May	Jun	Jul	Aug	Sep	Oct	Nov	Dec
2000-2005	12.68	15.44	18.9	21.96	22.81	20.84	16.13	16.64	17.25	17.83	15.76	14.38
2006-2011	17.6	19.49	23.63	27.75	28.7	25.95	20.33	20.92	21.95	22.25	21.21	19.36
Average Max Temp	14.64	17	20.69	24.19	25.17	22.95	17.65	18.22	19.19	19.62	18.26	17.56

Table 4.15 Trends in Monthly Average Maximum Temperature

	Jan	Feb	Mar	Apr	May	Jun	Jul	Aug	Sep	Oct	Nov	Dec
Slope	0.376	0.03	0.113	0.058	-0.02	0.027	0.108	0.13	0.043	-0.052	0.113	0.086
Constant	15.151	19.304	22.903	27.377	28.826	25.775	19.628	20.072	21.668	22.587	20.559	18.834
R^2	0.2462	0.001	0.032	0.017	0.011	0.001	0.027	0.079	0.008	0.032	0.093	0.041

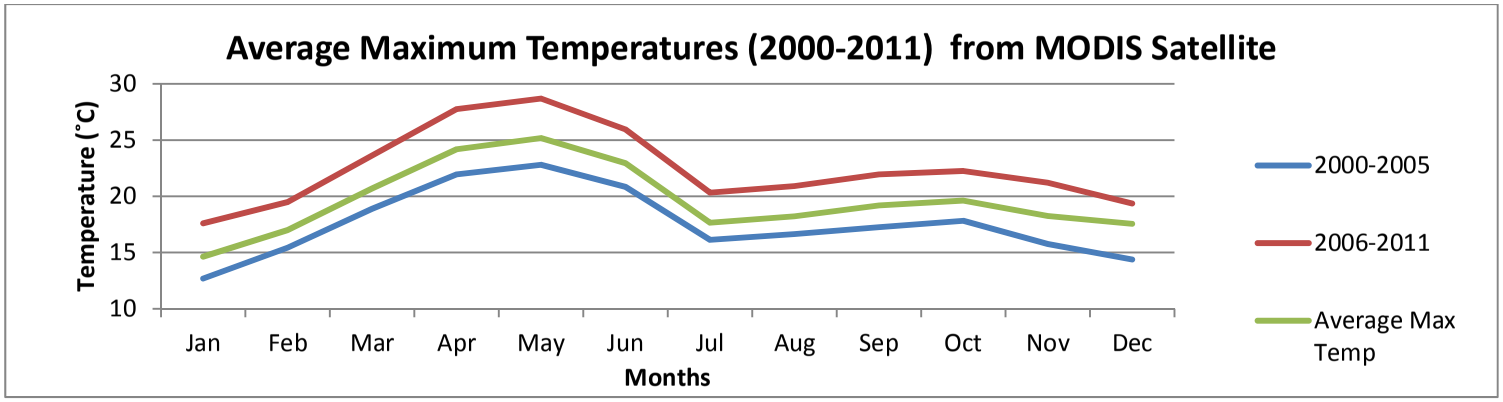

Figure 4.78 Average Maximum Temperature Compared with 2000-2005 and 2006-2011 Periods

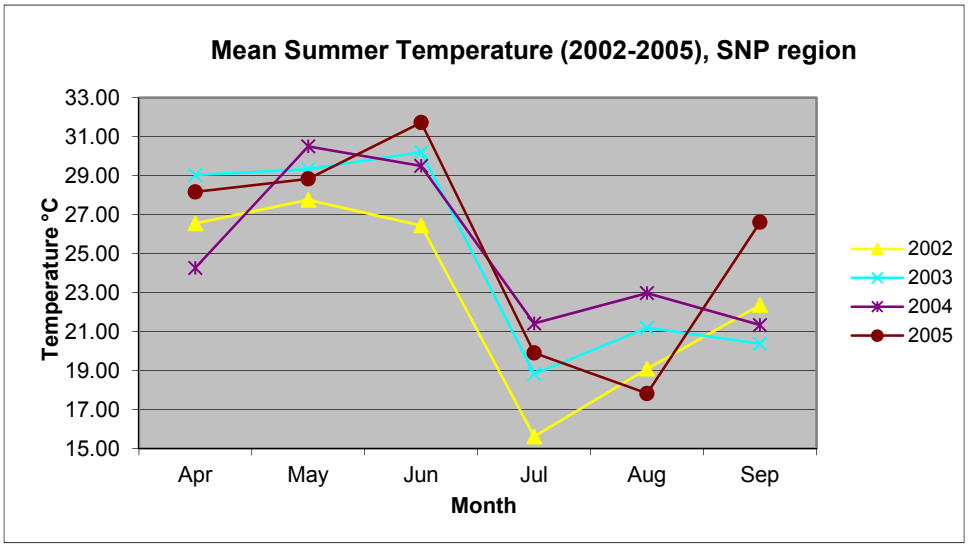

Figure 4.79 Temperature of The Study Area for the Period 2002-2005

4.4.1 Result and discussion for objective 3

I reject the third hypothesis because local temperature has increased during the study period. However, it was not validated with field data.

One of the study's limitations was ascertaining this information from one satellite MODIS which had 1km pixel size of the study area. Perhaps, if there were meteorological stations around the glacial area, high accuracy temperature information could have been acquired for temperature data interpretation.

CHAPTER V

CONCLUSION AND RECOMMENDATIONS

This study tried to bridge a data gap on mass balance of Himalayan glaciers employing the geodetic method for the period 2002-2005 and 2002-2008 using ASTER satellite images. This study also used Landsat images from 1972-2010 to evaluate temporal changes in glacier lake surface areas in inaccessible terrain, and determined the temperature variation over time around the study area using MOD11A product from MODIS satellite images. ASTER images showed a high accuracy in all of the statistical analyses as shown in Chapter 4 Results and Discussion. Uncertainty tests showed accuracy ±10m in between elevation changes of the DEMs when compared to the 1:50,000 topographic maps published by Department of Survey, Nepal. Hence, ASTER image can produce significant results in mass balance calculation using geodetic method.

Since, all glaciers were not covered in a particular DEM; glaciers common to at least two DEMs, their mass balances were estimated. Most of the studied glaciers in the study area showed a negative trend of mass balance which is commonly referred to as glacier mass reduction. For the period 2002-2005, an area of nearly 70 sq. km. average glacier surface of the overall study area lowered by -4.79m with a reduction in mass balance -2.978 ± 0.89 m.w.e.a-1. The results of the separate mass balance studies of 2002-2005 and 2005-2008 DEMs in the clean ice area referred to as accumulation (C-Type) and debris covered termed as (D-Type) were quantitatively analyzed (Table 4.3-

4.8). The results were compared to previously published peer reviewed journal for the same area by (Bolch et al. 2011b) as it has estimated mass balance with remote sensing employing various satellite images, aerial photographs, topographic maps coupled with field collected GCPs. Most of the glaciers within the SNP area showed negative mass balance in this study as well as Bolch et al., study. The research results were not validated with in-situ data from the SNP area; however, this study's results are very similar to the results obtained by (Bolch et al. 2011b). These two independent studies showed negative trends reflecting glacier mass balance reductions in the SNP region of the Himalayan mountain range.

To ascertain the causes of the negative mass balance of glaciers; further research was employed to evaluate surface profile changes along various glacier cross-sections caused by an increase in temperature. Interpretation of MODIS satellite temperature data of the study area from 2000-2011 showed an increase in temperature. The absence of meteorological stations introduced data gaps in climatic data such as precipitation, temperature, and solar radiation. Temperature data extracted from the MODIS images were not validated because of unavailability of temperature data from the field.

Almost all of transects showed lowering glacier surface over the evaluated years. This study's results provided evidence that multi-temporal DEMs can assist researchers in the determination of mass balance trends and glacial retreat that could not be realized utilizing in-situ methods. Geodetic method employed in this study is a cost-effective approach for scientists to continually monitor glaciers at regular intervals to create accurate glacier retreat and GLOF predictions. As proven in this study geodetic method is a research tool that provides more information over a short period than any other

methodology. The glacier surface profiles at all transects showed more melt occurred in later years indicating more glaciers will melt in the future if this trend continues. Hence, the future of this research would be improving accuracy of DEMs by introducing GCPs from the study. This will help to georeference and calibrate vertical elevation of DEMs for an improved elevation change analysis. Hence, more accurate mass balance estimation could be presented in local as well in regional areas.

Glacier mass melting is a normal phenomenon due to change in local and regional weather, as it helps millions of people providing sources of fresh water during the dry season. However, glacier mass melting more than normal presents the negative aspects of glacier melt at high altitudes in the Himalayas which causes the formation of glacial lakes. Glacial lakes are formed by melting ice and snow collected on relatively level surfaces or melt water from small glaciers at the end of glacier tongue over large amounts of time. This study illustrated the advantages of using remote sensing technology to monitor such lakes in high rough terrain utilizing Landsat images. This study evaluated three decades of surface analyses and quantified a linear increase in glacial lake surface of Imja Glacial Lake by 268%.

The recommendation to augment this thesis research is to acquire bathymetric data to calculate volume of water and generate a more accurate model to predict surface area and water volume increases in the future. Such studies should focus on moraine dam stability, moraine dam formation, geological material inside of these dams, and how these aforementioned factors are changing with time. This recommended study should ascertain information from local inhabitants that would facilitate understanding amongst scientists in regard to the amount of hazard mitigations that should be implemented to

protect their livelihoods without being overly costly to the society and preserve historically, culturally and socially attached emotions to one of the World Heritage Site listed under UNESCO.

More detailed studies coupling mass balance changes with temperature, precipitation, wind, solar radiation need to be performed. This helps to create long standing prediction pattern for glacier melts. Scientists and engineers can implement hazard mitigation structures in appropriate locations to protect the general population. The parameters from DEMs, surface slope, aspect, and solar radiation can be assimilated for generating models which will predict the possible areas for glacial lake development as well as creating an estimated rate of water discharge volume in the event of GLOFs.

This study provided evidence remote sensing is a good and convenient tool for glacier monitoring, glacier mass balance evaluation, and in ascertaining site specific information to make informed decisions in regards to crisis management in the case of possible GLOFs. Stating this doesn't mean, all variables associated with glacier studies can be acquired from satellite imagery. In fact, in-situ data and local interaction with people on changes they faced over period needs to be evaluated and will be the key information to validate the result.

REFERENCES

Ageta, Y., and T. Kadota. 1992. Predictions of changes of glacier mass balance in the Nepal Himalaya and Tibetan Plateau: a case study of air temperature increase for three glaciers. *Annals of Glaciology* 16: 89-94.

Ageta, Y., and K. Higuch. 1984. Estimation of mass balance components of a summer-accumulation type glacier in the Nepal Himalaya. *Geografiska Annaler* 66A: 249-255.

Ambinakudige, S. 2010. A study of the Gangotri glacier retreat in the Himalayas using Landsat satellite images. *International Journal of Geoinformatics* 6 (3): 7-12.

Ashish, A., V. Joshi, A. Sharma, and S. Anthwal. 2006. Retreat of Himalayan glaciers - indicator of climate change. *Nature and Science* 4: 53-60.

Asahi K., and T. Watanabe. 2001. "Past and recent glacier fluctuation in Kanchenjunga Himal, Nepal". *Journal of Nepal Geological Society* 22: 481-490.

Bajracharya, S., and P. Mool. 2009. Glaciers, glacial lakes and glacial lake outburst floods in the Mount Everest region, Nepal. *Annals of Glaciology* 50 (53): 81-86.

Bajracharya, S., P. Mool, and B. Shrestha. 2007. *Impact of Climate Change on Himalayan Glaciers and Glacial Lakes: Case Studies on GLOF and Associated Hazards in Nepal and Bhutan,169*. ICIMOD, Katmandu, Nepal.

Bamber, J., and R. Kwok, 2004. *Remote-sensing techniques, in: Mass balance of the Cryosphere: Observations and modeling of contemporary and future changes.* Eds: Bamber, J. L. and Payne, A. J. Cambridge University Press, Cambridge.

Bamber, J., and A. Rivera. 2007. A review of remote sensing methods for glacier mass balance determination. *Global and Planetary Change*, 59: 138-148.

Roger, B. 2006. The Status of Research on glaciers and Global glacier Recession: a Review. *Progress in Physical Geography,* 30 (3): 285-306.

Douglas, B., and L. Owen. 2002. "Himalayan Glacial Sedimentary Environments: a Framework for Reconstructing and Dating the Former Extent of glaciers in High Mountains." *Quaternary International* 3 (25): 97-98.

Berthier, E., Y Arnaud, R. Kumar, S. Ahmad, P. Wangnon, and P. Chevallier. 2007. Remote Sensing Estimates of Glacier Mass Balances in the Himachal Pradesh (Western Himalaya, India). *Remote Sensing of Environment* 108:327-338.

Bolch T., T. Pieczonka, and D. Benn. 2011. Multi-decadal mass loss of glaciers in the Everest area (Nepal, Himalaya) derived from stereo imagery. *Cryosphere* 5:349-358.

Bolch, T., M. Buchroithner, T. Pieczonka, & A. Kunert. 2008. Planimetric and volumetric glacier changes in Khumbu Himalaya since 1962 using Corona, Landsat TM and ASTER data. *Journal of Glaciology* 54: 592-600.

Bolstad, P. 2002. *GIS Fundamentals: A First Text on Geographic Information Systems*, 1st. ed. Minnesota: Eider Press.

Boresjo-Bronge, L. and C. Bronge. 1999: Ice and snow-type classification, using Landsat-TM data and ground radiometer measurements. *International Journal of Remote Sensing,* 20: 225-240.

Braithwaite, R. 2002. Glacier mass balance: the first 50 years of international monitoring. *Progress in Physical Geography,* 26 (1):76-95.

Casey, K., A. Kaab, and D. Benn. 2012. Geochemical characterization of supraglacial debris via in situ and optical remote sensing methods: a case study in Khumbu Himalaya, Nepal. *The Cryosphere* 6:85-100.

Church J., N. White, T. Aarup, W. Wilson, P. Woodworth, C. Domingues, J. Hunter, and K. Lambeck. 2008. Understanding global sea levels: past, present and future. *Sustainability Science,* 3 (1):9-22.

Clague, J., and S. Evans. 2000. A review of catastrophic drainage of moraine-dammed lakes in British Columbia. *Quaternary Science Reviews* 19: 1763-1783.

Dyurgerov, M., and M. Meier. 1997a. Mass balance of mountain and sub polar glaciers: a new assessment for 1961–1990. *Alpine Research* 29: 379-391.

Dyurgerov, M., and M. Meier. 1997b. Year-to-year fluctuations of global mass balance of small glaciers and their contribution to sea level changes. *Arctic and Alpine Research*, 29:392-402.

Dyurgerov, M. and M. Meier. 2000a. Analysis of Winter and Summer Glacier Mass Balances. *Geografiska Annaler*: Series A, *Physical Geography* 81 (4).

Dyurgerov, M. and M. Meier. 2000b. Twentieth century climate change: Evidence from small glaciers. *Proceedings of the National Academy of Science* 97(4):1406-1411.

Frenierre, Jeff. 2009. "Measuring the Mass Balance of Mountain glaciers: A Review of Techniques and Recent Investigations" (Geography 3720 Lecture: Mountain Environments and Sustainability), 1-23. http://www.lafrenierre.net/uploads/9/7/8/4/978415/mass_balance_of_mountain_glaciers.pdf. Last accessed on 11/27/2012.

Fujisada, H. 1994. Overview of ASTER instrument on EOS-AM1 platform. Proceedings of SPIE. *The International Society for Optical Engineering*, 2268: 14-36.

Fujisada, H. 1998. ASTER level 1 data processing algorithm. *IEEE Transactions on Geoscience and Remote Sensing* 36 (4): 1101–1112.

Fujita, K., T. Kadota, B. Rana, R. Kayastha, and Y. Ageta. 2001. Shrinkage of glacier Ax010 in Shorong region, Nepal Himalayas in the 1990s. *Bulletin of Glacier Research,* 18: 51-54.

Fujita, K., L. Thompson G., Y. Ageta et al. 2006. Thirty-year history of glacier melting in the Nepal Himalayas. *Journal of Geophysical Research*, 111(D03109).

Fujita, K., A. Sakai, T. Nuimura, S. Yamaguchi, and R. Sharma. R. 2009: Recent changes in Imja Glacial Lake and its damming moraine in the Nepal Himalaya revealed by in situ surveys and multi-temporal ASTER imagery, Environmental Research Letters, 4(045205).

Fushima, H. and T. Ohata. 1980. Fluctuations of glaciers from 1970 to 1978 in the Khumbu Himal. *Report of the Glaciological Expedition to Nepal: Part 4. Seppyo, Special Issue*, 41:71-81.

Gao, J., and Y. Liu. 2001. Applications of remote sensing, GIS and GPS in glaciology: a review Applications of remote sensing, GIS and GPS in glaciology: a review. *Progress in Physical Geography,* 25(4): 520-540.

Bamber, J.L. and A.J. Payne. 2004. *Mass balance of the cryosphere: observations and modeling of contemporary and future change*. Cambridge University Press, Cambridge, 11–42.

Higuchi, K. 1976. Glaciers and Climates of Nepal Himalayas. *Report of the Glaciological Expedition to Nepal. Seppyo, Special Issue*, 38:130.

Higuchi, K. 1977. Effect of nocturnal precipitation on the mass balance of the Rikha Samba Glacier, Hidden Valley, Nepal. *Report of the Glaciological Expedition to Nepal, Part 2. Seppyo, Special Issue,* 39: 43-49.

Higuchi, K. 1978. Outline of the glaciological expedition to Nepal (3). *Report of the Glaciological Expedition to Nepal: Part 3. Seppyo, Special Issue,* 40: 1-3.

Higuchi, K. 1980. Outline of the glaciological expedition to Nepal (4). *Report of the Glaciological Expedition to Nepal: Part 4. Seppyo, Special Issue,* 41: 1-4.

Hirano, A., W. Roy, and H. Lang. 2003. Mapping from ASTER Stereo Image Data: DEM Validation and Accuracy Assessment. *ISPRS Journal of Photogrammetry and Remote Sensing* 57(5-6): 356-370.

Hubbard, B., and N. Glasser. 2005. *Field Techniques in Glaciology and Glacial Geomorphology: Glacier Mass Balance and Motion*. John Wiley & Sons, Ltd. Chichester, England: 179-216.

Huggel, C., A. Kaab, W. Haeberli, P. Teysseire, and F. Paul. 2002. Remote sensing based assessment of hazards from glacier lake outbursts: a case study in the Swiss Alps. *Canadian Geotechnical Journal*, 39: 316-330.

Immerzeel, W., Van Beek L. and M. Bierkens. 2010. Climate change will affect the Asian water towers. *Science,* 328(5984): 1382-1385.

Iwata, S., Y. Ageta, N. Naito, A. Sakai, and C. Narama. 2002. Glacial lakes and their outburst flood assessment in the Bhutan Himalaya. *Global Environmental Research,* 6(1): 3-17.

Kaab, A. 2002. Monitoring high-mountain terrain deformation from air and spaceborne optical data: Examples using digital aerial imagery and ASTER data. *ISPRS Journal of Photogrammetry and Remote Sensing*, 57 (1-2): 39-52.

Kadota, T., K. Seko, and Y. Ageta. 1993. Shrinkage of Glacier Ax010 since 1978, Shorong Himal, East Nepal. *Snow and Glacier Hydrology*, Proceedings of the Kathmandu Symposium, November 1992. IAHS 218:145-154.

Kargel, J., M. Abrams, M. Bishop, A. Bush, and G. Hamilton. 2005. Multispectral imaging contributions to global land ice measurements from space. *Remote Sensing of Environment*, 99 (1-2): 187-219.

Kaser, G., A. Fountain, and P. Jansson. 2003. *A manual for monitoring the mass balance of mountain glaciers*. Technical Documents in Hydrology, 59:106. UNESCO, Paris.

Kattelmann, R. 2003. Glacial Lake Outburst Floods in the Nepal Himalaya: A Manageable Hazard? *Natural Hazards,* 28(1): 145-154.

Kulkarni, A. V., I. Bahuguna M., B. Rathore P., S. Singh K., S. Randhawa S., R. Sood K., and S. Dhar. 2007. Glacial retreat in Himalaya using Indian remote sensing satellite data. *Current Science,* 92(1): 69-74.

Kulkarni, A., B., Rathore, and S. Alex. 2004. Monitoring of glacial mass balance in the Baspa basin using accumulation area ratio method. *Current Science*, 86(1): 101−106.

Mayo, L., M., Meier, and W. Tangborn. 1972. A system to combine stratigraphic and annual mass-balance systems: A contribution to the international hydrological decade. *Journal of Glaciology*, 11 (61): 3-14.

Mergili, Martin, F. Wolfgang, S. Moreiras, and J. Stotter. 2012. Simulation of Debris Flows in the Central Andes Based on Open Source GIS: Possibilities, Limitations, and Parameter Sensitivity. *Natural Hazards,* 61(3): 1051-1081.

Mool, P. K., S. Bajracharya, and S. Joshi. 2001. *Inventory of glaciers, glacial lakes and glacial lake outburst floods, Nepal*. International Centre for Integrated Mountain Development, Kathmandu, Nepal.

Nakawo, M., Fuji, Y. and M. Shrestha L. 1976. Flow of glaciers in Hidden Valley, Mukut Himal. *Report of the Glaciological Expedition to Nepal. Seppyo, Special Issue*, 38: 39-43.

Nakawo, M., Y. Fujita, K. Ageta, A. Pokhrel P and Y. Tandong. 1997. Basic Studies for Assessing the Impacts of the Global Warming on the Himalayan Cryosphere, 1994-1996. *Bulletin of Glacier Research*, 15:53-58.

Narama, C., A. Kaab, M. Duishonakunov, and K. Abdrakhmatov. 2010. Spatial variability of recent glacier area changes in the Tien Shan Mountains, Central Asia, using Corona (1970), Landsat (2000), and ALOS (2007) satellite data. *Global & Planetary Change,* 71(1–2):42–54.

Nishida, K., K. Satow, M. Aniya, G. Casassa, and T. Kadota. 1995. Thickness change and flow of Tyndall Glacier, Patagonia. *Bulletin of Glacier Research,* 13: 29–34.

Nuimura, T., K. Fujita, S. Yamaguchi, and R. Sharma R. 2012. Elevation Changes of glaciers Revealed by Multitemporal Digital Elevation Models Calibrated by GPS Survey in the Khumbu Region, Nepal Himalaya, 1992–2008. *Journal of Glaciology,* 58(210): 648–656.

Paterson, W. 1994. *The Physics of Glaciers*, (3rd ed.). Pergamon, Oxford.

Paul, F., A. Kaab, and W. Haeberli. 2006. Recent glacier changes in the Alps observed by satellite: Consequences for future monitoring strategies. *Global and Planetary Change*, 56: 111–122.

Paul, F., and A. Kaab. 2005. Perspectives on the production of a glacier inventory from multispectral satellite data in the Arctic Canada: Cumberland Peninsula, Baffin Island. *Annals of Glaciology*, 42(1): 59-66.

Prima, O., and R.,Yokoyama. 2002. DEM generation method from contour lines based on the steepest slope segment chain and a monotone interpolation function. *ISPRS Journal of Photogrammetry and Remote Sensing,* 57(1-2): 86-101.

Qin, J., K.Yang, S. Liang, and X. Guo. 2009. The altitudinal dependence of recent rapid warming over the Tibetan Plateau. *Climatic Change*, 97: 321-327.

Quincey, D., R. Lucas, S. Richardson, N. Glasser, M. Hambrey. 2005. Optical remote sensing techniques in high-mountain environments: application to glacial hazards. *Progress in Physical Geography,* 29(4): 475-505.

Rabatel, A., J. Dedieu, C. Vincent. 2005. Using remote-sensing data to determine equilibrium-line altitude and mass-balance time series: validation on three French glaciers, 1994-2002. *Journal of Glaciology*, 51 (175): 539-546.

Racoviteanu, A., Y. Arnaud, M. Williams, and J Ordonez. 2008a. Decadal changes in glacier parameters in the Cordillera Blanca, Peru, derived from remote sensing. *Journal of Glaciology* 54(186): 499-510.

Racoviteanu A., M. Williams, and R. Barry. 2008b. Optical remote sensing of glacier characteristics: A review with focus on the Himalaya. *Sensors* 8(5): 3355-3383.

Raup, B., A. Kaab, J. Kargel, M. Bishop, G. Hamilton, E. Lee. 2007. Remote Sensing and GIS technology in the Global Land Ice Measurements from Space (GLIMS) Project, *Computers & Geoscience,* 33: 104-125.

Richardson, S., and J. Reynolds. 2000. An overview of glacial hazards in the Himalayas. *Quaternary International* , 65-66: 31-47.

Rott, H., W. Rack, P. Skvarca, and H. De Angelis. 2002. Northern Larsen Ice Shelf, Antarctica: further retreat after collapse, *Annals of Glaciology*, 34: 277-282.

San, B. & M. Suzen. 2005. Digital elevation (DEM) generation and accuracy assessment from ASTER stereo data. *International Journal of Remote Sensing*, 26(22): 5013-5027.

Scherzinger, B., J. Hutton, and M. Mostafa. 2007. Chapter 10: Enabling technologies. In *Digital elevation model technologies and applications*: *The DEM Users Manual, 2nd Edition*, 354-355. D.F. Maune, ed. Bethesda, Maryland: ASPRS.

Sobota, I. 2007. Selected methods in mass balance estimation of Waldemar Glacier, Spitsbergen. *Polish Polar Research,* 28(4): 249-268.

Stevens, N., V. Manville, and D. Heron. 2003. The sensitivity of a volcanic flow model to digital elevation model accuracy: experiments with digitized map contours and interferomegtric SAR at Ruapehu and Taranaki volcanoes, New Zealand. *Journal of Volcanology and Geothermal Research*, 119(1): 89-105.

Tangborn, W. 1999. A mass-balance model that uses low-altitude meteorological observations and the area-altitude of a glacier, *Geografiska Annaler*, 81(4): 753-765.

Thomas J., and S. Rai. 2005. *An overview of glaciers, glacier retreat, and subsequent impacts in Nepal, India and China*. WWF Nepal Program, Kathmandu. http://wwf.panda.org/?19092/An-Overview-of-Glaciers-Glacier-Retreat-and-Subsequent-Impacts-in-Nepal-India-and-ChinaLast accessed on 11/27/2012.

Toutin, T. 2008. ASTER DEMs for geomatic and geoscientific applications: a review. *International Journal of Remote Sensing*, 29(7):1855-1875.

Vuichard, D. and M. Zimmermann. 1987. The 1985 Catastrophic Drainage of a moraine Dammed Lake, Khumbu Himal, Nepal: Cause and Consequences. *Mountain Research and Development*, 7(2): 91-110.

Waldmann, N., D. Ariztegui, F. Anselmetti, A. Coronato, & J. Austin 2010. Geophysical evidence of multiple glacier advances in Lago Fagnano (54^0S), southernmost Patagonia. *Quaternary Science Reviews*, 29(9-10): 1188-1200.

Wessels, R., Kargel J., and H. Kiefffer. 2002. Aster Measurement of Supraglacial Lakes in the Mount Everest Region of the Himalaya. *Annals of Glaciology,* 34(1): 399-408.

Yamada, T. 1989. Outline of glaciological expedition of Nepal: Langtang Himal Project 1987-1988. *Bulletin of Glacier Research*, 7:191-193.

Yamada, T. 1993. *Glacier Lakes and Their Outburst Floods in the Nepal Himalaya*, Water and Energy Commission Secretariat (WECS) and Japan Co-operation Agency (JICA), Kathmandu, Nepal.

Yamada, T. 1998. *Glacier Lake and its outburst food in the Nepal Himalaya*, data Centre for Glacier Research, Monograph No. 1. Tokyo: Japanese Society of Snow and Ice, Japan.

Yamanda, T., and C. Sharma. 1993. Glacier Lakes Outburst Floods in the Nepal Himalaya. *Snow and Glacier Hydrology*, proceedings of the Kathmandu Symposium, November 1992. IAHS 218: 319-330.

Ye, Q. 2010. The generation of DEM from ALOS/PRISM and ice volume change in Mt. Qomolangma region. *Geophysical Research Abstracts*, 12.

APPENDIX A

T-TEST RESULTS FOR NON-GLACIALTED AND GLACIATED REGION FOR THE STUDY PERIOD 2002-2005 AND 2002-2008

T-Test on Non-glaciated region, 2002-2005

Paired Samples Statistics

		Mean	N	Std. Deviation	Std. Error Mean
Pair 1	**Year 2002**	4687.5601	55765	492.2051	2.0843
	Year 2005	4678.1853	55765	492.0478	2.0836

Paired Samples Correlations

		N	Correlation	Sig.
Pair 1	**Year 2002** and **Year 2005**	55765	.999	0.000

Paired Samples Test

		Paired Differences					t	df	Sig. (2-tailed)
		Mean	Std. Deviation	Std. Error Mean	95% Confidence Interval of the Difference Lower	Upper			
Pair 1	**Year 2002 - Year 2005**	9.3748	26.9099	.1139	9.1514	9.5981	82.268		0.00

T-Test on Non-glaciated region, 2002-2008

Paired Samples Statistics

		Mean	N	Std. Deviation	Std. Error Mean
Pair 1	**Year 2002**	4618.0944	50614	457.03093	2.03147
	Year_2008	4600.2941	50614	451.89234	2.00863

Paired Samples Correlations

		N	Correlation	Sig.
Pair 1	**Year 2002** and Year_2008	50614	.996	0.000

Paired Samples Test

		Paired Differences					t	df	Sig. (2-tailed)
		Mean	Std. Deviation	Std. Error Mean	95% Confidence Interval of the Difference Lower	Upper			
Pair 1	**Year 2002** - Year_2008	17.80034	42.32305	.18812	17.43162	18.16907	94.621	50613	0.000

T-Test on glaciated region, 2002-2005

Name = Ama Dablam_CI

Paired Samples Statistics[a]

	Mean	N	Std. Deviation	Std. Error Mean
Pair 1 Y02	5459.3787	331	448.32800	24.64234
Y05	5463.2813	331	445.86816	24.50713

a. Name = Ama Dablam_CI

Paired Samples Correlations[a]

	N	Correlation	Sig.
Pair 1 Y02 and Y05	331	.891	.000

a. Name = Ama Dablam_CI

Paired Samples Test[a]

	Paired Differences					t	df	Sig. (2-tailed)
				95% Confidence Interval of the Difference				
	Mean	Std. Deviation	Std. Error Mean	Lower	Upper			
Pair 1 Y02 - Y05	-3.90260	208.40426	11.45493	-26.43650	18.63130	-.341	330	.734

Name = Ama Dablam_DI

Paired Samples Statistics[a]

	Mean	N	Std. Deviation	Std. Error Mean
Pair 1 Y02	4963.9496	1150	140.00525	4.12853
Y05	4961.2560	1150	200.15146	5.90214

a. Name = Ama Dablam_DI

Paired Samples Correlations[a]

	N	Correlation	Sig.
Pair 1 Y02 and Y05	1150	.904	0.000

a. Name = Ama Dablam_DI

Paired Samples Test[a]

	Paired Differences					t	df	Sig. (2-tailed)
				95% Confidence Interval of the Difference				
	Mean	Std. Deviation	Std. Error Mean	Lower	Upper			
Pair 1 Y02 - Y05	2.69357	95.00000	2.80140	-2.80285	8.19000	.962	1149	.336

Name = Chukhung_CI

Paired Samples Statistics[a]

	Mean	N	Std. Deviation	Std. Error Mean
Pair 1Y02	5481.1647	1241	230.74474	6.55007
Y05	5460.6667	1241	230.09204	6.53154

a. Name = Chukhung_CI

Paired Samples Correlations[a]

	N	Correlation	Sig.
Pair 1Y02 and Y05	1241	.999	0.000

a. Name = Chukhung_CI

Paired Samples Test[a]

	Paired Differences					t	df	Sig. (2-tailed)
				95% Confidence Interval of the Difference				
	Mean	Std. Deviation	Std. Error Mean	Lower	Upper			
Pair 1Y02 - Y05	20.49795	12.12513	.34419	19.82269	21.17322	59.554	1240	0.000

a. Name = Chukhung_CI

Name = Chukhung_DI

Paired Samples Statistics[a]

	Mean	N	Std. Deviation	Std. Error Mean
Pair 1Y02	5010.7455	1073	103.92855	3.17274
Y05	4995.3024	1073	105.59599	3.22365

a. Name = Chukhung_DI

Paired Samples Correlations[a]

	N	Correlation	Sig.
Pair 1Y02 and Y05	1073	.994	0.000

a. Name = Chukhung_DI

Paired Samples Test[a]

	Paired Differences					t	df	Sig. (2-tailed)
				95% Confidence Interval of the Difference				
	Mean	Std. Deviation	Std. Error Mean	Lower	Upper			
Pair 1Y02 - Y05	15.44308	11.63451	.35518	14.74615	16.14000	43.480	1072	.000

a. Name = Chukhung_DI

Name = Gaunara_CI

Paired Samples Statistics[a]

	Mean	N	Std. Deviation	Std. Error Mean
Pair 1Y02	5644.2068	1432	112.00673	2.95987
Y05	5637.4975	1432	109.80912	2.90180

a. Name = Gaunara_CI

Paired Samples Correlations[a]

	N	Correlation	Sig.
Pair 1Y02 and Y05	1432	.992	0.000

a. Name = Gaunara_CI

Paired Samples Test[a]

	Paired Differences					t	df	Sig. (2-tailed)
				95% Confidence Interval of the Difference				
	Mean	Std. Deviation	Std. Error Mean	Lower	Upper			
Pair 1Y02 - Y05	6.70938	14.40267	.38060	5.96278	7.45598	17.628	1431	.000

a. Name = Gaunara_CI

Name = Gaunara_DI

Paired Samples Statistics[a]

	Mean	N	Std. Deviation	Std. Error Mean
Pair 1Y02	5259.4902	2073	165.49720	3.63489
Y05	5252.6866	2073	164.03340	3.60274

a. Name = Gaunara_DI

Paired Samples Correlations[a]

	N	Correlation	Sig.
Pair 1Y02 and Y05	2073	.998	0.000

a. Name = Gaunara_DI

Paired Samples Test[a]

	Paired Differences					t	df	Sig. (2-tailed)
				95% Confidence Interval of the Difference				
	Mean	Std. Deviation	Std. Error Mean	Lower	Upper			
Pair 1Y02 - Y05	6.80365	9.33796	.20509	6.40144	7.20586	33.173	2072	.000

a. Name = Gaunara_DI

Name = Imja_CI

Paired Samples Statistics[a]

	Mean	N	Std. Deviation	Std. Error Mean

Pair 1Y02	5852.0996	1205	444.48732	12.80460
Y05	5836.7862	1205	472.47607	13.61088

a. Name = Imja_CI

Paired Samples Correlations[a]

	N	Correlation	Sig.
Pair 1Y02 and Y05	1205	.978	0.000

a. Name = Imja_CI

Paired Samples Test[a]

	Paired Differences					t	df	Sig. (2-tailed)
				95% Confidence Interval of the Difference				
	Mean	Std. Deviation	Std. Error Mean	Lower	Upper			
Pair 1Y02 - Y05	15.31340	99.15385	2.85638	9.70937	20.91744	5.361	1204	.000

Name = Imja_DI

Paired Samples Statistics[a]

	Mean	N	Std. Deviation	Std. Error Mean
Pair 1Y02	5211.9501	3701	189.88464	3.12126
Y05	5187.9693	3701	188.07547	3.09152

a. Name = Imja_DI

Paired Samples Correlations[a]

	N	Correlation	Sig.
Pair 1Y02 and Y05	3701	.998	0.000

a. Name = Imja_DI

Paired Samples Test[a]

	Paired Differences					t	df	Sig. (2-tailed)
				95% Confidence Interval of the Difference				
	Mean	Std. Deviation	Std. Error Mean	Lower	Upper			
Pair 1Y02 - Y05	23.98077	13.44425	.22099	23.54749	24.41405	108.514	3700	0.000

a. Name = Imja_DI

Name = Khumbu_CI

Paired Samples Statistics[a]

	Mean	N	Std. Deviation	Std. Error Mean
Pair 1Y02	5873.6481	4376	444.56297	6.72039
Y05	5860.2100	4376	442.63917	6.69131

a. Name = Khumbu_CI

Paired Samples Correlations[a]

	N	Correlation	Sig.
Pair 1Y02 and Y05	4376	.993	0.000

a. Name = Khumbu_CI

Paired Samples Test[a]

	Paired Differences					t	df	Sig. (2-tailed)
				95% Confidence Interval of the Difference				
	Mean	Std. Deviation	Std. Error Mean	Lower	Upper			
Pair 1Y02 - Y05	13.43815	51.53789	.77909	11.91073	14.96556	17.249	4375	.000

Name = Khumbu_DI

Paired Samples Statistics[a]

		Mean	N	Std. Deviation	Std. Error Mean
Pair 1	Y02	5248.9981	6827	195.57869	2.36705
	Y05	5238.6643	6827	209.55320	2.53618

a. Name = Khumbu_DI

Paired Samples Correlations[a]

		N	Correlation	Sig.
Pair 1	Y02 and Y05	6827	.965	0.000

a. Name = Khumbu_DI

Paired Samples Test[a]

		Paired Differences					t	df	Sig. (2-tailed)
		Mean	Std. Deviation	Std. Error Mean	95% Confidence Interval of the Difference Lower	Upper			
Pair 1	Y02 - Y05	10.33371	55.07520	.66656	9.02704	11.64038	15.503	6826	.000

a. Name = Khumbu_DI

Name = Lhotse Shar_CI

Paired Samples Statistics[a]

		Mean	N	Std. Deviation	Std. Error Mean
Pair 1	Y02	5624.4790	134	337.37005	29.14433
	Y05	5455.6061	134	219.76982	18.98522

a. Name = Lhotse Shar_CI

Paired Samples Correlations[a]

		N	Correlation	Sig.
Pair 1	Y02 and Y05	134	.558	.000

a. Name = Lhotse Shar_CI

Paired Samples Test[a]

		Paired Differences					t	df	Sig. (2-tailed)
		Mean	Std. Deviation	Std. Error Mean	95% Confidence Interval of the Difference Lower	Upper			
Pair 1	Y02 - Y05	168.87291	281.83793	24.34709	120.71531	217.03051	6.936	133	.000

a. Name = Lhotse Shar_CI

Name = Lhotse Shar_DI

Paired Samples Statistics[a]

		Mean	N	Std. Deviation	Std. Error Mean
Pair 1	Y02	5367.3745	891	436.16659	14.61213
	Y05	5268.2501	891	305.52961	10.23563

a. Name = Lhotse Shar_DI

Paired Samples Correlations[a]

		N	Correlation	Sig.
Pair 1	Y02 and Y05	891	.856	.000

a. Name = Lhotse Shar_DI

Paired Samples Test[a]

	Paired Differences								
	Mean	Std. Deviation	Std. Error Mean	95% Confidence Interval of the Difference		t	df	Sig. (2-tailed)
				Lower	Upper			
Pair 1 Y02 - Y05	99.12439	235.45280	7.88797	83.64321	114.60557	12.567	890	.000

a. Name = Lhotse Shar_DI

Name = Lhotse_CI

Paired Samples Statistics[a]

		Mean	N	Std. Deviation	Std. Error Mean
Pair 1	Y02	5375.8426	400	99.57628	4.97881
	Y05	5350.5256	400	101.12352	5.05618

a. Name = Lhotse_CI

Paired Samples Correlations[a]

		N	Correlation	Sig.
Pair 1	Y02 and Y05	400	.990	0.000

a. Name = Lhotse_CI

Paired Samples Test[a]

		Paired Differences					t	df	Sig. (2-tailed)
		Mean	Std. Deviation	Std. Error Mean	95% Confidence Interval of the Difference Lower	Upper			
Pair 1	Y02 - Y05	25.31705	14.43801	.72190	23.89785	26.73625	35.070	399	.000

a. Name = Lhotse_CI

Name = Lhotse_DI

Paired Samples Statistics[a]

		Mean	N	Std. Deviation	Std. Error Mean
Pair 1	Y02	5090.1980	2289	126.85093	2.65137
	Y05	5072.4517	2289	124.00934	2.59198

a. Name = Lhotse_DI

Paired Samples Correlations[a]

		N	Correlation	Sig.
Pair 1	Y02 and Y05	2289	.997	0.000

a. Name = Lhotse_DI

Paired Samples Test[a]

		Paired Differences					t	df	Sig. (2-tailed)
		Mean	Std. Deviation	Std. Error Mean	95% Confidence Interval of the Difference Lower	Upper			
Pair 1	Y02 - Y05	17.74628	9.55499	.19971	17.35464	18.13792	88.859	2288	0.000

a. Name = Lhotse_DI

Name = Nojumba_CI

Paired Samples Statistics[a]

		Mean	N	Std. Deviation	Std. Error Mean
Pair 1	Y02	5463.2008	2718	285.37291	5.47379
	Y05	5452.3628	2718	270.85799	5.19538

a. Name = Nojumba_CI

Paired Samples Correlations[a]

		N	Correlation	Sig.
Pair 1	Y02 and Y05	2718	.974	0.000

a. Name = Nojumba_CI

Paired Samples Test[a]

		Paired Differences					t	df	Sig. (2-tailed)
		Mean	Std. Deviation	Std. Error Mean	95% Confidence Interval of the Difference Lower	Upper			
Pair 1	Y02 - Y05	10.83802	64.87297	1.24434	8.39807	13.27797	8.710	2717	.000

a. Name = Nojumba_CI

Name = Nojumba_DI

Paired Samples Statistics[a]

		Mean	N	Std. Deviation	Std. Error Mean
Pair 1	Y02	4976.6089	7800	180.78583	2.04700
	Y05	4970.4264	7800	185.09278	2.09576

a. Name = Nojumba_DI

Paired Samples Correlations[a]

		N	Correlation	Sig.
Pair 1	Y02 and Y05	7800	.967	0.000

a. Name = Nojumba_DI

Paired Samples Test[a]

		Paired Differences					t	df	Sig. (2-tailed)
		Mean	Std. Deviation	Std. Error Mean	95% Confidence Interval of the Difference Lower	Upper			
Pair 1	Y02 - Y05	6.18253	47.01344	.53232	5.13903	7.22602	11.614	7799	.000

a. Name = Nojumba_DI

Name = Nuptse_CI

Paired Samples Statistics[a]

		Mean	N	Std. Deviation	Std. Error Mean
Pair 1	Y02	5766.2963	357	291.35026	15.41989
	Y05	5699.4157	357	243.66257	12.89599

a. Name = Nuptse_CI

Paired Samples Correlations[a]

		N	Correlation	Sig.
Pair 1	Y02 and Y05	357	.771	.000

a. Name = Nuptse_CI

Paired Samples Test[a]

		Paired Differences					t	df	Sig. (2-tailed)
		Mean	Std. Deviation	Std. Error Mean	95% Confidence Interval of the Difference Lower	Upper			
Pair 1	Y02 - Y05	66.88062	186.41409	9.86608	47.47749	86.28374	6.779	356	.000

a. Name = Nuptse_CI

Name = Nuptse_DI

Paired Samples Statistics[a]

		Mean	N	Std. Deviation	Std. Error Mean
Pair 1	Y02	5297.2365	1455	246.43151	6.46048
	Y05	5276.2953	1455	221.83079	5.81554

a. Name = Nuptse_DI

Paired Samples Correlations[a]

		N	Correlation	Sig.
Pair 1	Y02 and Y05	1455	.914	0.000

a. Name = Nuptse_DI

Paired Samples Test[a]

		Paired Differences					t	df	Sig. (2-tailed)
		Mean	Std. Deviation	Std. Error Mean	95% Confidence Interval of the Difference Lower	Upper			
Pair 1	Y02 - Y05	20.94128	100.08392	2.62381	15.79442	26.08814	7.981	1454	.000

Name = Gaunara_CI

Paired Samples Statistics[a]

	Mean	N	Std. Deviation	Std. Error Mean
Pair 1Y02	5644.2068	1432	112.00673	2.95987
Y08	5627.6150	1432	108.45304	2.86596

a. Name = Gaunara_CI

Paired Samples Correlations[a]

	N	Correlation	Sig.
Pair 1Y02 and Y08	1432	.990	0.000

a. Name = Gaunara_CI

Paired Samples Test[a]

	Paired Differences					t	df	Sig. (2-tailed)
				95% Confidence Interval of the Difference				
	Mean	Std. Deviation	Std. Error Mean	Lower	Upper			
Pair 1Y02 - Y08	16.59186	15.98060	.42230	15.76346	17.42025	39.289	1431	.000

a. Name = Gaunara_CI

Name = Gaunara_DI

Paired Samples Statistics[a]

	Mean	N	Std. Deviation	Std. Error Mean
Pair 1Y02	5259.4902	2073	165.49720	3.63489
Y08	5246.8621	2073	158.90386	3.49008

a. Name = Gaunara_DI

Paired Samples Correlations[a]

	N	Correlation	Sig.
Pair 1Y02 and Y08	2073	.998	0.000

a. Name = Gaunara_DI

Paired Samples Test[a]

	Paired Differences					t	df	Sig. (2-tailed)
				95% Confidence Interval of the Difference				
	Mean	Std. Deviation	Std. Error Mean	Lower	Upper			
Pair 1Y02 - Y08	12.62810	13.21369	.29022	12.05895	13.19725	43.512	2072	.000

a. Name = Gaunara_DI

Name = Khumbu_CI

Paired Samples Statistics[a]

	Mean	N	Std. Deviation	Std. Error Mean
Pair 1Y02	5728.1323	3539	318.73672	5.35787
Y08	5701.4293	3539	315.73172	5.30735

a. Name = Khumbu_CI

Paired Samples Correlations[a]

	N	Correlation	Sig.
Pair 1Y02 and Y08	3539	.987	0.000

a. Name = Khumbu_CI

Paired Samples Test[a]

	Paired Differences					t	df	Sig. (2-tailed)
				95% Confidence Interval of the Difference				
	Mean	Std. Deviation	Std. Error Mean	Lower	Upper			
Pair 1Y02 - Y08	26.70303	50.59683	.85052	25.03548	28.37059	31.396	3538	.000

a. Name = Khumbu_CI

Name = Khumbu_DI

Paired Samples Statistics[a]

	Mean	N	Std. Deviation	Std. Error Mean
Pair 1Y02	5253.1528	6927	197.67202	2.37505
Y08	5220.4248	6927	182.82615	2.19667

a. Name = Khumbu_DI

Paired Samples Correlations[a]

	N	Correlation	Sig.
Pair 1Y02 and Y08	6927	.963	0.000

a. Name = Khumbu_DI

Paired Samples Test[a]

	Paired Differences					t	df	Sig. (2-tailed)
				95% Confidence Interval of the Difference				
	Mean	Std. Deviation	Std. Error Mean	Lower	Upper			
Pair 1Y02 - Y08	32.72799	54.11903	.65025	31.45331	34.00267	50.332	6926	0.000

a. Name = Khumbu_DI

Name = Nojumba_CI

Paired Samples Statistics[a]

	Mean	N	Std. Deviation	Std. Error Mean
Pair 1 Y02	5440.4806	3059	281.11555	5.08271
Y08	5429.7952	3059	261.77529	4.73303

a. Name = Nojumba_CI

Paired Samples Correlations[a]

	N	Correlation	Sig.
Pair 1 Y02 and Y08	3059	.972	0.000

a. Name = Nojumba_CI

Paired Samples Test[a]

	Paired Differences					t	df	Sig. (2-tailed)
				95% Confidence Interval of the Difference				
	Mean	Std. Deviation	Std. Error Mean	Lower	Upper			
Pair 1 Y02 - Y08	10.68536	66.99340	1.21127	8.31037	13.06036	8.822	3058	.000

a. Name = Nojumba_CI

Name = Nojumba_DI

Paired Samples Statistics[a]

	Mean	N	Std. Deviation	Std. Error Mean
Pair 1 Y02	4963.6814	7459	171.19468	1.98221
Y08	4960.3708	7459	175.74923	2.03495

a. Name = Nojumba_DI

Paired Samples Correlations[a]

	N	Correlation	Sig.
Pair 1 Y02 and Y08	7459	.965	0.000

a. Name = Nojumba_DI

Paired Samples Test[a]

	Paired Differences					t	df	Sig. (2-tailed)
				95% Confidence Interval of the Difference				
	Mean	Std. Deviation	Std. Error Mean	Lower	Upper			
Pair 1 Y02 - Y08	3.31061	46.03258	.53300	2.26578	4.35543	6.211	7458	.000

a. Name = Nojumba_DI

Name = Nuptse_CI

Paired Samples Statistics[a]

	Mean	N	Std. Deviation	Std. Error Mean
Pair 1Y02	5788.4418	334	288.13547	15.76607
Y08	5631.0526	334	132.40859	7.24508

a. Name = Nuptse_CI

Paired Samples Correlations[a]

	N	Correlation	Sig.
Pair 1Y02 and Y08	334	.589	.000

a. Name = Nuptse_CI

Paired Samples Test[a]

	Paired Differences					t	df	Sig. (2-tailed)
	Mean	Std. Deviation	Std. Error Mean	95% Confidence Interval of the Difference Lower	Upper			
Pair 1Y02 - Y08	157.38916	235.75318	12.89984	132.01371	182.76461	12.201	333	.000

a. Name = Nuptse_CI

Name = Nuptse_DI

Paired Samples Statistics[a]

	Mean	N	Std. Deviation	Std. Error Mean
Pair 1Y02	5299.5314	1478	245.22780	6.37870
Y08	5248.1961	1478	191.82913	4.98973

a. Name = Nuptse_DI

Paired Samples Correlations[a]

	N	Correlation	Sig.
Pair 1Y02 and Y08	1478	.914	0.000

a. Name = Nuptse_DI

Paired Samples Test[a]

	Paired Differences					t	df	Sig. (2-tailed)
	Mean	Std. Deviation	Std. Error Mean	95% Confidence Interval of the Difference				
				Lower	Upper			
Pair 1Y02 - Y08	51.33534	104.81700	2.72643	45.98725	56.68343	18.829	1477	.000

a. Name = Nuptse_DI